ABSTRACT

BEHAVIOUR OF INDIRECTLY LOADED REINFORCED CONCRETE THIN-WALL RIBBED PANELS

IQBAL S. PAUL

The method of load application, the nature of loading, the amount of web reinforcement and the details of the reinforcement invariably influence the behaviour and in particular, the shear strength of reinforced concrete flexural members. The effects are significant in the case of deep beams.

This report investigates the strength and behaviour of wall panels having shear span-to-depth ratio of 1 and with a single concentrated load at mid-span. Effects of direct loading and indirect loading are examined and comparable results are presented.

The Finite Element model, developed at Concordia University, is used to obtain the behaviourial pattern, principal stresses and loading history of the panels.

The crack and stress patterns for each panel, simulated from the results of the finite element model, are presented for comparison purposes.

ACKNOWLEDGEMENTS

ACKNOWLEDGEMENTS

The author expresses his sincerest gratitude to
Dr. Z.A. Zielihski for his invaluable advice and guidance
throughout the preparation of this thesis.

Grateful thanks are due to many fellow graduate
students at the University, who assisted during testing,
modifying and running the "Finite Element Model" developed
at the University.

The author is indebted to Concordia University for
the use of the computer facilities which enabled him to
complete this report.

A very special thanks to my wife Birte for her
constant encouragement and her patience in correcting the
manuscript.

Special words of appreciation go to W.J. Kedzierski,
Eng., a colleague at work, who helped with the occasional
translations from German and Polish references, and to
Miss M. Stredder, who typed this report.

TABLE OF CONTENTS

TABLE OF CONTENTS

LIST OF TABLES

LIST OF TABLES

LIST OF FIGURES

LIST OF FIGURES

NOTATIONS

NOTATIONS

A_s, A_v area of reinforcement; tension and shear, respectively

a shear span (measured from centre of support to centre of load)

b width of beam or panel

b_w width of web

C, T longitudinal force; compressive and tensile, respectively

$[D], [D]'$ stress-strain matrix in general and local coordinates, respectively

d effective depth of beam or panel

E_c, E_s Young's modulus of elasticity; concrete and steel, respectively

f'_c compressive strength of concrete

f_{ct} compressive stress in concrete subject to biaxial tension-compression

f_t tensile strength of concrete

f_{ti} splitting strength of concrete

f_y yield strength of reinforcement

G shear modulus $\dfrac{E_c}{2(1+\nu)}$

h overall depth of panel

$[K]$ structure stiffness matrix

ℓ_n total length of the panel

ℓ_s support bearing plate length

P point load on panel

P_u ultimate load

s spacing of web reinforcement

s_1 spacing of vertical web reinforcement

s_2 spacing of horizontal web reinforcement

$[T]$ transformation matrix

V shear force

V_a shear force carried by aggregate interlock

V_c shear force carried by concrete

V_d shear force carried by dowel action

V_h' shear force transferred by horizontal shear reinforcement

V_s shear force transferred by vertical or inclined shear reinforcement

V_u ultimate shear

V_{cr} shear cracking resistance

v_b basis shear stress

α angle of inclination of bent up reinforcement to the axis of a beam

β shear retention factor

γ_{xy} shearing strain in general coordinates

$\{\delta\}$ vector of nodal displacement

$\varepsilon_x, \varepsilon_y$ strains in general coordinates

$\{\varepsilon\}, \{\varepsilon'\}$ strain vector in general and local coordinates respectively

θ angle between x-axis and the crack direction measured counter-clockwise

λ Factor: 1 for normal weight concrete
                0.75 for light-weight concrete

ν Poisson's ratio

σ_x, σ_y stress in general coordinates

$\{\sigma\}, \{\sigma'\}$ stress vector in general and local coordinates

ρ_ω, ρ_t ratio of web and flexural reinforcement

ϕ strength factor: 0.85 for shear

τ_{xy} shearing stress in general coordinates

x, y general (Cartesian) coordinates

ξ, η local curvilinear coordinates for stiffness matrix formulation

CHAPTER I

INTRODUCTION

CHAPTER I

INTRODUCTION

1.1 GENERAL

For the first time, the 1971 ACI Building Code (2) and CSA Standard A23.3 - 1973 (8), Canadian equivalent, recognizes the need to assess the shear strength of deep beams. The present recommendations, in both the Codes, are still restricted to members if they are loaded on the top and supported on the bottom face.

A beam is classified as deep beam when its clear span ℓ_n to effective depth, d ratio is less than 5. CEB (7) defines deep beams as members with span-to-depth ratios of 2 or 2.5 for simple and continuous beams.

Concentrated loads or reactions may be applied to beams on the extreme compression or tension faces or through other structural members framing into the sides of the beam. While the former is the case most frequently simulated in the laboratory and has been the subject of numerous research papers, the latter case is most generally representative of the actual structural systems.

Examples of the top loaded deep members would be pile caps and transfer girders while bins and silo walls, where the load of contents is transferred at the bottom or at the intermediate levels, would be representative of the other

loading situations. Fig. 1.1 show three cases of loading.

The members loaded on top or compression face are generally referred to as "directly loaded" and the provisions of the ACI Building Code apply only to such loaded members. When the load transfer from one member to the other is by shear rather than bearing, the members are considered to be "indirectly loaded." The ACI Building Code does not yet specify the analysis of shear for indirectly loaded members, therefore, the ordinary shear design methods proposed for normal proportion beams, are assumed applicable.

In deep beams the inclined cracks are much steeper compared to normal beams and this affects the shear transfer mechanism. The modes of shear failures in deep beams, therefore, differ considerably from those in normal beams.

Considerable research has been done in order to establish the major differences in behaviour between the deep beams and the normal proportional beams.

1.2 PREVIOUS RESEARCH

Since the introduction of the concept of elasticity there have been many contributions in solving such problems. Guyon [13] investigated the stresses in the end block of a prestressed concrete beam by means of stress trajectories or isostatics. Deep beams can be considered as analogous to bearing blocks at the end of prestressed concrete I-beams turned on their sides. In 1932 Dischinger [10] used trigono-

.metric series to determine stresses in continuous deep girders. PCA [31] presented solutions of Dischinger and included solutions for simply-supported spans.

Chow, Conway and Winter [6] used finite difference equations to give solutions for single span deep beam problems. Cheng and Pei [5] contributed much to the theory of deep beams by solving the case in which no displacement at supports is permitted.

Leonhardt et al [22,23,24] undertook extensive investigation of deep beams under all loading and support conditions and presented comprehensive findings for directly and indirectly loaded beams.

Kaar [18] conducted tests on centrally loaded simply supported deep beams made of aluminum and of steel in order to establish the non-linear stress stage which departs from simple linear flexural relationship (Navier's hypothesis). It was shown that stresses in deep members are highly non-linear and if computed by using ordinary flexural formulas, (Euler-Bernoulli Theory) it would give erroneous results.

Deep beams were mostly analysed by the theory of vertical plates or by photoelasticity, with beams assumed to be made of homogeneous material. The members were simply designed as beams in the plane stress state with linear strain behaviour and tensile reinforcing was added, in the regions, where tensile stresses were above the estimated tensile strength of concrete.

Leonhardt and Walther (24) considered two states -
the uncracked and cracked. Their tests showed that the theory
of vertical plates apply fairly well to reinforced concrete
deep beams as long as no cracks occur. After cracking, how-
ever, which initiate in most deep beams before or at working
load, the actual stresses deviate quite significantly from
the theoretical ones calculated for the homogeneous material.
Due to the reduction of the lever arm the tensile stresses in
the main reinforcement tend to be less than the values given
by the elastic theory at mid-span. The compressive stresses
at supports tend to be more for deep beams and could be critical
for thin, heavily loaded beams.

Zielinski (42) considered four strength limit stages
of beams and derived simple formulas giving the ultimate
strength in deep thin wall panels based on strength limit stage
2 - when 45° inclined cracks appear due to pure shear action,
and strength limit stage 3 - at ultimate diagonal splitting.
Tests (1,36) proved that beams with well anchored tensile re-
inforcing continue working beyond strength limit stage 2 until
stage 3 is reached.
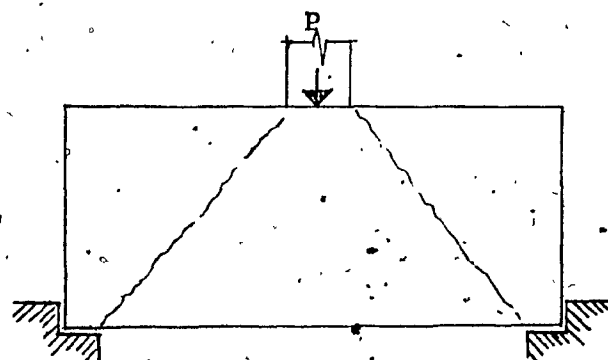
TOP LOADING
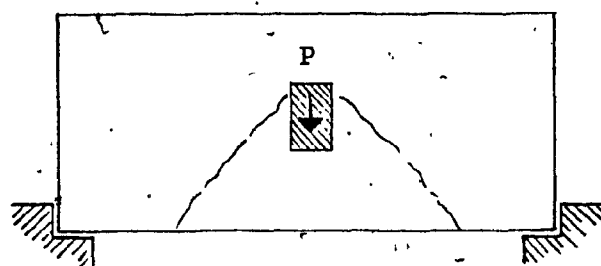
IN-DEPTH LOADING
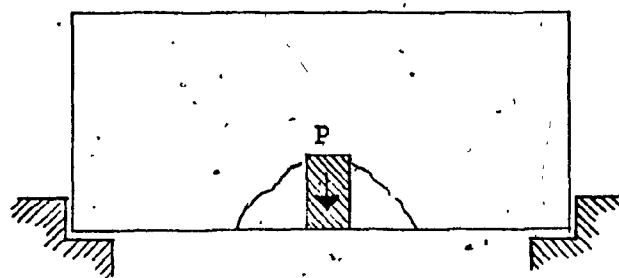
BOTTOM LOADING

FIG. 1.1   TYPICAL LOADING CASES

CHAPTER II

BEHAVIOR OF DEEP BEAMS

CHAPTER II

BEHAVIOUR OF DEEP BEAMS

2.1 INTRODUCTION

In view of St. Venant's principle, with reference
to a beam in which no point is more than the amount of the
height of the beam from a concentrated force such as a load
or reaction, we should not attempt to apply conventional
flexural theory or to think in terms of bending moments.
In case of deep beams this criterion influences the behavior
of the member.

Mechanism and complexities developed in reinforced
concrete beams point out that deep beams display tied-arch
action and cannot be explained in terms of Navier's assump-
tions. Actual distribution of strain would differ even
more from that assumed by Navier's if reinforcement is not
bonded between supports.

2.2 MECHANISM OF SHEAR TRANSFER

In reinforced concrete members shear is transferred
from one plane to another by various means such as shear
strength of uncracked concrete, shear reinforcement, interface
shear transfer and dowel action. In deep beams, arch action
plays a significant role in transferring load to supports.
Other means of shear transfer are not that predominant as

these would be in ordinary proportioned beams. Arch action could develop immediately after the concrete cracks provided the main longitudinal tensile reinforcing is well anchored.

Shear stresses and vertical normal stresses may require more attention than the flexural stresses in the design of deep beams. Bi-axial tension and compression stresses, acting normal and parallel respectively to the line joining the load and the support, cause diagonal cracks to appear immediately within the span inside the reaction plates.

The forces in a reinforced concrete beam with a diagonal crack are shown in Fig. 2.1. The longitudinal forces T and C, are related to the flexural resistance of the member. The forces along the diagonal tension crack, V_{ax} and V_{ay} are due to the interface shear transfer or aggregate interlock. The V_s and V_d forces are web reinforcement and the "dowel shear" forces respectively and V_c represents the shear carried by compression zone. Total shear capacity V_u of the member, therefore, is:

$$V_u = V_c + V_s + V_a + V_d \qquad (2.1)$$

At elastic state, before flexural cracking, most of shear is carried by uncracked concrete. Between flexural and inclined cracking the external shear is resisted by the concrete V_c; interface shear transfer, V_a; and by dowel action, V_d. A portion of the shear is carried by the web

reinforcement V_s, which intersects the inclined cracks. When web reinforcement can no longer carry additional shear due to its yielding, any additional shear must be carried by V_c V_d and V_a . The interface shear transfer, V_a , decreases as the cracks widen. This results in accelerated increase in V_d and V_c until either splitting failure occurs or compression zone failes due to combined shear and compression.

2.3 MODES OF FAILURE

The usual modes of failure in deep beams generally involve cracking and crushing of concrete and yielding of reinforcement under complex states of stress. Primarily, there are two failure modes in deep beams, i.e., flexural failure and shear failure. Both the modes directly relate to failure of the tied arch.

A flexural failure, or a ductile failure, results either from crushing at the crown of the concrete rib of the tied arch or by rupture of the longitudinal steel acting as a tie at the bottom. A shear failure, on the other hand, occurs when the inclined concrete strut that forms between the load point and the support is destroyed.

There are other secondary modes of failure such as anchorage failure and bearing failure. Although these are also undesirable modes, but with careful detailing of anchorage and bearing plates at load points and at supports, these

two modes of failure can be eliminated. Fig. 2.2 shows failure modes in a deep beam.

2.3.1 Flexural Failure

Zielinski [42], Kani [17] and others have pointed out that for deep beams, the concrete in the vicinity of loads is in biaxial compression and has greater strength. The load, if calculated by usual ultimate strength design, for flexure, will be significantly underestimated since it is based on yield stress of the reinforcement. In case of flexural failure, the tension steel may rupture or usually be in strain-hardening regions before the concrete crushes. de Paiva and Siess [9] reported that if the ultimate strain in the concrete in compression is taken as 0.008 and the corresponding steel stress is obtained from the steel stress-strain diagram, a good estimate of flexural capacity can be obtained.

Present flexural provisions of ACI Code for deep beams are conservative and do not represent correctly the flexural capacity of the deep beams, however, they do represent the lower limit of ductile behaviour at failure.

2.3.2 Shear Failure

The shear failure in concrete beams may be caused by destruction of one or a combination of various means by which the shear is transferred across the section. Since the tied arch mechanism is most predominant in deep beams, the shear

failures of deep beams generally related to the destruction of diagonal strut.

2.3.2.1 Failure initiated by yielding of web reinforcement

The most common case of shear failure involves the yielding of web reinforcement. Diagonal splitting is accompanied by a sudden increase in steel stress since from the moment of splitting, the total tension must be carried by web reinforcement. The beam would attain its limit strength at this stage if the web reinforcement was insufficiently provided. Otherwise, the beam will continue to work until either reinforcement yields or concrete fails in compression. In deep beams with $\frac{a}{d}$ ratio 0 to 1, horizontal web reinforcement becomes more effective because of shear friction mechanism [15] and decrease with an increase in $\frac{a}{d}$ ratio until $\frac{a}{d}$ ratio of 2.5, when it disappears and vertical web reinforcement takes over. The contribution of horizontal web reinforcement to the shear strength of a member, V_h, due to shear friction can be calculated from equation:

$$V_h = \phi[\frac{A_v f_y d}{s} (1 - \frac{a}{2d})]$$ (2.2)

This equation is similar to Equation (2.4.3) proposed by the Joint ACI-ASCE Committee on shear [15].

2.3.2.2 Failure Initiated by Crushing of Arch Rib

The failure of a deep beam could take place from crushing of the arch rib which forms after the inclined cracking. Shearing stresses particularly, in narrow web beams are much larger compared to normal beams. Crushing of arch ribs, which form between the inclined cracks takes place under the action of diagonal compression forces [30]. To prevent such failures, the diagonal compression stresses, thus the shearing stresses, must be limited. CEB [7] recommends that these stresses must not exceed $0.2 f'_c$ in beams with vertical web reinforcement and $0.25 f'_c$ in beams with 45° web reinforcement.

Manuel [ACI-SP42] developed a rational approach to predict the failure load based on web crushing. Fig. 2.3 shows the basis of his approach.

2.3.2.3 Failure Initiated by Anchorage Distress

Due to the tied arch action, after the inclined cracks, the tensile force in longitudinal reinforcement is constant from support to support and, therefore, it is essential to anchor these bars to resist the tensile force. Anchorage must be designed to resist at least 80% of the yield strength of the bar.

2.4   SHEAR STRENGTH OF DEEP BEAMS

Conventionally, ACI Code [2] and CSA Standard [8] assume that the values of V_a and V_d are small and hence ignore them and express the shear strength of beams in the form:

$$V_u \leq \phi(V_c + V_s + V_h) \qquad (2.4)$$

shear force carried by concrete, V_c, is given by

$$V_c = (2\frac{d}{a})v_b b_w d \qquad (2.5)$$

but not less than $v_b b_w d$, where

$$v_b = (0.8 + 120\rho_w)\lambda\sqrt{f'_c} \qquad (2.6)$$

but not greater than $2.3\lambda\sqrt{f'_c}$ nor less than $\lambda\sqrt{f'_c}$

$$\rho_w = \frac{A_s}{b_w d}$$

λ = 1 for normal weight concrete; 0.75 for light-
   weight concrete

Shear force transferred by vertical web reinforcement, V_s, is given by:

$$V_s = \frac{A_v f_y (a - \frac{d}{2})}{s_1} \qquad (2.7)$$

but not more than $\dfrac{A_v f_y d}{s}$ and not less than zero

where
$$A_v \geq 50 \, b_w \, s_1/f_y$$

and
$$s_1 \leq d/4 \text{ or } 18 \text{ inches}$$

Shear force V_h transferred by horizontal stirrups is given by:

$$V_h = \frac{A_{vh} f_y (1.5d - a)}{s_2} \qquad (2.8)$$

but not more than $\dfrac{A_{vh} f_y d}{s_2}$

where
$$A_{vh} \geq 50 \, b_w \, s_2/f_y$$

and
$$s_2 \leq d/3 \text{ or } 18 \text{ inches}$$

The contribution of web reinforcement in transferring shear force $V_s + V_h$ must not exceed $8b_w d\lambda\sqrt{f_c'}$, and maximum shear force $V_c + V_s + V_h$ not to exceed $0.2b_w df_c'$ nor $800 \, b_w d$.

A number of commonly used methods are available for predicting the shear strength of reinforced concrete deep beams. Although most of the relationships are developed for "directly loaded" deep beams, these also can be applied to "indirectly loaded" deep members provided properly designed suspension or hanger reinforcements are provided and well anchored in the top compression zone. The present study showed that indirectly loaded deep beams with hanger reinforcement attained equivalent strength to those of directly loaded beams.

The most commonly used methods are outlined below:

2.4.1 de Paiva and Seiss [9] Method

This is a modification of the original equation and applies to deep beams $0 \leq \frac{a}{d} \leq 1.0$.

$$V_u = [0.8bd(1-0.6\tfrac{a}{d})(200+0.188f_c'+21,300\rho_t')] \quad (2.9)$$

where

$$\rho_t' = \frac{1}{bd}[(A_s+A_v)(1-\sin\alpha)]$$

A_s = main longitudinal reinforcement area

A_v = total horizontal web reinforcement area
in shear span.

α = angle of inclination of bent up reinforcement
to the axis of the beam.

2.4.2 Ramakrishnan and Ananthanarayana [32] Method

This approach to calculate the shear strength is based on the diagonal splitting strength of concrete. Web reinforcement does not contribute to strength in this formula:

$$V_u = \beta K f_t bd \quad (2.10)$$

where

β = 2 for symmetrical loading; two-point, single
and uniform

$$K = \frac{\pi}{2} = 1.571 \text{ for cylinder split test}$$

1.363 for diagonal cube split test

$f_t =$ splitting strength of 6in x 12 in cylinder

2.4.3 Kong and Robins [18,19] Method

This formula evolved from the Nottingham tests conducted on simple span deep beams with low $\frac{a}{d}$ ratios and with various web reinforcement configurations. The formula was revised when it was revealed from further tests that concrete cylinder splitting tensile strength rather than the cube strength, as previously suggested, was more related to the ultimate shear strength.

The ultimate shear strength of a deep beam, V_u, is given by:

$$V_u = C_1 (1-0.35\frac{a}{d}) f_t bd + C_2 \sum^{n} \frac{AY}{d} - \sin^2\alpha \quad (2.11)$$

where

C_1 = 1.4 for normal weight concrete and
1.0 for light-weight concrete

C_2 = 18,900 psi for plain bars and
43,500 psi for deformed bars

f_t = cylinder splitting tensile strength psi or
10% of cube strength

A = area of an individual web bar including main
tensile longitudinal reinforcement

Y = depth of individual web bar, measured from top of the beam, at which it intersects the line joining the inside edge of the bearing block at the support of the outside edge of that at the loading point

n = total number of web bars

α = angle between web bar and diagonal line as described above in definition of Y.

2.4.4 - Zielinski [42] Method

This approach again is based on diagonal splitting strength of concrete. The presence of web reinforcement slightly increases the splitting force. Shear load can be expressed as:

$$V_u = f_{ct}(\frac{bd^2}{a} + m \Sigma A_s \sin\alpha) \qquad (2.12)$$

where

$$f_{ct} = 1.17f_t = 0.117f_c'$$

m = ratio of Modulus of steel to concrete $\frac{E_s}{E_c}$

A_s = area of individual web bar including main tensile longitudinal steel along the diagonal

α = angle between the web bar and principal tension direction

2.4.5 Manuel Method (ACI - SP42)

This method was advanced to include web crushing as another mode of failure in deep beams and is given as follows:

$$V_u = \frac{0.85f'_c \, L_s \, b_w}{1 + (\frac{a}{d})^2} \qquad (2.13)$$

where

L_s = support bearing plate length

b_w = web thickness

The bearing length on the web thickness can be adjusted so that:

$$\frac{V_u}{L_s \, b_w} \leq \frac{0.85f'_c}{1 + (\frac{a}{d})^2}$$

This relationship is shown in Fig.2.3.

2.5 COMPARISON OF SHEAR STRENGTH METHODS

Generally, the formulas based on cylinder splitting analogy under-estimated the ultimate capacity for over-reinforced panels. Over-estimation for over-reinforced panels would result using Kong et al's formula. Zielinski's formula gave good results for under-reinforced panels but under-estimated the over-reinforced panels.

The finite element method which will be pursued in this study, proved [36,37] that ultimate loads observed experimentally and obtained using finite element models were in good agreement. The results indicate that the finite element analysis will be valuable to the design engineers, as it offers a complete picture of the stress distribution, both in concrete and in steel.
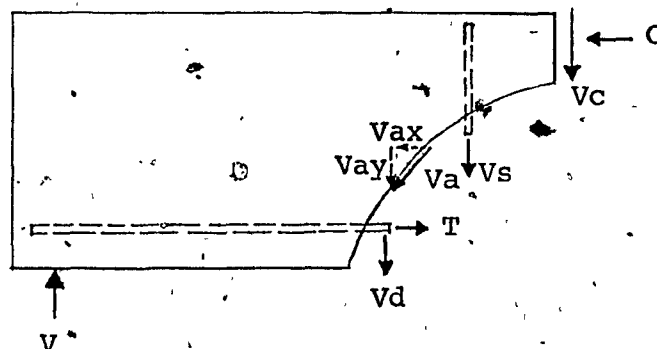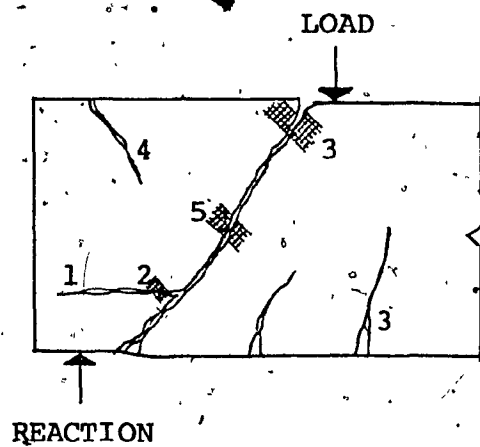
FIG. 2.1 FORCES ACTING AT INCLINED CRACK

FIG. 2.2 MODES OF FAILURE OF DEEP BEAMS
(SCHEMATIC)

Type of failure

1. Anchorage failure
2. Bearing failure
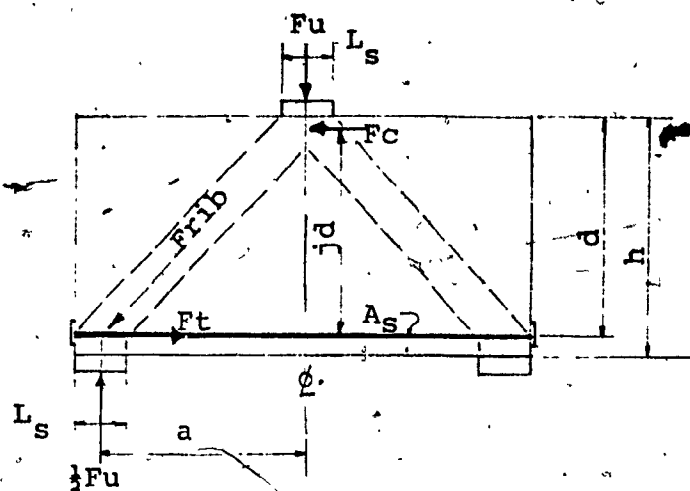3. Flexure failure
4&5. Arch-rib failure

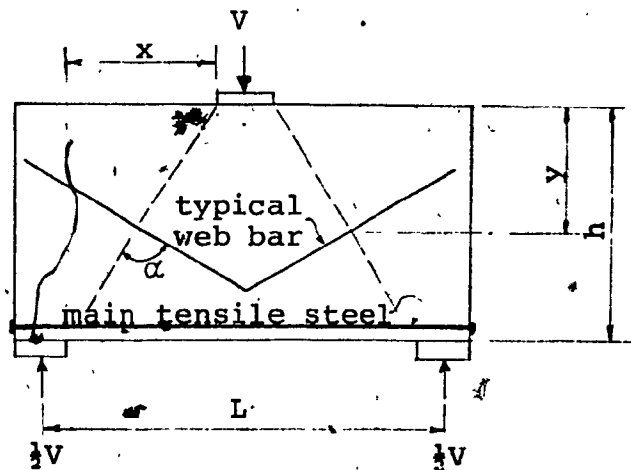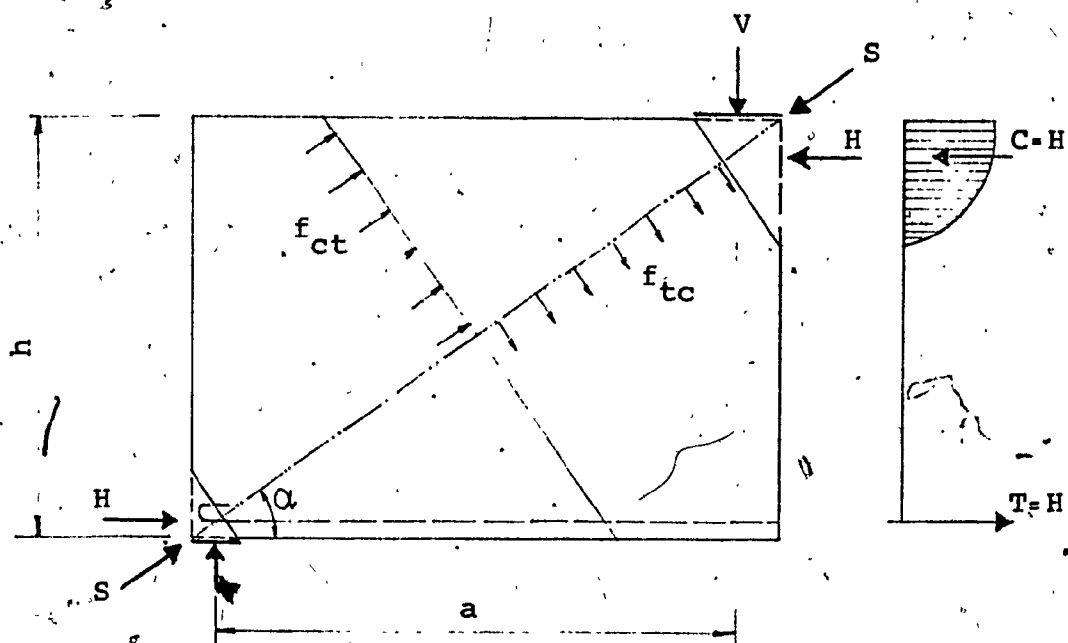FIG. 2.3   THE WEB COMPRESSION METHOD
(according to Manuel)

FIG. 2.4 DESCRIPTION OF VARIABLES USED IN
EMPIRICAL FORMULA BY KONG et al.

$$\alpha = \arctan\left(\frac{h}{a}\right)$$

$$V = S \sin\alpha$$

$$H = S \cos\alpha$$

$$f_{ct} = \frac{H}{hb}$$

$$f_{tc} = \frac{V}{ab}$$

where b is width of member

FIG. 2.5 SIMPLIFIED STRESS DISTRIBUTION UNDER
DIAGONAL COMPRESSION
(According to Zielinski)

CHAPTER III

TEST PROGRAMME

CHAPTER III

TEST PROGRAMME

3.1 INTRODUCTION

The majority of research, to gain insight into the behaviour of deep beams, has been based on tests conducted on beams with direct loads, applied on top face and supported on the bottom face. Most frequently in practice, however, loads or reactions are applied indirectly, as shear on the sides of a beam. These loads could occur somewhere between the top and bottom faces of a beam. Effects of such loading on the behaviour of beam panels is the subject of this study.

3.2 A BRIEF REVIEW OF PREVIOUS CONCORDIA TESTS

Analytical studies and experimental research has been undertaken at Concordia University to study the behaviour of reinforced concrete thin-wall ribbed panels and the results [1,36,37,41] reported. The tests [1,41] were conducted on fourteen full-size "UCOPAN" panels "directly" loaded with one concentrated load at mid-span or one-third point loading. Thin webs (1½") of the panels gave an opportunity of studying the propagation of cracks and inclined splitting stresses.

The results indicated that in all panels a tied arch action developed at around 45% to 50% of the ultimate load, and diagonal splitting cracks appeared at about 80% of the

ultimate load. Without the web reinforcement the panel would have failed at this stage. According to Zielinski [42] the work of a flexural member does not terminate at the occurrence of diagonal splitting cracks, provided sufficient web reinforcement is present to take over the splitting forces.

Taner [36] continued analytical and experimental research on full-size "directly loaded" modified "UCOPAN" thinwall ribbed panels, and developed a finite element model to predict ultimate shear strength and behaviour of reinforced concrete members subject to monotonically increasing, static in-plane loading.

3.3 THE SCOPE OF THIS STUDY

3.3.1 Objective

The main objective of this study has been to investigate analytically the behaviour and strength variations in an "indirectly loaded" modified "UCOPAN" thin-wall ribbed panel, and to compare the results with existing analytical and experimental test data. Panels for this study were identical to test panels used by Taner [36]. The effects of location of loading, the amount and details of web reinforcements were studied.

A finite element model, developed at Concordia University [36], with slight modifications, was used to obtain the stress patterns and load-deflection characteristics in the panels. A brief description of the finite element model

is given in Chapter IV.

3.3.2 Description of Test Panels

. The panels were 44" x 89" with a perimeter rib 6"
thick and web wall thickness of 1.5". The rib was provided
to accommodate the reinforcing bars and to impart lateral
rigidity to the panel. The main longitudinal reinforcement in
the bottom rib and web reinforcement varied in the panel but
the reinforcement in the vertical and top rib consisted of
2 #3 and was constant for all the panels. An additional
vertical reinforcement in the form of a "suspender" or
hanger bar was also provided for those panels where the load
was applied below the compression face. Typical panel details
are shown in Fig. 3.1 and details of the panel reinforcing
are given in Table 3.1.

All the panels were simply supported at their under-
side by means of 10" x 6" bearing blocks. A single concen-
trated load was applied either at the top face, mid-depth,
or at the bottom face of the panel. The ratio a/d was less
than 1.

The main variables were the amount of tensile flexur-
al steel and the web reinforcement. The notation "Panel ijk"
used for the panels, identified these variables:

"i" denotes location of the load:

    1 - load at compression face

    2 - load at mid-depth of panel

    3 - load at tension face

"j" denotes the amount of flexural tensile steel:

    1 - 2 #3 bars

    2 - 2 #4 bars

    3 - 2 #10 bars

"k" denotes type of web reinforcement:

    1 - welded wire mesh 6 x 6/6-6

    2 - welded wire mesh 6 x 6/4-4

    3 - welded wire mesh 4 x 4/4-4

    3A- as 3 plus 4 #4 hanger bars

The tensile flexural steel was assumed welded to steel angles at the ends assuring a full anchorage of main tensile reinforcement.

3.3.3 Material Properties

3.3.3.1 Concrete

Normal weight concrete with 28 days compressive strength f_c' of 5,648 psi and tensile strength $f_t = 1.38(f_c')^{2/3}$

= 407 psi was adopted for all panels. These values are identical to the ones used in previous tests [36]. Modulus of Elasticity for concrete E_c was determined at 4.5562 x 10⁶ psi and Poisson's ratio was assumed at 0.17.

3.3.3.2 Reinforcing Steel

The following values for yield strength f_y was used for the model and were obtained from tensile tests conducted at Concordia University. [36]

Reinforcement Designation	f_y (psi)
Wire Gauge 6 and 4	78,506
#3 bar	60,088
#4 bar	57,500
#10 bar	50,000

Panel #	Longitudinal main tensile reinforcement	As sq.in	web reinforcement welded wire mesh		suspension reinforcement
			horizontal	vertical	
111*	2#3	0.22	6g @ 6"	6g @ 6"	
112*	2#3	0.22	4g @ 6"	4g @ 6"	
121*	2#4	0.4	6g @ 6"	6g @ 6"	
122*	2#4	0.4	4g @ 6"	4g @ 6"	
131*	2#10	2.54	6g @ 6"	6g @ 6"	
132*	2#10	2.54	4g @ 6"	4g @ 6"	
211	2#3	0.22	6g @ 6"	6g @ 6"	
212	2#3	0.22	4g @ 6"	4g @ 6"	
213	2#3	0.22	4g @ 4"	4g @ 4"	4#4 U-bars
221	2#4	0.4	6g @ 6"	6g @ 6"	
222	2#4	0.4	4g @ 6"	4g @ 6"	
223	2#4	0.4	4g @ 4"	4g @ 4"	4#4 U-bars
231	2#10	2.54	6g @ 6"	6g @ 6"	
232	2#10	2.54	4g @ 6"	4g @ 6"	
233	2#10	2.54	4g @ 4"	4g @ 4"	4#4 U-bars
311	2#3	0.22	6g @ 6"	6g @ 6"	
312	2#3	0.22	4g @ 6"	4g @ 6"	
313	2#3	0.22	4g @ 4"	4g @ 4"	4#4 U-bars
321	2#4	0.4	6g @ 6"	6g @ 6"	
322	2#4	0.4	4g @ 6"	4g @ 6"	
323	2#4	0.4	4g @ 4"	4g @ 4"	4#4 U-bars
331	2#10	2.54	6g @ 6"	6g @ 6"	
332	2#10	2.54	4g @ 6"	4g @ 6"	
333	2#10	2.54	4g @ 4"	4g @ 4"	4#4 U-bars

*Panels experimentally tested previously at Concordia (36)

TABLE 3.1 REINFORCEMENT DETAILS

DETAIL 'A'

welding

L-3½x2½x½

Tensile rebars.
Spacers ½" thick.

SECTION B-B

B

B

6"

44.0"

2¾" 2⅜" 2¾" 2¾"

SYMM.

2¾" 1¾" 2¾"
1¾"

44.5"

½"

2¾"

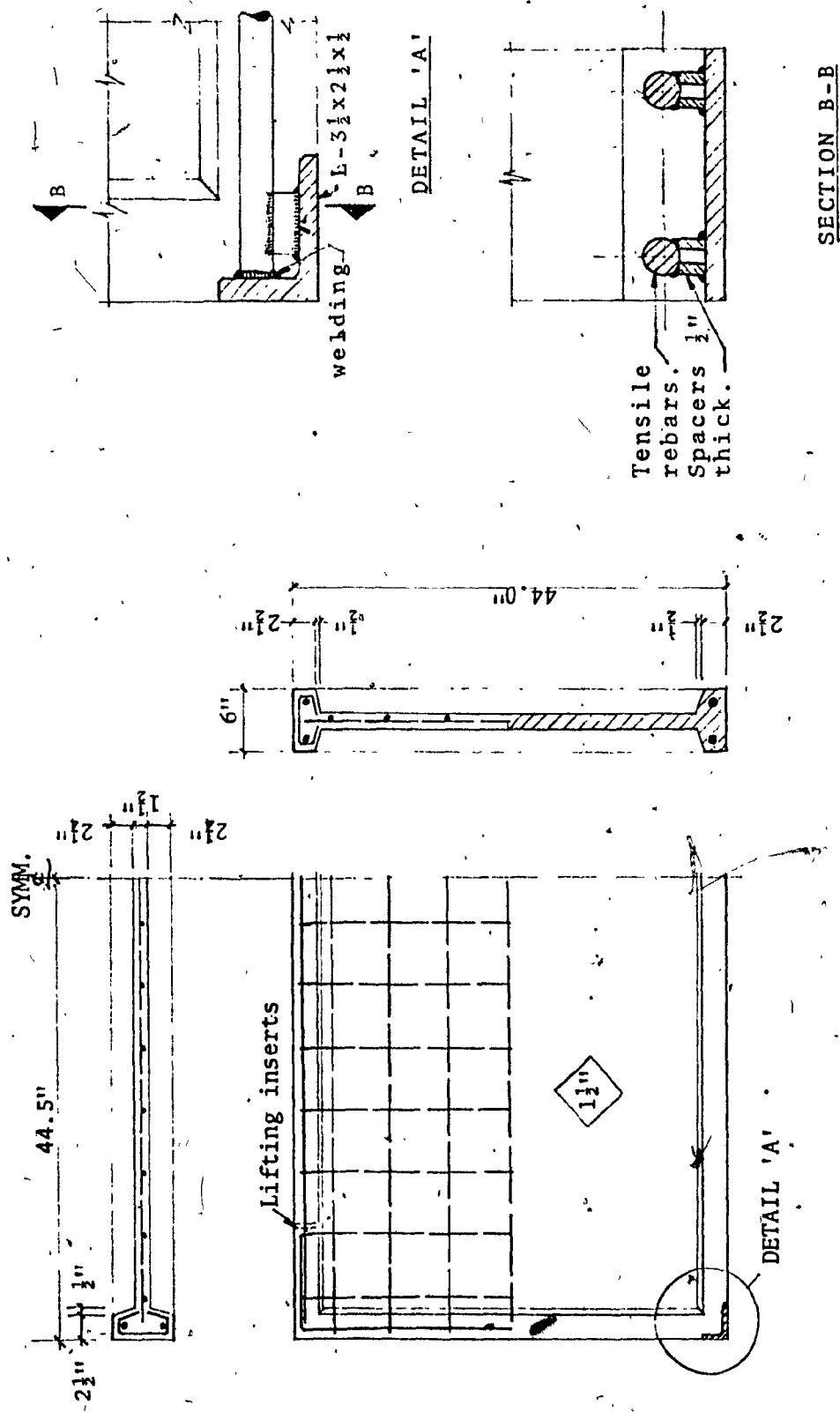Lifting inserts

1¾"

DETAIL 'A'

FIG. 3.1 TYPICAL WALL PANEL

CHAPTER IV

FINITE ELEMENT MODEL

CHAPTER IV

FINITE ELEMENT MODEL

4.1 INTRODUCTION

It becomes quite a complicated problem to determine displacements, deformations and internal stresses in a reinforced concrete member. The complications arise because:

(a) a member is composed of two materials - concrete and steel;

(b) constant changes in topology of the member due to cracking under increasing loads;

(c) non-linear stress-strain relationship of concrete and difficulty in obtaining constitutive relationship and failure criteria under combined stress state;

(d) difficulties in modelling bond between concrete and steel, dowel action, aggregate interlock and bond slip.

In fact, an analysis of a reinforced concrete member becomes a non-linear, inelastic analysis of a non-homogeneous anisotropic body, making it almost impossible to analyse principal stresses in concrete by means of continuum mechanics principles.

The finite element method provides an appropriate framework around which can be built the analytic capability of dealing with complexities.

4.2 HISTORICAL BACKGROUND

In 1967, Ngo and Scordelis [28] presented the first analytical model most commonly used for analysis of reinforced concrete beams. Bond links to interconnect steel and concrete were used. Nilson [29] extended this approach to include non-linear material properties and bond slip relationship. Mufti et al [26,27] included effects of tensile cracking by a "variable stiffness" procedure.

Valliapan and Nath [39] investigated an alternative approach to the effects of tensile cracking using an "initial stress" procedure. Steel is represented as beam element connected to the nodes of concrete finite elements and all bond slip is neglected. Valliapan and Doolan [38] incorporated the simple elasto-plastic behaviour of both the concrete and steel into the solution procedure. Cervenka [4] used a constant strain finite element to analyze reinforced concrete wall panels subject to monotonically increasing and cyclic loads with reinforcement in two orthogonal directions. Yuzugullu and Schnobrich [40] used quadrilateral elements composed of four constant strain triangles to represent wall-frame systems. A constant shear retention factor was introduced to simulate aggregate interlock and dowel action.

Franklin [12] developed a non-linear analysis which accounted automatically for cracking with infinite elements and redistribution of stresses into the system. This made possible one continuous computer analysis in tracing the response of two-dimensional systems from their initial loading to failure.

4.3 CONCORDIA FINITE ELEMENT MODEL AND PRESENT STUDY

4.3.1 General Description

A quadratic edge displacement isoparametric rectangle, as shown in Fig. 4.1, is used for the finite element study. This particular element produces exact results in flexure, and does not have the shape and loading limitations of the linear edge displacement isoparametric rectangle with incompatible modes. The element is curvilinear with 4 corner and 4 mid-side nodes. The element is shown in Fig. 4.1.a. The model is restricted to short-term static loading and effects of creep, shrinkage of concrete and bond slip are not included. A detailed description of the model, idealization of materials and formulation is given in reference [36].

4.3.2 Modelling of the Test Panels

A medium finite element mesh was selected for the idealization of the panel. The panel was divided into 25 elements interconnected at 96 nodes, as shown in Fig. 4.2.

Since the panel and loadings were symmetrical, only half of the panel was considered and nodes on the centre-line of the panel and nodes on the support block were respectively restrained in a longitudinal and vertical direction.

4.3.2.1 Allocation of Body Forces

Physically, the result would be the same if body force is equally divided to all nodes, but in a finite element, the forces are not allocated to the nodes, according to common sense. In a quadratic element family, the equivalent nodal forces would not be equal, in fact, they would not all act in the same direction. Fig. 4.3 shows the allocation of a body force to the nodes in an element.

4.3.2.2 Modelling of Material Properties

The concrete, in its uncracked state, is assumed to behave as a linear elastic isotropic material. The uniaxial stress-strain relationship for concrete is shown in Fig. 4.4. The stresses are related to strains, according to Hooke's Law, as:

$$
\begin{Bmatrix} \sigma_x \\ \sigma_y \\ \tau_{xy} \end{Bmatrix} = \frac{E_c}{1-\nu^2} \begin{bmatrix} 1 & \nu & 0 \\ \nu & 1 & 0 \\ 0 & 0 & \frac{1-\nu}{2} \end{bmatrix} \begin{Bmatrix} \varepsilon_x \\ \varepsilon_y \\ \gamma_{xy} \end{Bmatrix} \tag{4.4}
$$

or

$$\{\sigma\} = [D]\{\epsilon\}$$

When one of the principal stresses exceeds the tensile strength of concrete, cracks will occur in a direction perpendicular to that principal stress. Normal stress at cracks drops to zero. Since cracked concrete is capable of transferring shear stress along the crack, as shown in Fig. 4.5, the stress-strain relation in cracked elastic concrete becomes:

$$\begin{Bmatrix} \sigma'_x \\ \sigma'_y \\ \tau'_{xy} \end{Bmatrix} = \begin{bmatrix} E & 0 & 0 \\ 0 & 0 & 0 \\ 0 & 0 & \beta G \end{bmatrix} \begin{Bmatrix} \epsilon'_x \\ \epsilon'_y \\ \gamma'_{xy} \end{Bmatrix} \quad (4.2)$$

or

$$\{\sigma'\} = [D']\{\epsilon'\}$$

where

β = cracked concrete shear factor with upper and lower limits of 1 and 0, and

$$G = \frac{E_c}{2(1+\nu)}$$

If both the principal stresses exceed the tensile strength of the concrete, it will crack in both principal directions. Stress-strain relation can be written as

$$\begin{Bmatrix} \sigma'_x \\ \sigma'_y \\ \tau'_{xy} \end{Bmatrix} = \begin{bmatrix} 0 & 0 & 0 \\ 0 & 0 & 0 \\ 0 & 0 & \beta G \end{bmatrix} \begin{Bmatrix} \varepsilon'_x \\ \varepsilon'_y \\ \gamma'_{xy} \end{Bmatrix} \qquad (4.3)$$

Above are the constitutive relations in local coordinates and can be transformed to general coordinates using the following transformations.

$$\{\delta\} = [T]^T\{\sigma'\} \qquad (4.4a)$$

$$\{\varepsilon'\} = [T]\{\varepsilon\} \qquad (4.4b)$$

$$\{D\} = [T]^T[D'][T] \qquad (4.4c)$$

where

$$[T] = \begin{bmatrix} \cos\theta & \sin\theta & \sin\theta\cos\theta \\ \sin^2\theta & \cos^2\theta & -\sin\theta\cos\theta \\ -2\sin\theta\cos\theta & 2\sin\theta\cos\theta & \cos^2\theta-\sin^2\theta \end{bmatrix}$$

when θ is the angle between the x-axis and the crack direction measured counter-clockwise.

4.3.2.3 Plasticity and Failure Criteria of Concrete

The assumed yield criteria for plain concrete in a biaxial state of stresses was proposed by Kupfer et al [21] and is shown in Fig. 4.6. Behaviour of concrete under uni-axial and biaxial stresses differ considerably. Concrete under biaxial compressive stress exhibits higher strength than the

uniaxial compressive strength, however, concrete subject to combined tensile and compressive stresses, reaches cracking limit earlier than concrete subject to uniaxial tensile strength.

The following relationships are used for Concordia Model, subject to biaxial stresses:

(a) Kupfer et al [21] for biaxial tension

$$\sigma_2 = f_t \qquad (4.5)$$

(b) Von Mises' yield criterion for biaxial compression

$$\sigma_1^2 + \sigma_2^2 - \sigma_1 \sigma_2 = (f_c')^2 \qquad (4.6)$$

(c) Kupfer et al for tension compression

$$\sigma_2 - \frac{0.8 f_t}{f_c'} \sigma_1 = f_t \qquad (4.7)$$

Concrete is assumed crushed when it reaches the limiting compression strain $\varepsilon_{\ell c}$. In uncracked concrete subject to biaxial compression, crushing occurs approximately when ε_{eq} reaches $\varepsilon_{\ell c}$, where

$$\varepsilon_{eq} = (\varepsilon_x^2 + \varepsilon_y^2 - \varepsilon_x \varepsilon_y + 1.5 \gamma_{xy}^2)^{\frac{1}{2}} \qquad (4.8)$$

Cracked concrete in tension is assumed to crack again in a direction perpendicular to the first crack. Both the crushed concrete and concrete with ■ cracks are unable to carry any further load and the stress-strain matrix [D] becomes zero.

4.3.2.4 Plasticity and Yielding of Steel

Reinforcing steel is assumed to be elastic,perfect plastic in both compression and tension, as shown in Fig. 4.7. Yielding of steel occurs when σ_s reaches f_y. Prior to yielding the stress-strain matrix is:

$$[D'] = \begin{bmatrix} \rho E_s & 0 & 0 \\ 0 & 0 & 0 \\ 0 & 0 & 0 \end{bmatrix} \tag{4.9}$$

where

ρ = ratio of reinforcement volume to element volume.

Transformation is identical to that of cracked concrete, as in Equations (4.4c). At yield $E_s = 0$, therefore $[D] = 0$.

4.3.2.5 Composite Material

The reinforcement is assumed "smeared" over the concrete element and elasticity matrix of composite material $[D]_{comp}$ is the result of superposition of the concrete stress-

strain matrix and steel stress-strain matrix. Therefore:

$$[D]_{comp} = [D]_{concrete} + \Sigma[D]_{steel} \qquad (4.10)$$

Idealization of concrete-reinforcement composite is shown in Fig. 4.8.
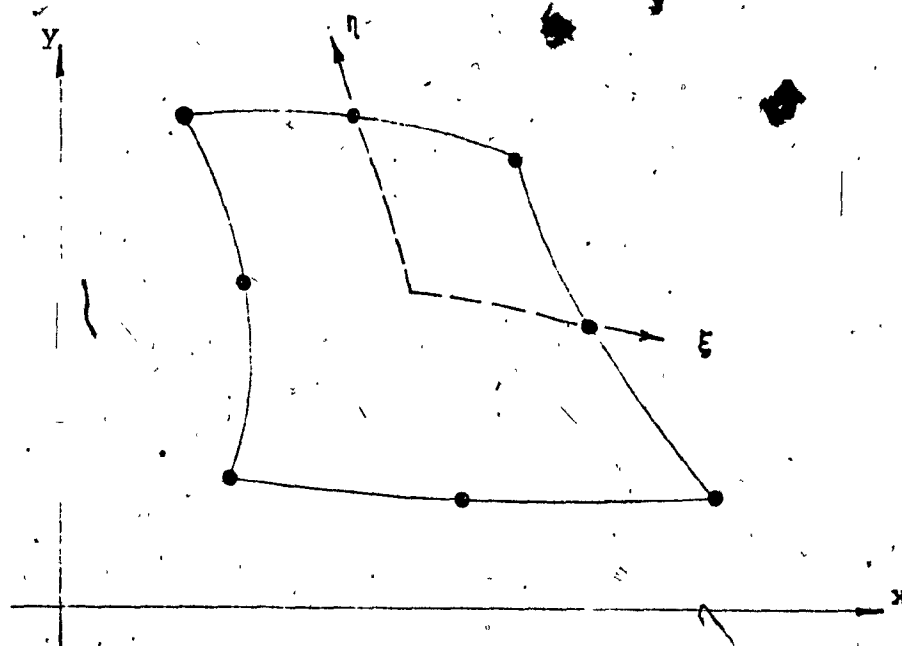
(a) In General Coordinates

+ Integration Points
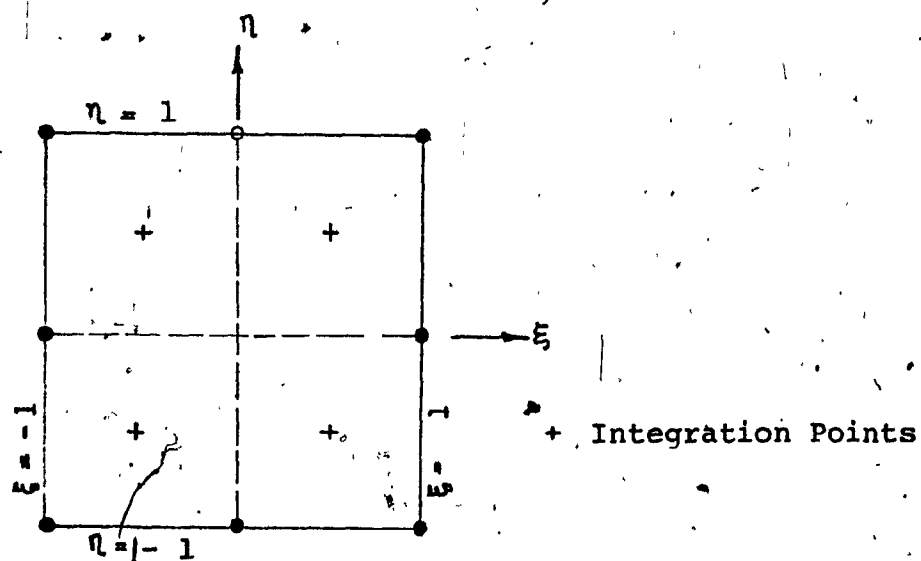
(b) In Normalized, Local Coordinates

FIG. 4.1 A QUADRATIC EDGE DISPLACEMENT
ISOPARAMETRIC RECTANGLE
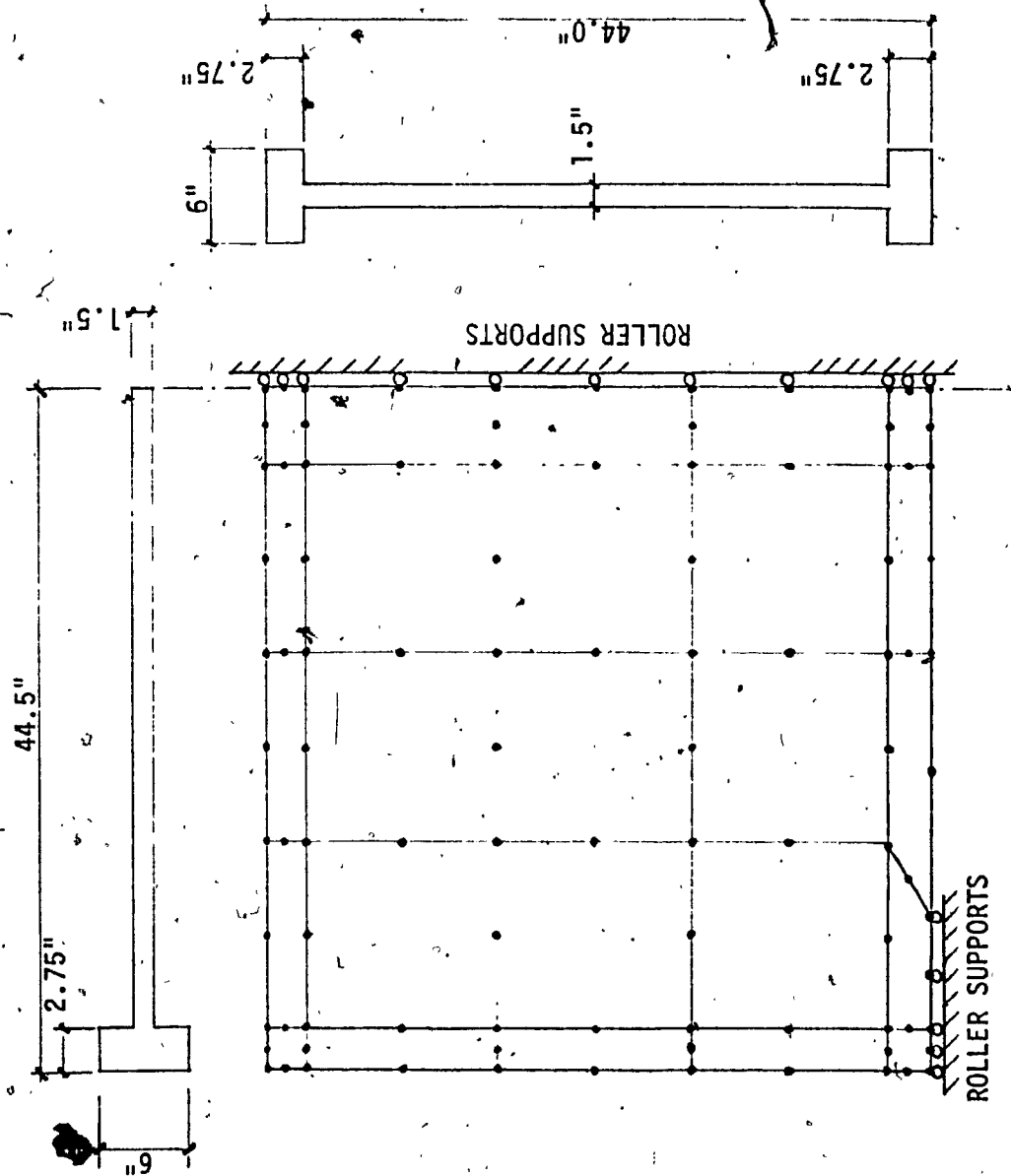
FIG. 4.2 FINITE ELEMENT MESH USED FOR ANALYSIS
(25 ELEMENTS; 96 NODES)

$-\dfrac{1}{12}$ $\dfrac{1}{3}$ $-\dfrac{1}{12}$

$\dfrac{1}{3}$ P $\dfrac{1}{3}$

$-\dfrac{1}{12}$ $\dfrac{1}{3}$ $-\dfrac{1}{12}$
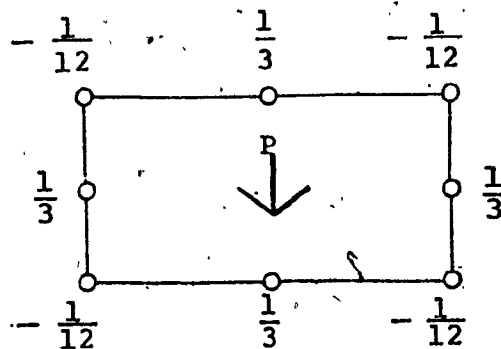
FIG. 4.3   ALLOCATION OF A UNIFORM BODY FORCE
TO NODES-- RECTANGULAR ELEMENT FAMILY
(Fractions of total weight shown)
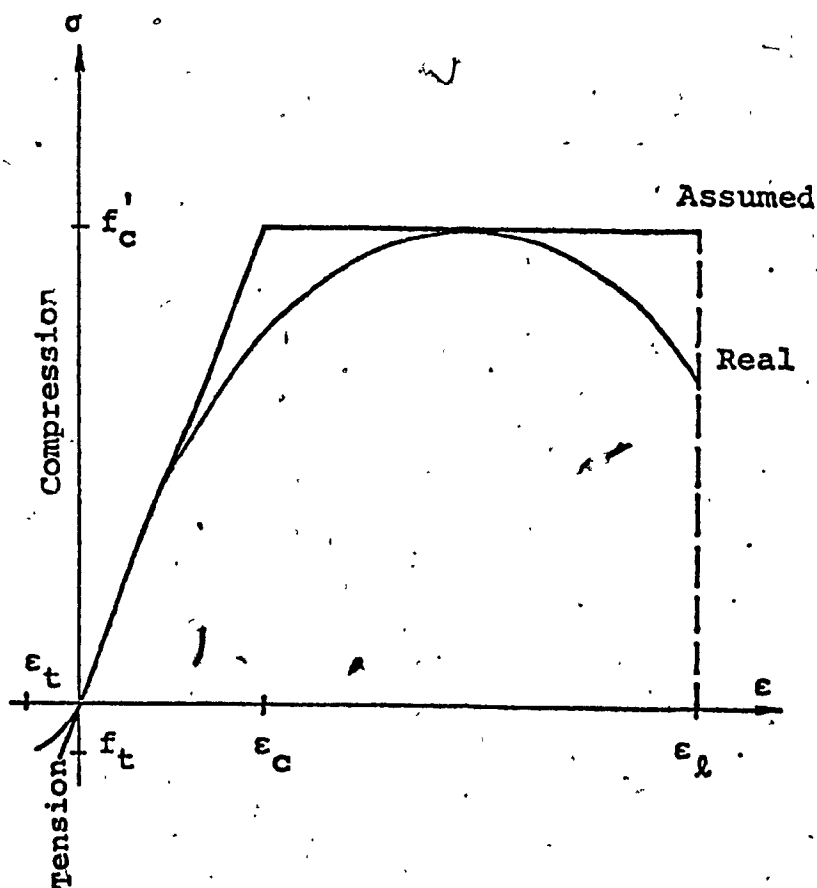
FIG. 4.4   UNIAXIAL STRESS-STRAIN RELATIONSHIP
FOR CONCRETE
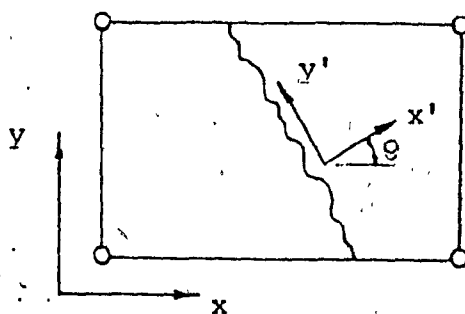
FIG. 4.5 SHEAR TRANSFER MECHANISM OF
CRACKED CONCRETE ELEMENT

—————— Kupfer et al

—·——·—— Liu et al

—··——··— Van Mises

— — — — Suwalski and Zalewski
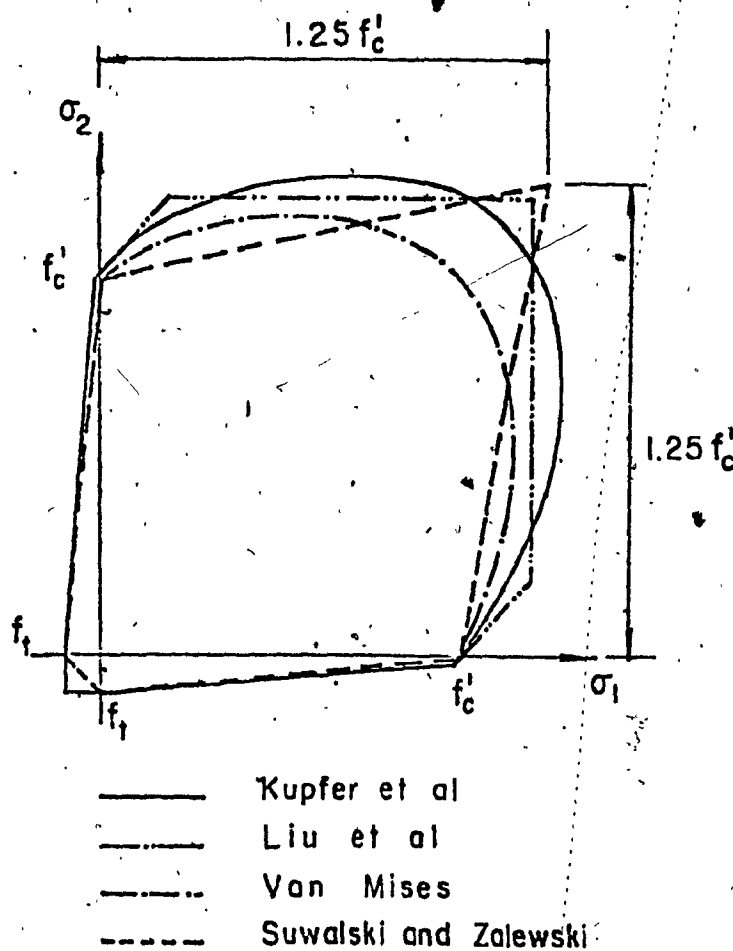
FIG. 4.6 BIAXIAL STATE OF STRESSES IN
PLAIN CONCRETE
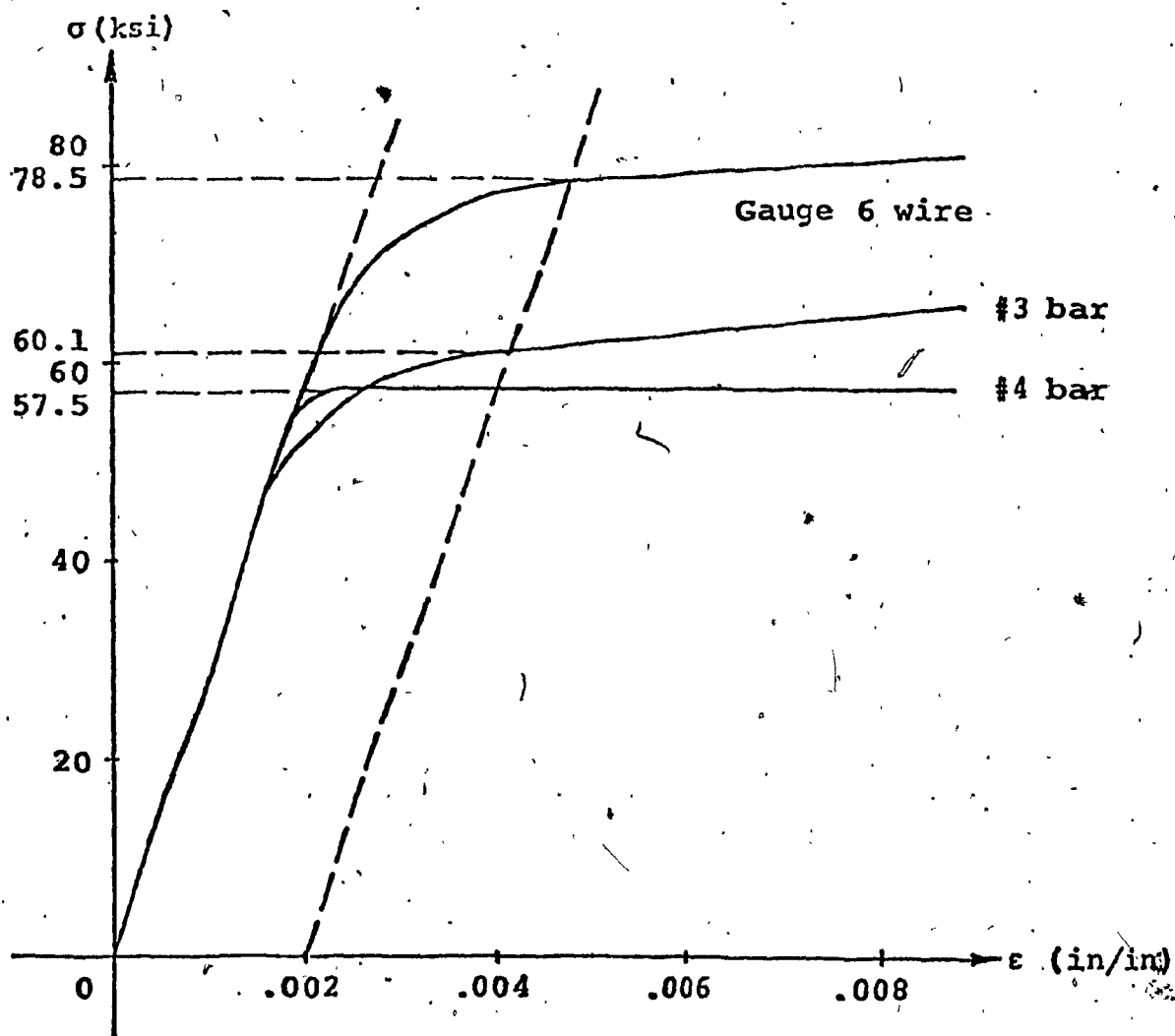
FIG. 4.7 STRESS-STRAIN RELATIONSHIP FOR
REINFORCEMENT
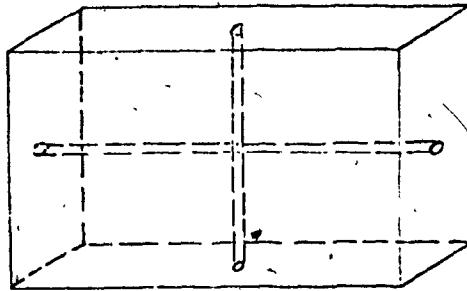
Uncracked – Real
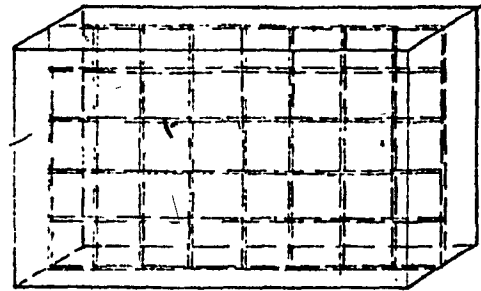
Uncracked – Assumed
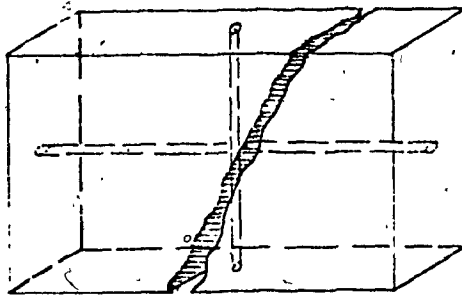
Cracked – Real
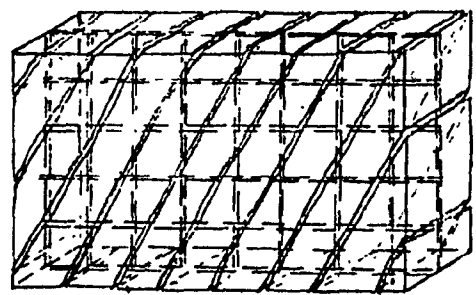
Cracked – Assumed

FIG. 4.8   IDEALIZATION OF THE CONCRETE-
REINFORCEMENT COMPOSITE

CHAPTER V

DESCRIPTION OF THE RESULTS OF INDIVIDUAL PANELS - SPECIFIC OBSERVATIONS FINITE ELEMENT METHOD

CHAPTER V

DESCRIPTION OF THE RESULTS OF INDIVIDUAL
PANELS - SPECIFIC OBSERVATIONS
FINITE ELEMENT METHOD

5.1   LOADING TYPE I - PANELS LOADED AT TOP FACE WITH ONE CONCENTRATED LOAD AT MID-SPAN

5.1.1   Panel 111 (Fig. 5.1)

The first vertical flexural cracks appeared after the elastic limit load of 24.4^k, and the cracks reached the top of the web at an increase in the load to 29.3^k. Most of the cracks were directly under the load and concentrated in the middle 1/4 of the span. Maximum stress in the main steel, at this stage was in the region of 45 ksi. Shear-flexural cracks were apparent at the next load increment to 35.2^k, when these cracks spread over most of the area below the line joining the load and the support and some of the previous cracks penetrated slightly into the top rib. Yielding of the main tensile reinforcing steel and that of the horizontal bars of the web reinforcement, near the bottom rib, started at a load of 50.6^k. Failure of the panel occurred at a load of 60^k by yielding of the reinforcing steel.

5.1.2   Panel 112 (Fig. 5.2)

After the elastic limit load of 24.4^k was increased to 25.1^k, the vertical flexure cracks appeared directly under the load and extended to 3/4 depth of the panel. The shear-flexural cracks did not appear intil a load of 28.3^k. These cracks

spread in most of the area below the line joining the load and the support. Diagonal-splitting cracks were indicated at 40.8^k. At a load of 57^k the main tensile and the horizontal web reinforcement yielded and failure of the panel was recognized. The stress in the main reinforcement at the cracking load was only 2.4 ksi and deflection was 0.005", while deflection before failure was 0.0755".

5.1.3 Panel 121 (Fig. 5.3)

The elastic limit load was reached at 23.7^k stressing the main tensile reinforcement to 2.25 ksi. At a load of 27.3^k, familiar patterns of the vertical flexure cracks appeared. The cracks spread over the middle third of the span, extending to the top of the web just below the top rib. At 31.4^k the shear-flexural cracks spread over the remaining area below the line joining the load and the support. Further propagation of the existing cracks and the new diagonal cracks were recorded at a load of 41.5^k. The panel failed at a load of 54.9^k when the yield occurred in the main tensile steel and in the web reinforcement, both vertical and horizontal bars. Some of the cracks also penetrated into the top rib.

5.1.4 Panel 122 (Fig. 5.4)

The cracking load for this panel was reached at 23.8^k and at a load of 27.3^k the flexural cracks extended up to 3/4 depth of the panel. At 36.2^k most of the shear-flexural cracks appeared in the usual manner and spread over most of the area

under the line joining the load and the support. No further
changes in cracking pattern occurred until a load of 55^k was
reached. When the cracks penetrated the top rib, the main
reinforcing in the bottom rib and the web reinforcement yielded.
Failure load was determined at 55^k. Deflection before failure
was 0.106" compared to a deflection of 0.0048" at the cracking
load.

5.1.5   Panel 131 (Fig. 5.5)

The elastic load limit reached at 19.3^k deflection at the
mid-span at this stage was 0.00362" and stress in the main
tensile reinforcement was only 1.3 ksi. Flexural cracking
appeared directly under the load in the bottom rib at a load of
22.2^k. The shear-flexural cracks did not appear until at a
load of 35^k. The existing cracks propagated and extended to
the top of the web. Maximum tensile stress in the bars in the
bottom rib, at this stage was 7.5 ksi. The panel failed at a
load of 99.3^k due to crushing of the concrete in the top rib
and part of the web below it. Maximum tensile stress in the
main bars in the bottom rib was only 24.7 ksi at failure.

5.1.6   Panel 132 (Fig. 5.6)

The first flexural cracks in the bottom rib, directly
under the load, appeared at a load of 19.3^k. At 29.3^k the
existing flexural cracks propagated to 1/4 of depth of the
panel. Shear cracks along with diagonal splitting cracks
appeared at 35.2^k and covered the usual area under the diagonal.

Further diagonal splitting cracks occurred at the incremental loads of 50.7^k and at 70.9^k. Failure occurred at 99.3^k due to crushing of the concrete in the web above the support and under the load.

5.2 LOADING TYPE II - PANELS LOADED AT MID-DEPTH WITH ONE CONCENTRATED LOAD AT MID-SPAN

5.2.1 Panel 211 (Fig. 5.7)

The elastic limit for this panel reached at a load of 20.6^k. At the next increment of load to 20.7^k most of the panel below the line joining the top centre-line of the panel to the bearing plate, was covered with cracks. Stress at this stage in the main tensile reinforcement was 31.6 ksi and deflection was only 0.0049 in. No further cracks appeared until the load of 39.1^k was reached when a second set of diagonal cracks, above the first set, appeared. The main tensile reinforcement and vertical bars of web reinforcement in the vicinity of load showed yield. The panel was considered failed at 40.2^k by yielding of the main tensile reinforcing.

5.2.2 Panel 212 (Fig.5.8)

The panel below the diagonal line was covered with flexural and diagonal cracks as soon as the load increased from elastic limit load of 20.6^k to 20.8^k. At 28.9^k further diagonal cracks appeared above the mid-depth of the panel. At 33.1^k the tensile reinforcement at the bottom showed a yield and at

39.2^k the vertical and horizontal web reinforcement yielded and the panel finally failed at a load of 41^k. Deflection before failure was 0.0658 in.

5.2.3 Panel 213 (Fig. 5.9)

The elastic load limit terminated at 20.2^k and with an increment of the load to 20.7^k, the flexural cracks appeared and extended to the top of the web. The cracks were concentrated within a strip equal in width to the load width. The cracks below the load were vertical while the cracks above inclined at a shallow angle towards the centre of the panel. The diagonal shear cracks appeared at 22.3^k and covered the middle 3/4 of the span and extended to the top of the web. A second set of diagonal shear cracks appeared outside the first set. Failure occurred in the panel at 50^k due to the yielding of the main tensile reinforcing in the bottom rib. There was no yielding present in the web reinforcing or in the suspender bars. The suspender reinforcing was stressed to 33 ksi indicating that it was carrying about 64% of the applied load and transmitting it to the compression zone.

5.2.4 Panel 221 (Fig. 5.10)

The cracking load was established at 20.1^k. The flexural cracks appeared above and below the load at 20.6^k. The cracks below the load were vertical in direction while the cracks above inclined sharply towards the centre of the panel. At 21.6^k the shear cracks spread over the entire area below the

line, joining the top of the load to the inside face of the support plate. Failure occurred at a load of 23.3^k when horizontal and vertical components of the web reinforcement yielded.

5.2.5 Panel 222 (Fig. 5.11)

The elastic limit terminated at a load of 20.1^k. At 20.6^k the flexural cracks appeared above and below the load in a manner similar to the panel 221. At 23.3^k most of the area below the diagonal line, joining the load to the support, was covered with the shear cracks inclining towards the load. First set of the diagonal shear cracks appeared out of the diagonal line at a load of 29.3^k. Failure of the member was determined at 35.2^k due to yielding of the web reinforcing above the load.

5.2.6 Panel 223 (Fig. 5.12)

The elastic limit for this panel was determined as 19.6^k. At 20.1^k the vertical flexural cracks appeared below the load and the cracks above the load were inclined at a shallow angle towards the centre of the panel. The diagonal shear cracks appeared at 26.3^k and covered most of the area below the diagonal line and extended to the top of the web. At 31.8^k diagonal splitting cracks appeared indicating tied arch action. Further diagonal splitting cracks appeared until the load of 56.3^k. A further increase in load induced the failure of the panel due to yielding of main reinforcing, web reinforcing and the suspender bars.

5.2.7 Panel 231 (Fig. 5.13)

The elastic action terminated at a load of 16.4^k and stress in main tensile reinforcing was only 1.3 ksi. At 21.8^k, vertical cracks appeared in the bottom rib under the load. When the load was increased to 35^k, the existing cracks propagated to the underside of the load and new diagonal cracks appeared and covered the area below the diagonal line. Additional shear cracks followed outside the existing cracks at a load of 46.3^k and at 53.3^k. The web reinforcement above the load yielded with a further increase in load and the failure load for this panel was determined at 61.3^k.

5.2.8 Panel 232 (Fig. 5.14)

The flexural cracks appeared in the bottom rib at a location directly under the load at a load of 16.4^k. Stress in the main tensile reinforcement, at this stage, had a nominal value of 1.31 ksi. The diagonal shear cracks, in a similar pattern as that of panel 231, under the diagonal line appeared at 28.9^k and were followed by the additional cracks outside the previous diagonal cracks at the loads of 40.3^k and 61.3^k. The vertical bars of web reinforcement yielded, above the load, at a load of 70.5^k. This was considered to be the failure load for the panel.

5.2.9 Panel 233 (Fig. 5.15)

The elastic limit load was established at 16^k. At a load of 25.9^k, the flexural cracks propagated from the "bottom rib under the load" pattern to the top of the web. The cracks also extended for a short distance above the bottom rib to the support. The diagonal shear cracks appeared at 28.4^k. A second and third set of diagonal splitting cracks were indicated at 45.8^k and 73.8^k, respectively. These cracks appeared above the existing diagonal cracks. The failure in the panel occurred at a load of 98.2^k when the concrete crushed in the web in the region of the supported. The stress in the suspender bars was 39.5 ksi and in the main tensile reinforcing in the bottom rib was 22.7 ksi.

5.3 LOADING TYPE III - PANELS LOADED AT BOTTOM FACE WITH ONE CONCENTRATED LOAD AT MID-SPAN

5.3.1 Panel 311 (Fig. 5.16)

The elastic limit for the panel was recorded at load of 8.9^k. At this stage the deflection at midspan was 0.00315" and the main tensile steel was stressed to 1.9 ksi. At 9.8^k, the cracks spread over an area 1/2 the span by 1/3 depth of the panel. The cracks in the bottom rib were only under the load and the remaining cracks were in the web. The vertical bars of the web reinforcing showed yielding at this load, above the load. At 10.7^k load, the failure occurred by yielding of the main tensile reinforcement and the web reinforcing.

5.3.2 Panel 312 (Fig. 5.17)

The elastic limit was set at a load of 8.9^k. At a load of 9.8^k, the cracks developed in an area 1/3 the span by 1/2 the depth of the panel. The vertical component of the web reinforcing was showing yield above the load. The stress in the main reinforcing in the bottom rib, at this stage, was registered at 42.5 ksi. Further diagonal cracks appeared in the web at 11.8^k. The main reinforcing in the bottom rib and vertical web reinforcing on the side of the load were in near yield. The panel failed at a load of 13^k.

5.3.3 Panel 313 (Fig. 5.18)

The elastic load for this panel was established at 8.25^k. At 11^k, the cracks appeared in the immediate vicinity of the load which covered an area middle 1/4 span by 1/4 depth of the panel. More cracks, directly above the load, appeared at a load of 12.1^k. These cracks above the load inclined downward indicating tension cracks due to hanger bars transmitting load to the compression zone. The diagonal shear cracks appeared at 19.4^k and extended almost to the top of the web. A second set of the diagonal shear cracks developed above the existing cracks at a load of 25.9^k and extended into the vertical rib at the support. At 34.4^k, the main tensile bars in the bottom .

rib showed yielding and failure due to yielding of tensile
bars occurred at 37.9^k. The stress in the suspender bars was
41.6 ksi and the load carried by these bars was 100% of the
applied load.

5.3.4 Panel 321 (Fig.5.19)

At a load of 9.2^k, the panel showed cracks in the
immediate vicinity of the load and vertical web reinforcement
was in yield above the load. The stress in the main reinforce-
ment had reached 36.1 ksi. At an increase in the load to 9.4^k,
further yielding of vertical web bars was evident. The panel
failed at a load of 10.4^k apparently in yielding of web rein-
forcing.

5.3.5 Panel 322 (Fig. 5.20)

The load-history of this panel was similar to panel 321
except that failure of the panel occurred at a load of 13^k.

5.3.6 Panel 323 (Fig. 5.21)

The cracking load for this panel was established at 8.3^k.
At 9.5^k some tension cracks appeared in the immediate vicinity
of the load. The cracks which had normally developed in the
bottom rib did not appear at this stage, indicating a very low
stress in the main tensile reinforcement. The flexural cracks
appeared at 12.6^k in the bottom rib and more tension cracks
developed above the load. Further diagonal cracks covered an

area, 1/2 the span by 1/2 the depth of the panel, at a load of 16.7^k. A first set of diagonal shear cracks appeared at 21.6^k. The stresses in the main tensile reinforcement and in the suspender bars, at this stage, were 28 ksi and 23.8 ksi, respectively. There was yielding of horizontal web reinforcing at the centre and 1/2 way up the panel. At a load of 23.8^k, all the applied load was carried by the suspender bars and was transmitted to the compression zone at the top of the panel. A second set of the diagonal shear cracks developed above the first set at a load of 28.8^k and extended to the top of the web and to the vertical rib over the support. The panel failed at a load of 31.6^k.

5.3.7 Panel 331 (Fig. 5.22)

The elastic limit load was determined at 8.6^k and maximum stress in main longitudinal steel and vertical web bars was only 1308 and 2058 psi respectively. First cracks appeared at 9.5^k over and on the side of the load location. The vertical web reinforcement immediately above the load yielded when the load increased to 12.6^k. The panel failed at a load of 13.9^k by yielding of web reinforcement.

5.3.8 Panel 332 (Fig. 5.23)

The elastic limit was established at 8.6^k and the stress in the main tensile steel and web reinforcement at this stage was identical to that of panel 331. At 9.5^k cracks appeared in the immediate vicinity of the load and increased in number

at 18.5^k and covered most of the area below the diagonal line joining the load plate and reaction plate. At 15.3^k vertical web bars above the load showed yield and some crushing of web was evident. The panel continued to work until at a load of 24.4^k when panel failed in yielding of vertical web reinforcement.

5.3.9 Panel 333 (Fig. 5.24)

Elastic load was given at 8.6^k and cracks appeared in the vicinity of the load and generally inclined at an angle of 30° and nearly vertical above and below the location of load respectively. The cracks seemed to stabilize until the load reached 12.7^k and then increased in number at load of 16.9^k, upwards and towards the support. The cracks covered most of the area below the diagonal at 24.6^k. Some cracks also appeared above the support. Horizontal web bars above the load showed plasticity changes but panel continued to work. The stress in the hanger reinforcement and main bars was 44 ksi and 19 ksi respectively at this stage. The panel failure load was determined at 54 kips since at that stage the hanger reinforcement yielded and concrete crushed in the web at mid depth of the panel above the load.

Elastic limit 24403 lb
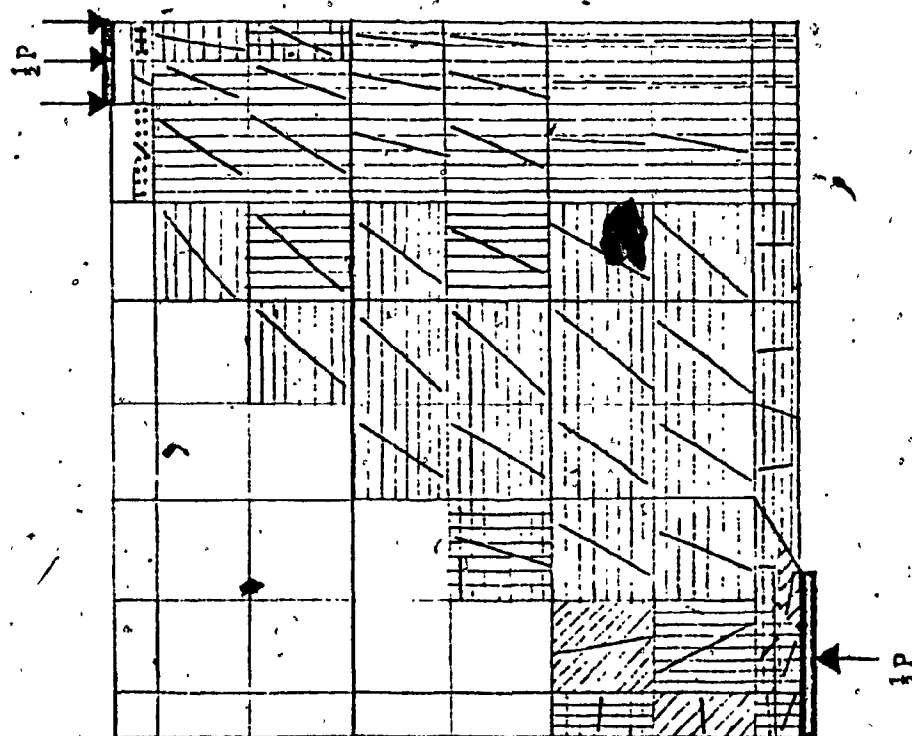
FIG. 5.1 ANALYTICAL CRACK PATTERNS - PANEL 111

57

Elastic limit 24444 lb.

57.1^k

40.8^k

28.3^k

25.1^k

$\frac{1}{2}$P

$\frac{1}{2}$P
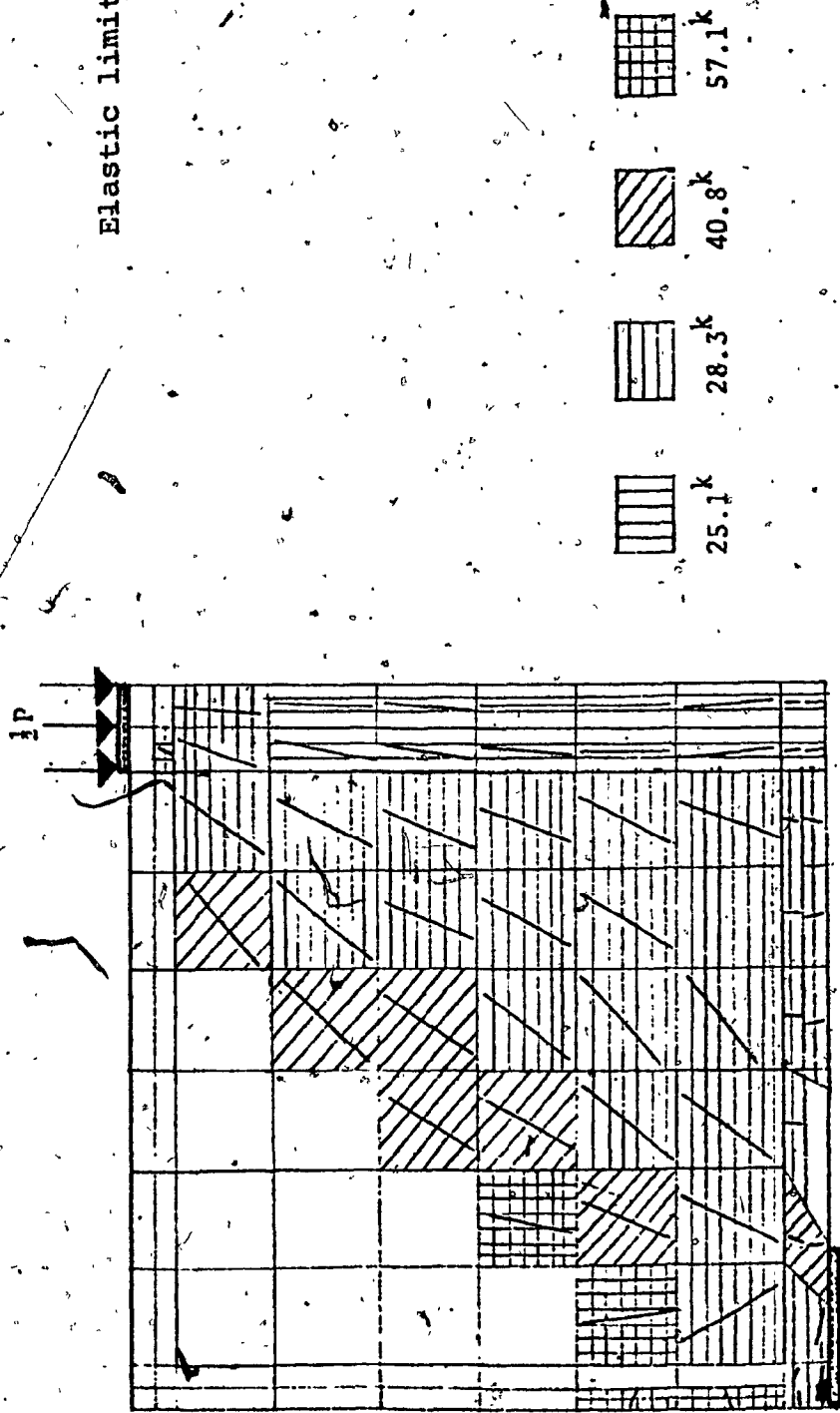
FIG. 5.2 ANALYTICAL CRACK PATTERNS - PANEL 112

Elastic limit 23740 lb.

47.8^k

41.5^k

36.1^k

31.4^k

27.3^k

54.9^k

$\frac{1}{2}$P

$\frac{1}{2}$P

FIG. 5.3 ANALYTICAL CRACK PATTERNS - PANEL 121

Elastic limit 23778 lb

27.3^k 36.2^k 55.0^k

$\frac{1}{2}$P

$\frac{1}{2}$P'
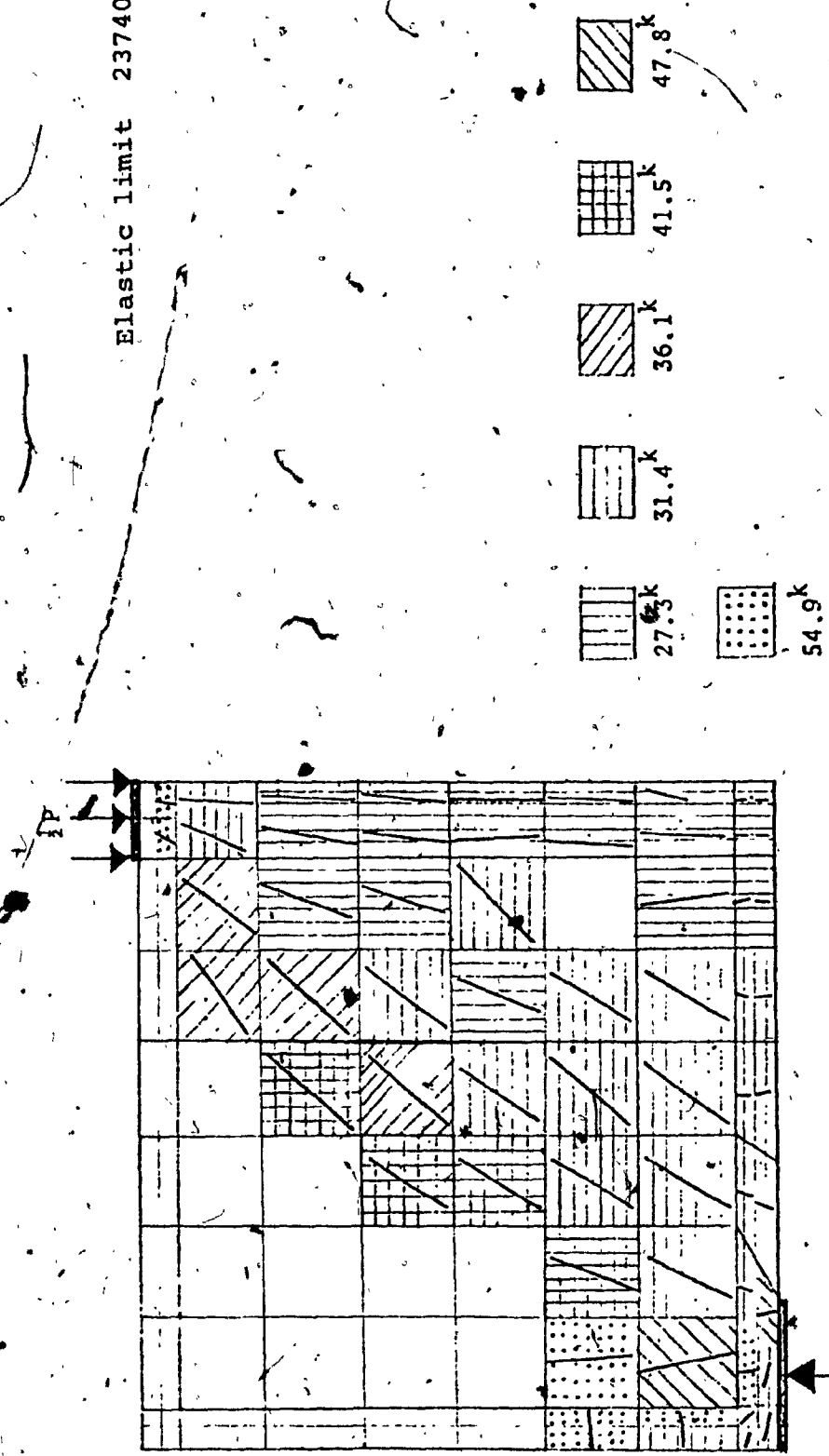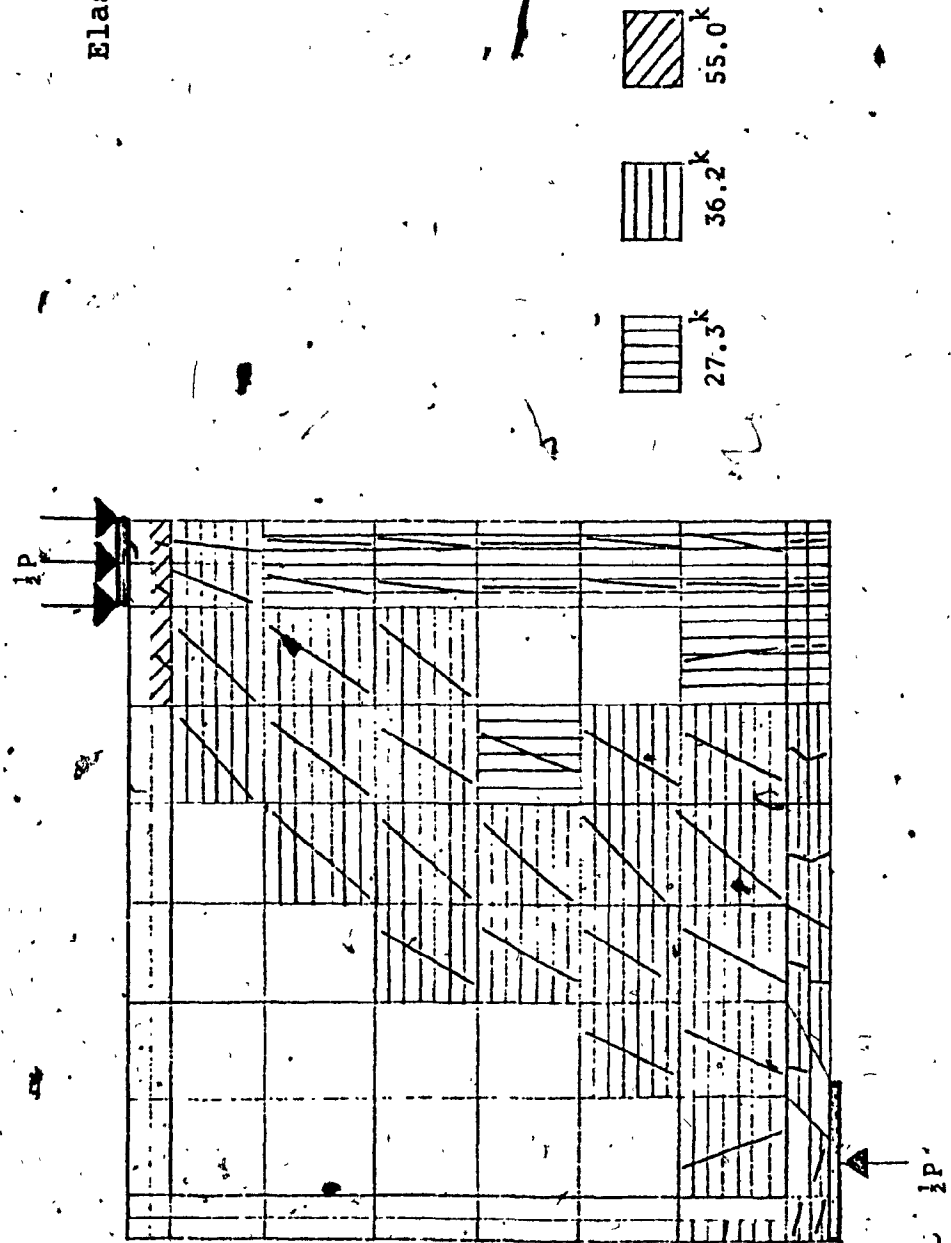
FIG. 5.4 ANALYTICAL CRACK PATTERNS - PANEL 122

Elastic limit 19273 lb.

50.7^k

42.2^k

35.2^k

29.3^k 99.3^k

22.2^k 70.9^k

1P

$\frac{1}{2}$P
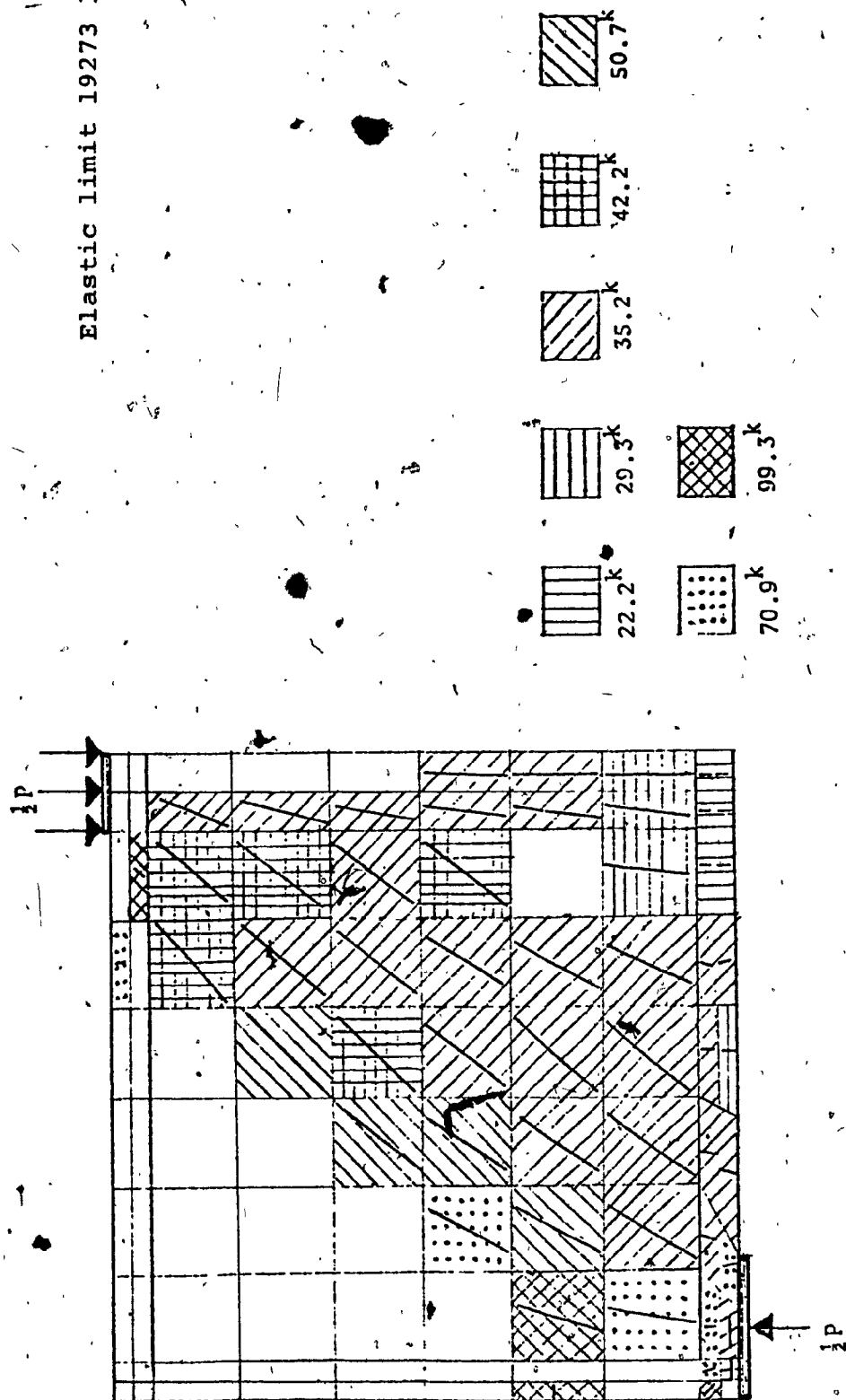
FIG. 5.5 ANALYTICAL CRACK PATTERNS - PANEL 131

Elastic limit 19292 lb.

50.7^k

42.3^k

35.3^k

29.3^k 99.4^k

22.2^k 71.0^k
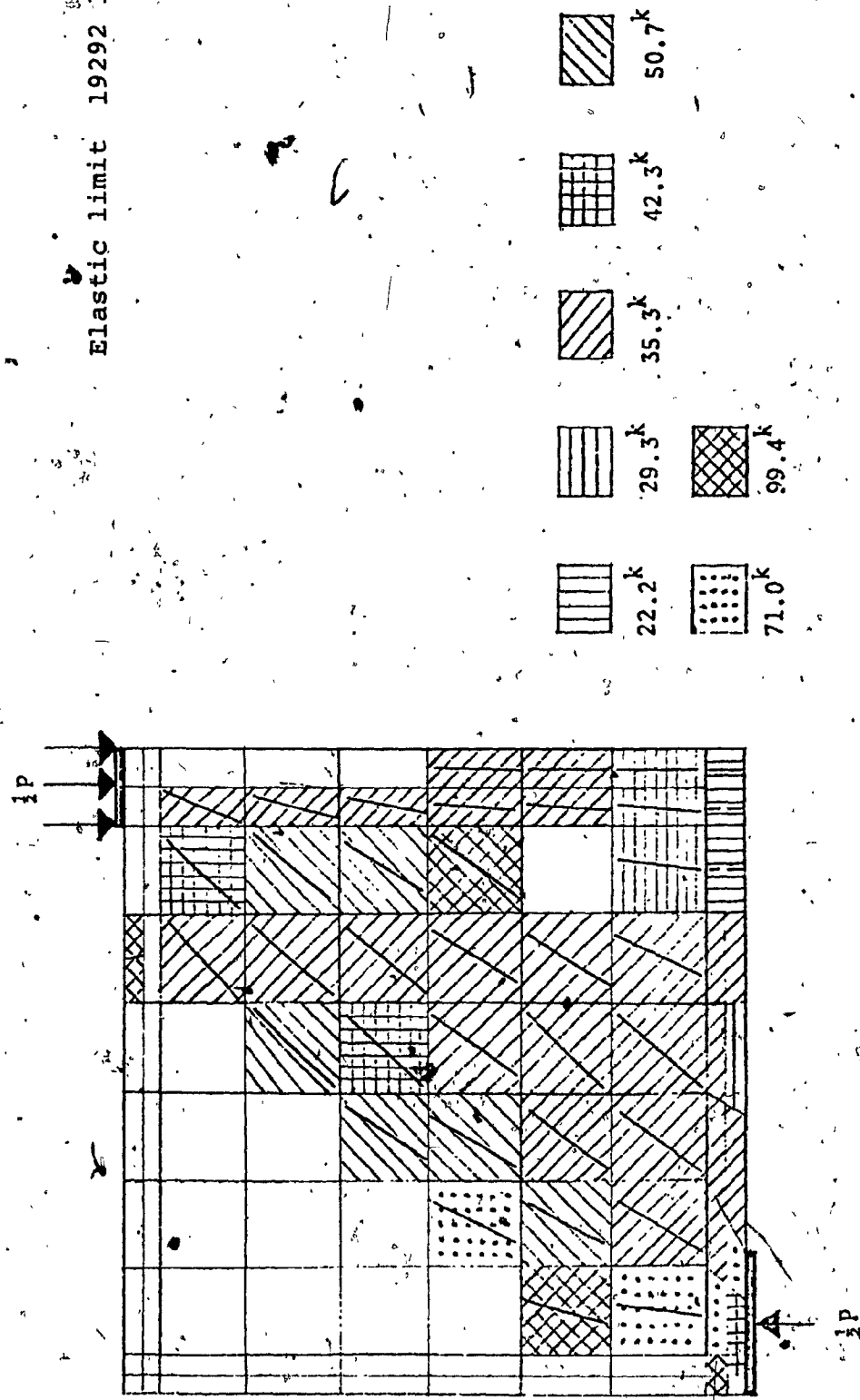
FIG. 5.6 ANALYTICAL CRACK PATTERNS – PANEL 132

Elasic limit 20601 lb.
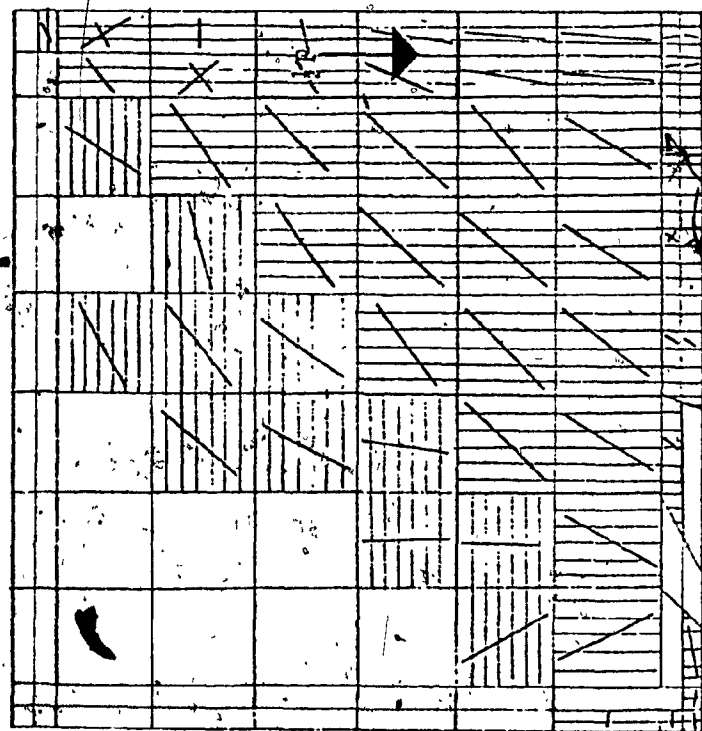
39.1

20.7

FIG. 5.7. ANALYTICAL CRACK PATTERNS - PANEL 211.

$\frac{1}{2}$P.

Elastic limit 20635 lb.

| | 20.8 | | 28.7 | | 33.0 | | 39.2 | | 41.0 |
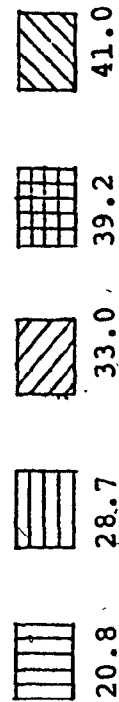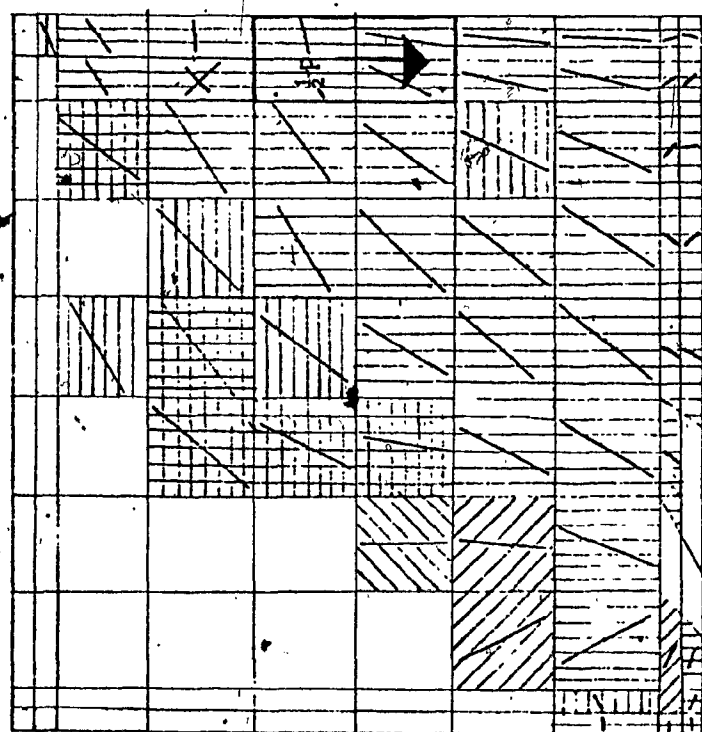
FIG. 5.8 ANALYTICAL CRACK PATTERNS - PANEL 212

Elastic limit 20150, lb.

32.6^k

26.7^k

22.3^k

21.7^k

20.6^k

43.4^k

$\frac{1}{2}P$
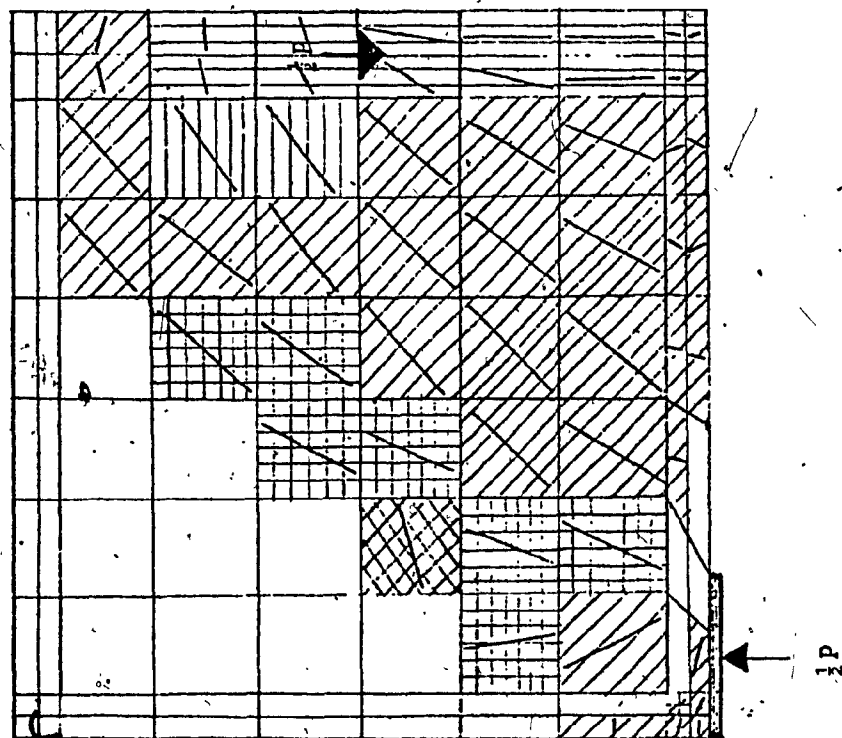
FIG. 5.9 ANALYTICAL CRACK PATTERNS - PANEL 213

Elastic limit 20059 lb.

20.6^k 21.6^k 23.25^k

$\frac{1}{2}P$

$\frac{1}{2}P$
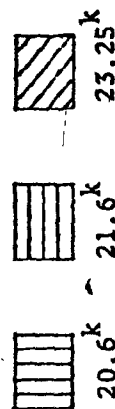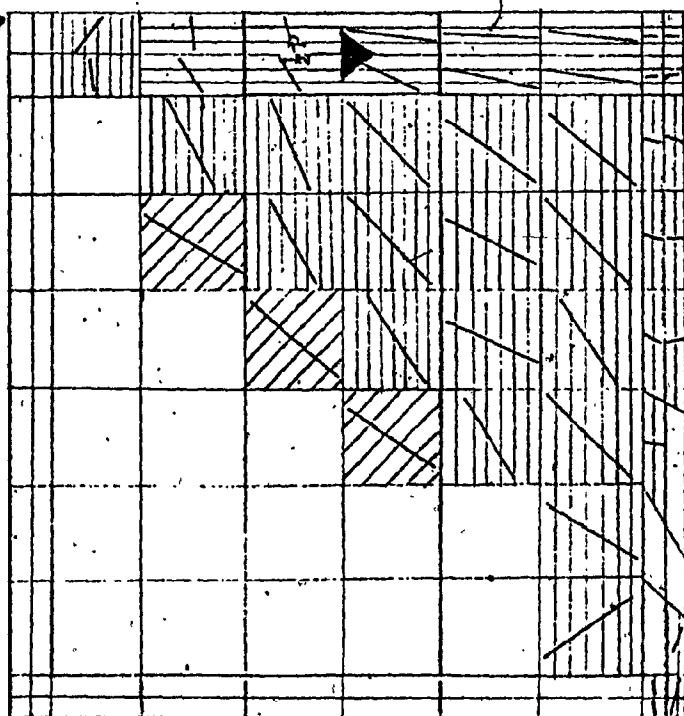
FIG. 5.10 ANALYTICAL CRACK PATTERNS - PANEL 221.

Elastic limit 20090 lb.
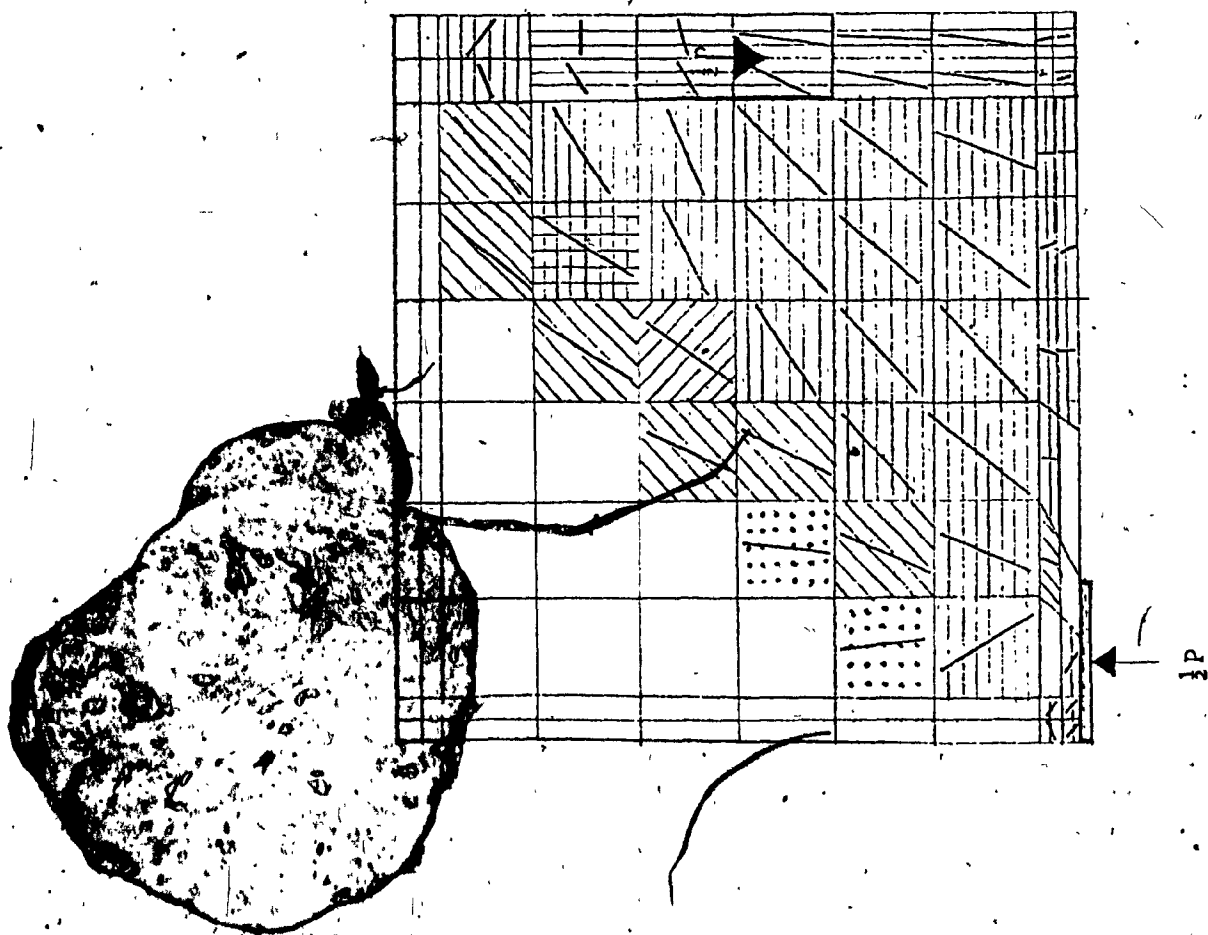
FIG. 5.11 ANALYTICAL CRACK PATTERNS - PANEL 222

Elastic limit 19611 lb

20.1^k 26.3^k 31.8^k 51.1^k
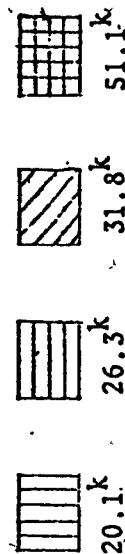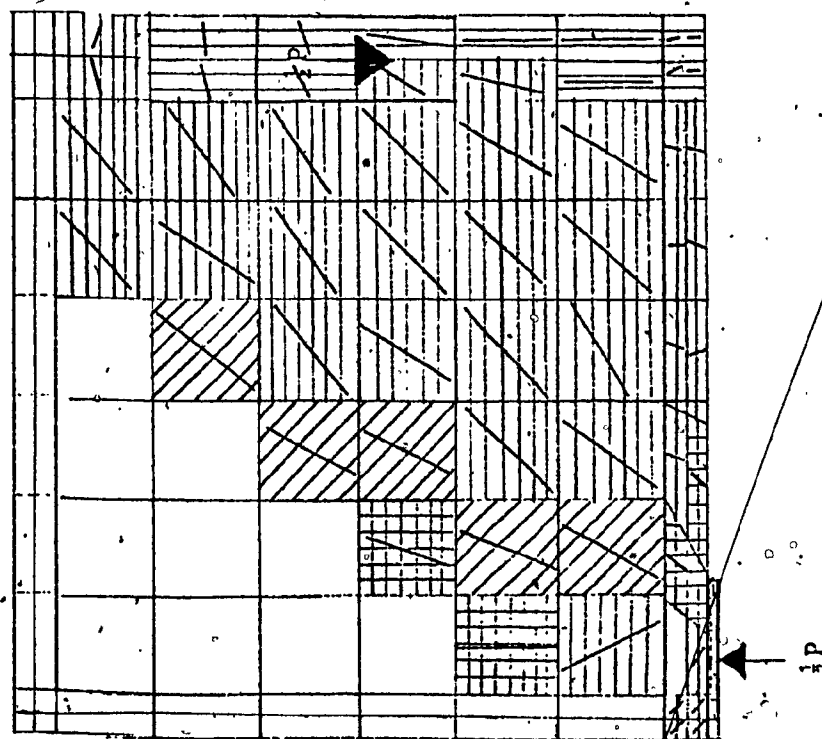
FIG. 5.12 ANALYTICAL CRACK PATTERNS - PANEL 223

Elastic limit 16348 lb.
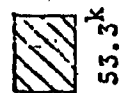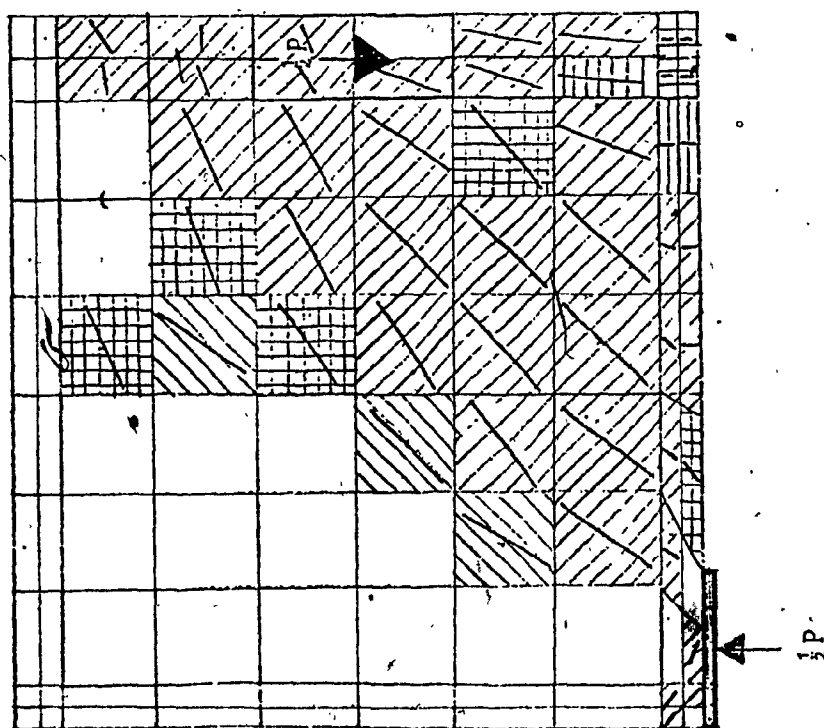
53.3^k	
46.3^k	
35.1^k	
23.9^k	
21.8^k	
61.3^k	

FIG. 5.13 ANALYTICAL CRACK PATTERNS - PANEL 231

Elastic limit 16363 lb.
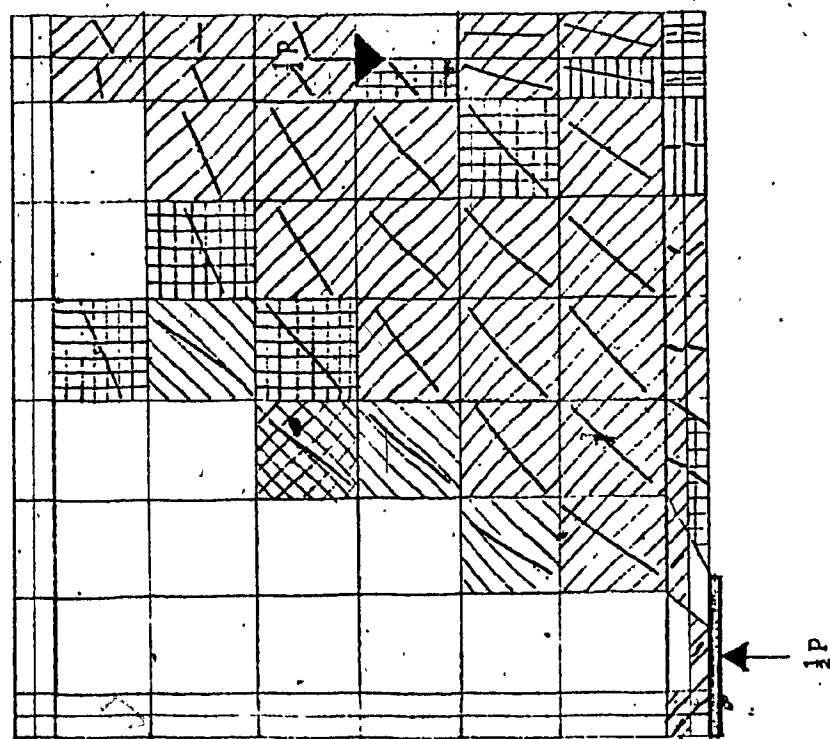
53.3^k 40.3^k 29.0^k 24.0^k

18.0^k 61.3^k

FIG. 5.14 ANALYTICAL CRACK PATTERNS - PANEL 232
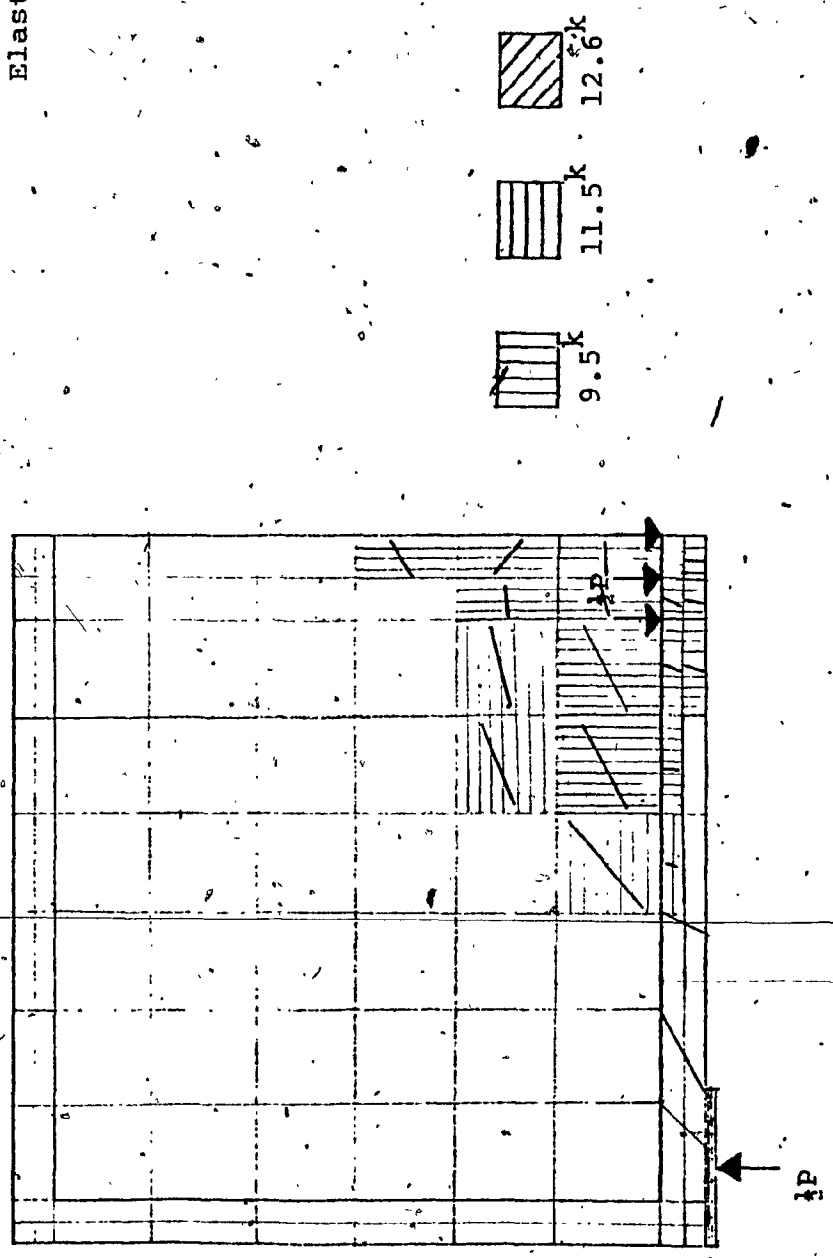
FIG. 5.22 : ANALYTICAL CRACK PATTERNS - PANEL 331

Elastic limit 8613 lb.

9.5 k

11.5 k

12.6 k

Elastic limit—8630 lb.
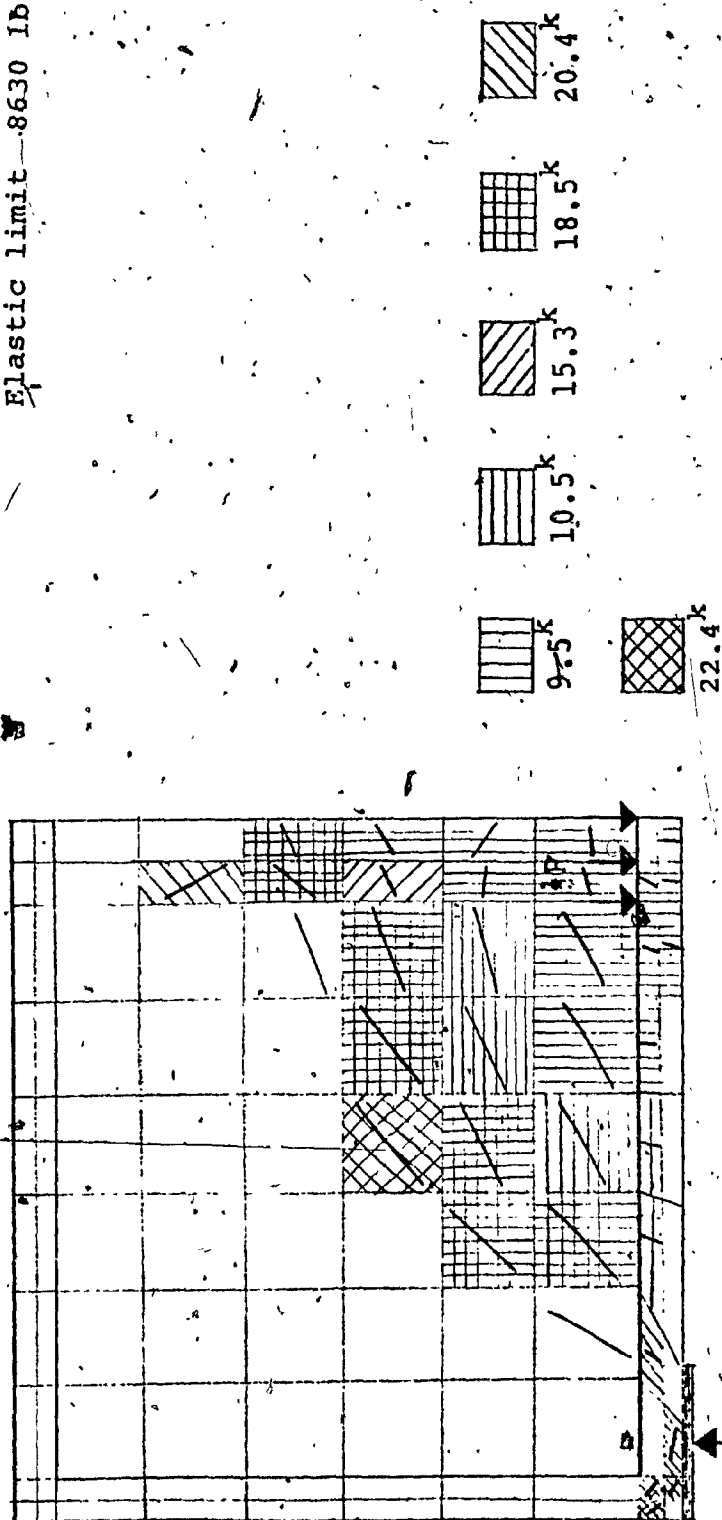
FIG. 5.23 ANALYTICAL CRACK PATTERNS — PANEL 332

Legend: 9.5^k, 10.5^k, 15.3^k, 18.5^k, 20.4^k, 22.4^k

1P

8.8^k 12.7^k 16.8^k 24.7^k 29.8^k 43.7^k

1P

½P
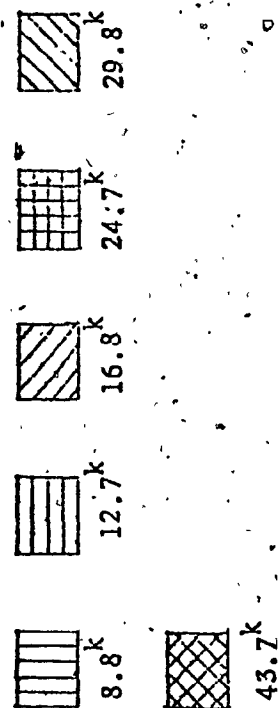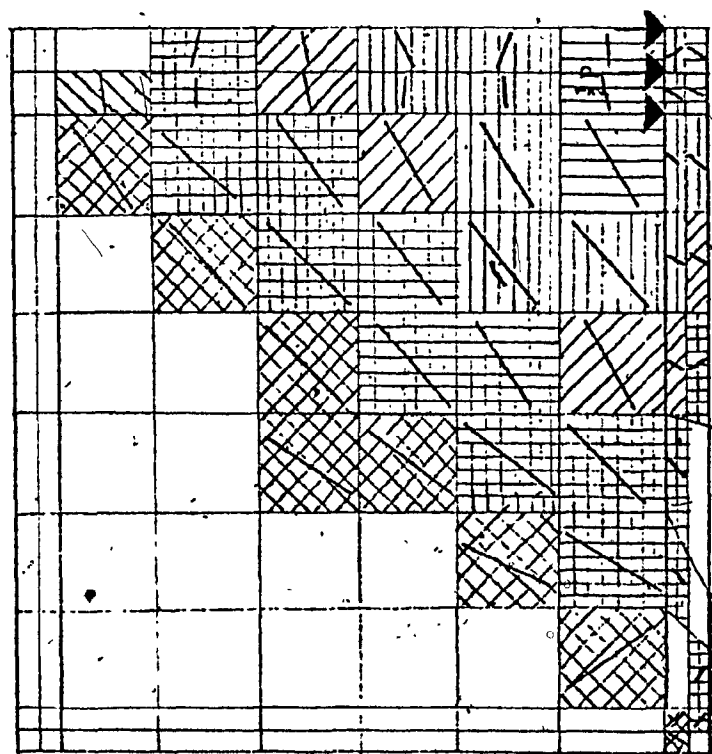
FIG. 5.24 ANALYTICAL CRACK PATTERNS - PANEL 333

CHAPTER VI

SUMMARY AND CONCLUSIONS

CHAPTER VI

SUMMARY AND CONCLUSIONS.

6.1 SUMMARY

The finite element concept, which permits the study of the behaviour of reinforced concrete elements through the entire range of loading, from zero load to failure, has been used as the basis for the investigation in this study. Reinforced concrete thin-wall ribbed panels, with $\frac{a}{d} \approx 1$, indirectly loaded with a single concentrated load at mid-depth (loading type II) and at tension face (loading type III) are analysed taking into account the non-homogeneity and non-linear material properties. No account, however, of the effects of torsion, buckling, shrinkage, creep, bond slip, etc., is taken in this study.

The accuracy of the model has already been established [36,37] during the research on top loaded panels. A small sacrifice, perhaps in exactness of the results, is made, in favour of economy in computer time, by using a medium mesh in modelling the beam panels. The model, however, presents a complete picture of the behaviour, stress distribution and crack propagation in the entire panel. The results are generally not obtained easily by other analytical and experimental methods.

The simulated crack patterns along with incremental loading are presented in Figures 5.1 through 5.24. For simplicity purposes crack direction is determined and drawn at the integration points and is assumed to be constant over that particular quarter of the element. Since the integration points are symmetrically located in the element, if a crack appears at the integration point, the whole element is assumed to be cracked. The crack direction is drawn to true angles and the flow of the stress trajectories can easily be visualized.

Load displacement curves and σ_x and σ_y curves are also presented in Appendix A and Appendix B respectively. These are also simulated from the results of the finite element model and can safely be regarded as representative of the actual behaviour of panels indirectly loaded.

6.2 CONCLUSIONS AND RECOMMENDATIONS

As discussed in Chapter III, the main objective of this study was to investigate the effects on the behaviour and strength of deep panels due to factors such as the location of the load, amount of longitudinal tensile reinforcement, contribution of web reinforcement and thin webs. Following are the conclusions, based on the influence of the above-mentioned factors on the behaviour and strength of the panels.

6.2.1   Effects of Location of Loading

Results show that the panels loaded below the compression zone, i.e., indirectly loaded, are weaker than the panels which were directly loaded at compression face under similar conditions, such as material properties and reinforcement. At the elastic load stage, the cracking load for panels loaded with Type II and Type III loading is 85% and 35% respectively, when compared to the panels loaded with Type I loading. The failure load for panels with Type II and Type III loading is 65% and 20%, respectively, of the load for panels with Type I loading. One of the reasons is that a full arch action cannot develop and panels tend to fail in diagonal tension at the inclined cracking load.

It is shown in this investigation that by means of providing adequate suspension or hanger reinforcement at the loaction of the load and anchoring it well in the compression zone, the load-carrying capacity of indirectly loaded beams can be increased significantly. It is strongly recommended that hanger reinforcement be provided to transfer 100% of the load. Hanger reinforcement is generally not required for indirectly loaded beams with $\frac{a}{d}$ ratios greater than 3 [3,11,22,23].

6.2.2 Effects of Amount of Longitudinal Reinforcement

It is quite evident from the results that a cracking load is larger for panels reinforced with smaller ratios of main longitudinal reinforcement. The flexural cracks appear sooner in members with greater ratios of tensile reinforcement, however, these cracks do not extend to greater depth in the panel.

Results also show that shear strength of panels drop significantly for under-reinforced panels. This agrees well with the findings of other researchers [16,30,33]. Equation (2.5) is developed based on the observed effects of ρw and $\frac{a}{d}$ ratios on the shear, and is now proposed· [15] as a replacement for ACI Equation 11-4.

CEB [7] recommends a reduction in the allowable shear stress if ρw is less than 1.5% at 2d from the support. The reason for this reduction is explained in two ways. First, by reducing ρ, the flexural cracks are wider and therefore extend higher into the panel reducing both the shear capacity of the compression zone and interface shear transfer V_a, and secondly the dowel shear V_d is smaller resulting in large deflection.

A tied arch action generally develops at about 40% to 50% of the ultimate load. This is evident from the results and it is of utmost importance to detail that the anchorage

of the main tensile steel at the supports. Anchorage must be designed to resist at least 80% of the tensile capacity of the bar.

6.2.3 Effects of Web Reinforcement

The web reinforcement plays a very little role in the behaviour of deep beams before cracking. At their elastic state, very small tensile stresses are recorded in the web reinforcement. Once the diagonal cracking occurs the web reinforcement shows a sudden increase in tensile stresses indicating a significant role in the redistribution of internal forces.

Web reinforcement has very little effect on the ultimate capacity of deep panels loaded on their compression face, i.e., directly loaded panels, and a small amount of orthogonal web reinforcement would be sufficient to ensure a gradual shear compression failure. ACI [2] provisions are adequate for all conditions in case of directly loaded panels and no serviceability problem should exist.

Results indicate that indirectly loaded beams show much more response to the gain of strength with increased ratio of web reinforcement. Increase in the horizontal web reinforcement seems to be more effective for $\frac{a}{d}$ ratio in this study. Hanger reinforcement at the location of a load, when properly detailed and well anchored in the compression zone, will increase the capacity of indirectly loaded panels

similar to directly loaded panels.

It is also evident from the results, that the presence of web reinforcement reduces the deflection in the panel. An increase in the ratio of web reinforcement results in a decrease in deflection. Generally, deflection does not present a serviceability problem in deep beams.

It is desirable that web reinforcement is closely spaced and when detailed in accordance with CEB [7] recommendations will provide adequate protection against wide cracks and deflection.

6.2.4   Effects of Thin Webs

In beams with thin webs, as is the case in study, shearing stresses in webs are larger than flexural stresses when compared to normal proportioned beams. Although no problem was indicated in our investigation, webs may crush due to inclined compressive stresses prior to yielding of stirrups. Tensile cracks may also begin in the webs due to principal tensile stresses associated with shearing stresses.

Diagonal compressive stresses thus shearing stresses in thin webs must be limited to a maximum of $0.2 f_c'$ in beams with vertical stirrups and $0.25 f_c'$ in beams with inclined stirrups at $45°$ [7]. Lapped U-shaped stirrups with laps equal to a class C splice, are preferable. Zsutty [47]

equation for shear cracking resistance of web is given below and is a good measure for predicting the strength of deep beams.

$$V_{cr} = [8(f'_c \frac{100 \times A_s}{b_w d})^{1/3} b_w d] \frac{a}{d} \qquad (6.1)$$

$$= [12(f'_c)^{1/3} b_w d] \frac{a}{d} \qquad (6.2)$$

6.3 OBSERVATIONS FROM σ_x AND σ_y CURVES

It becomes obvious from observing the σ_y curves in Appendix B, particularly in the case of indirectly loaded panels, the need of suspending the load by means of hangers. In Fig. B-1 the transverse stresses σ_y are compressive for the entire depth of the panel indicating no need of hangers. However, the curves differ completely for the cases when the load is located at the mid-depth and at bottom. Fig. B-2 and Fig. B-3 show clearly the need of suspension reinforcement. The transverse stresses tend to diminish fairly rapidly as they approach the mid shear-span as is indicated by Fig. B-5 and Fig. B-6. Based on these observations it is recommended that the suspension reinforcement be provided at the location of load for all cases of indirectly loaded panels. It is further recommended that such reinforcement extend atleast $\frac{d}{2}$ distance on each side of the load.

REFERENCES

REFERENCES

[1] Abdulezer, A., "Ultimate Strength in Diagonal Splitting of Reinforced Concrete Thin Wall Ribbed Panels," M.Eng. Thesis, Department of Civil Engineering, Sir George Williams University, Montreal, 1974.

[2] ACI Standard 318-71, "Building Code Requirements for Reinforced Concrete (ACI 318-71)," American Concrete Institute, Detroit, Mich., 1971. Section 11.9.

[3] Baumann, T., and Rüsch, H., "Shear Tests With Indirect Loading," (in German) Deutscher Ausschuss Für Stahlbeton, Vol. 210, Wilhelm Ernst und Sohn, Berlin, 1970.

[4] Cervenka, V., "Inelastic Finite Element Analysis of Reinforced Concrete Panels Under In-Plane Loads," Ph.D. Thesis, Department of Civil Engineering, University of Colorado, Boulder, 1970.

[5] Cheng, D., and Pei, M., "Continuous Deep Beams," ASCE Journal, V.80, Separate #450, June 1954.

[6] Chow, L., Conway, H., and Winter, G., "Stresses in Deep Beams," ASCE Journal, V.78, Separate #127, May 1952.

[7] Comité Européan du Béton - Federation Internationale de la Precontrainte, "International Recommendations for the Design and Construction of Concrete Structures," Cement and Concrete Association, London, England, 1970.

[8] CSA Standard A23.3-1973, "Code for the Design of Concrete Structures for Buildings," Canadian Standards Association, Rexdale, Ont., 1973, Section 9.10.

[9] de Paiva, H.A.R., and Siess, C.P., "Strength and Behaviour of Deep Beams in Shear," J. Structural Division, ASCE, Vol. 91, No. ST5, Oct.1965, pp.19-42.

[10]   Deschinger, F., "Contributions to the Theory of
       Wall Type Girders," IABSE Publication, Vol.1, 1932.
       pp.69-93.

[11]   Ferguson, P.M., "Some Implications of Recent Diagonal
       Tension Tests," ACI Journal, Vol.53, August 1956,
       pp.157-172.

[12]   Franklin, H.A., "Non-Linear Analysis of Reinforced
       Concrete by the Finite Element Method," ACI Journal,
       Vol.65, No.9, September 1968.

[13]   Guyon, Y., Prestressed Concrete, published by
       John Wiley and Sons Inc., New York, 1960.

[14]   Isenberg, J., and Adham, S., "Analysis of Orthotropic
       Reinforced Concrete Structures," J. Structural Division,
       ASCE, V.96, No.ST.12, Dec. 1970.

[15]   Joint ASCE-ACI Task Committee 426, "The Shear Strength
       of Reinforced Concrete Members," J.Structural Division,
       ASCE, Vol.99,No.ST.6, June 1973, pp.1091-1187.

[16]   Kani, G.N.J., "Basic Facts Concerning Shear Failures,"
       ACI Journal, Vol.63, June 1966, pp.675-692.

[17]   Kani, G.N., "The Riddle of Shear Failure and its
       Solution," ACI Journal, Vol.61,No.4, April 1964, pp.441-
       462.

[18]   Kaar, P.H., "Stresses in Centrally Loaded Deep Beams,"
       Portland Cement Association, Development Department
       Bulletin D.18.

[19]   Kong, F.K., Robins, P.J., and Cole, D.F., "Web Rein-
       forcement Effects on Deep Beams," ACI Journal, Vol.67,
       No.12, December 1970. pp.1010-1017.

[20]   Kong, F.K., Robins, P.J., Singh, A., and Sharp, G.R.,
       "Shear Analysis and Design of Reinforced Concrete Deep
       Beams," The Structural Engineer, Vol.50, No.10,
       October 1972. pp.405-409.

[21] Kupfer, H., Hilsdorf, H.K., and Rusch, H., "Behaviour of Concrete Under Biaxial Stresses," ACI Journal,Vol.66, No.8, August 1969, pp.656-666.

[22] Leonhardt, F., Koch, R., and Rostásy,F.S., "Hanger Reinforcement for Indirectly Loaded Prestressed Concrete Beams, Test Report and Recommendations," (in German), Beton Und Stahlbeton, Vol.66,Oct.1971, pp:233-241.

[23] Leonhardt, F., Walther, R., and Dilger, W. "Shear Tests on Indirectly Loaded Simple and Continuous Rein-forced Beams," (in German) Deutscher Ausschuss für Stahlbeton,Vol.201, Verlag Von Wilhelm Ernst Sohn, Berlin, 1968.

[24] Leonhardt, F., and Walther, R., "Wandertige Trager," Deutscher Ausschuss für Stahlbeton,Vol.178, Wilhelm Ernst Und Sohn, Berlin, 1966.

[25] Leonhardt, F., and Walther, R., "The Stuttgart Shear Tests 1961," Translation No.111, Cement and Concrete Association, London, England, 1964.

[26] Mufti, A.A., et al., "A Study of the Non-Linear Be-haviour of the Structural Concrete Elements," Proc. Speciality Conf. on Finite Element Method in Civil Engineering, Montreal, June 1972, pp.767-802.

[27] Mufti, A.A., Mirza, M.S., McCutcheon,J.O., and Houde,J., "A Study of the Behaviour of Reinforced Concrete Elements Using Finite Elements," Structural Concrete Series No.71-1, McGill University, Montreal, March 1971.

[28] Ngo, D., and Scordelis, A.C., "Finite Analysis of Reinforced Concrete by the Finite Element Method," ACI Journal, Vol.64, No.3, March 1967, pp.152-163.

[29] Nilson, A.H., "Non-Linear Analysis of Reinforced Concrete by the Finite Element Method," ACI Journal, Vol.65, No.9, September 1968, pp.757-766.

[30] Placas, A., and Regan, P.E., "Shear Failures of Reinforced Concrete Beams," ACI J. Vol.68,No.10,Oct.1971, pp.763-773.

[31] Portland Cement Association,"Design of Deep Girders," Concrete Information Series, ST:66, 10 pages.

[32] Ramakrishnan,V., and Ananthanarayana, Y., "Ultimate Strength of Deep Beams in Shear," ACI Journal,Vol.65,No.2, February 1968,pp.87-98.

[33] Rajagopalan,K.S., and Ferguson,P.N., "Exploratory Shear Tests Emphasizing Percentage of Longitudinal Steel," ACI Journal, Vol.65, No.8, August 1968, pp.634-638.

[34] Scordelis, A.C., "Finite Element Analysis of Reinforced Concrete Structures," Proc. Speciality Conf. on Finite Element Methods in Civil Engineering, Montreal, June 1972, pp.71-113.

[35] Suidan,M., and Schnobrich, W.C., "Finite Element Analysis of Reinforced Concrete," J. Structural Division,ASCE, Vol.99, No.ST10, October 1973, pp.2109-2121.

[36] Taner, N., "Prediction of Strength Limits of Thin Wall Beam Panels Using the Finite Element Method," D.Eng. Thesis, Department of Civil Engineering,Concordia University, Montreal, April 1976.

[37] Taner, N., Fazio, P.P., and Zielinski, Z.A., "Strength and Behaviour of Beam Panels - Tests and Analysis," ACI Journal, V.74, No.10, October 1977, pp.511-520.

[38] Valliappan,S., and Dodan, T.F., "Non-Linear Stress Analysis of Reinforced Concrete," Journal of the Structural Division,ASCE,Vol.98, No.ST.4, April 1972, pp.885-897.

[39] Valliappan, S., and Nath, P., "Tensile Crack Propagation in Reinforced Concrete Beams by Finite Element Techniques," International Conference on Shear, Torsion and Bond in Reinforced Concrete, Coimbatore, India, January 1969.

[40] Yuzugullu, O., and Schnobrich, W.C., "A Numerical Procedure for the Determination of the Behaviour of a Shear Wall Frame System," ACI Journal, Vol.70,No.7, July 1973. pp.474-479.

[41] Zielinski, Z.A., Abdulezer, A., "Ultimate Strength in Diagonal Splitting of Reinforced Concrete Thin Wall Panels," Canadian Journal of Civil Engineering, Vol.4, No.2, June 1977, pp.226-239.

[42] Zielinski, Z.A., "Behaviour and Ultimate Strength of Rectangular Reinforced Concrete Beams in Bending and High Shear," North Carolina State University Bulletin No. 81, 1967.

[43] Zielinski, Z.A., "A New Approach to Ultimate Strength of Reinforced Concrete Beams in Inclined Cracking and Reduction of Web Reinforcement in Bridge Girders," ACI Second International Symposium on Concrete Bridge Design, Paper SP-26-17, Vol.1, April 1969, pp.411-456.

[44] Zienkiewicz, O.C., The Finite Method in Engineering Science, McGraw-Hill, London, 1971.

[45] Zienkiewicz, O.C., Brotton, D.M., and Morgan, L.; "A Finite Element Primer for Structural Engineering," The Structural Engineer, Vol,54, No.10, October 1976, pp.387-397.

[46] Zsutty, T.C., "Beam Shear Strength Prediction by Analysis of Existing Data," ACI Journal, Vol.65, No.11, November 1968, pp.943-.

[47] Zsutty, T., "Shear Strength Predictions for Separate Categories of Simple Beam Tests," ACI Journal, Vol.68, No.2, February 1971, pp.138-143.

APPENDIX A

PANEL 111

LOAD (kip)

80

60

40

20

0

1   2   3   4   5   6   7   8   δ

DEFLECTION (10^{-2}) in.

PANEL 112

LOAD (kip)

80

60

40

20

0

1   2   3   4   5   6   7   8   δ

DEFLECTION (10^{-2}) in.

PANEL 121
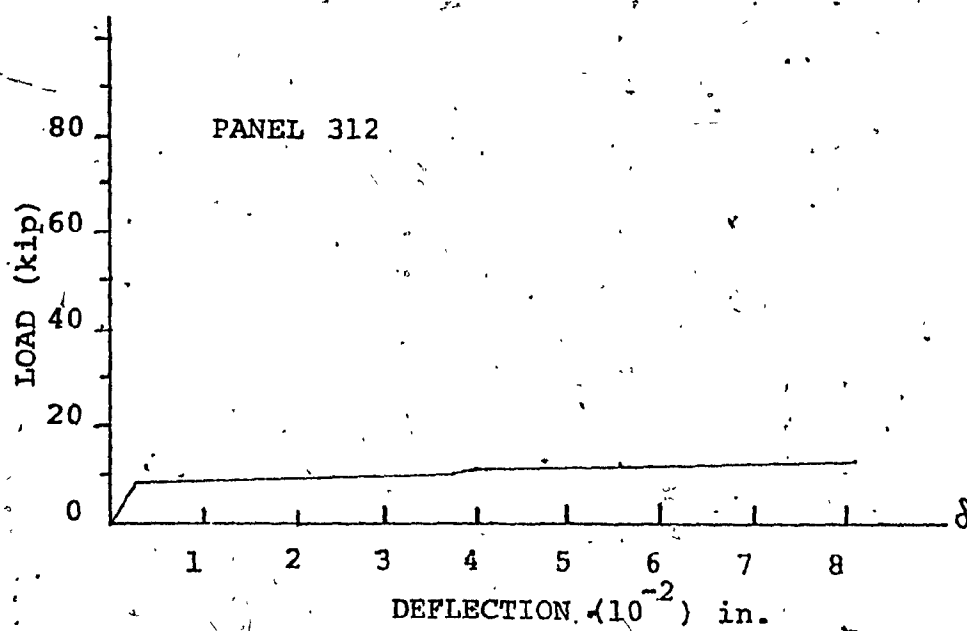
LOAD (kip)

80

60

40

20

0

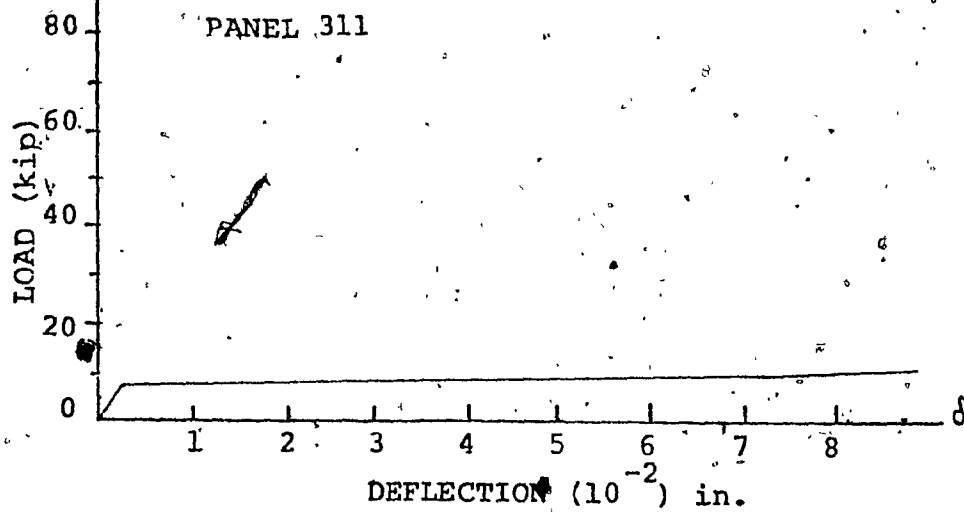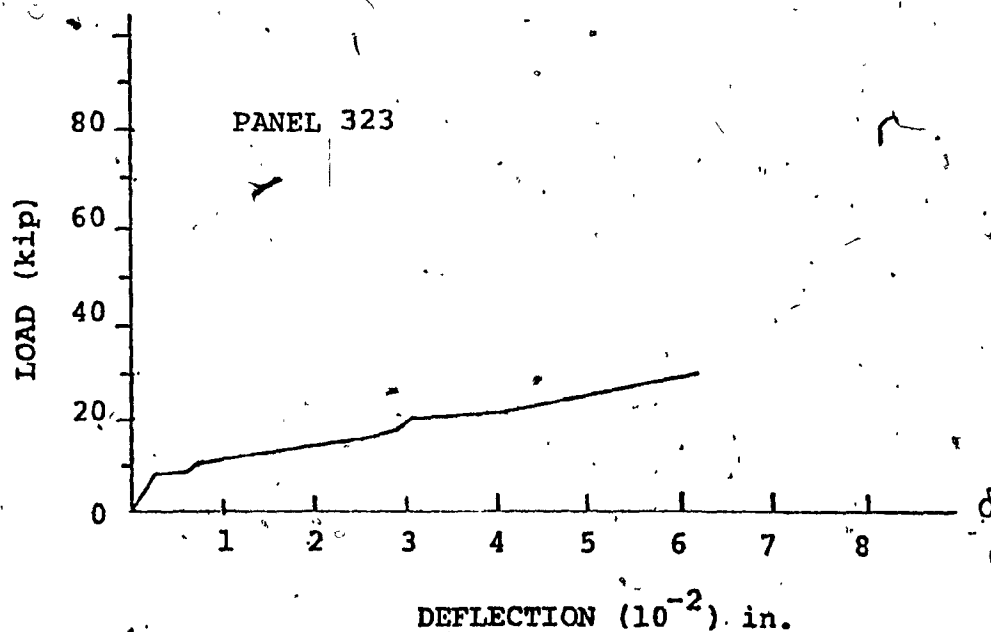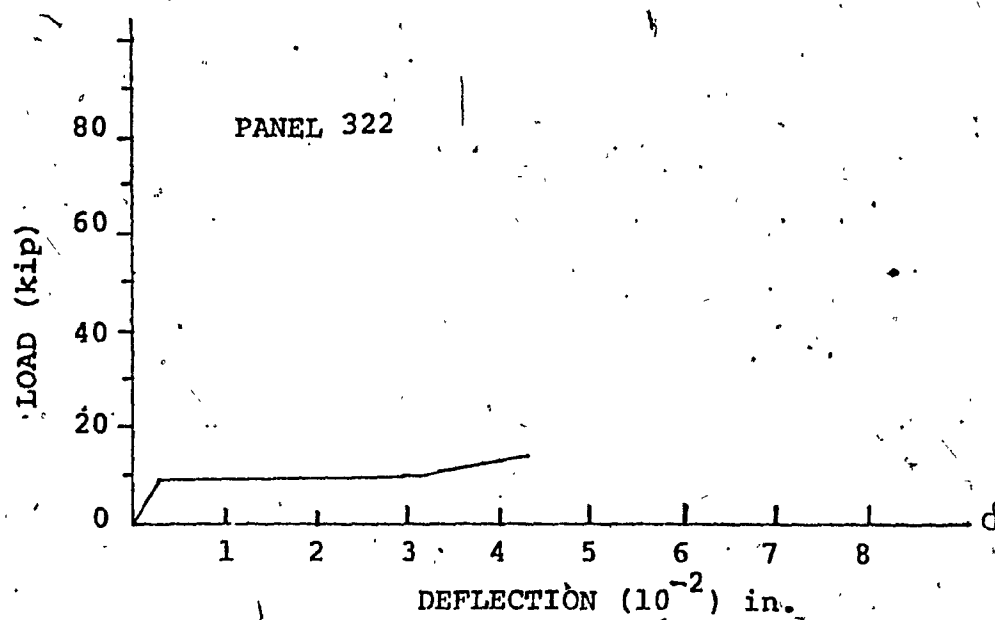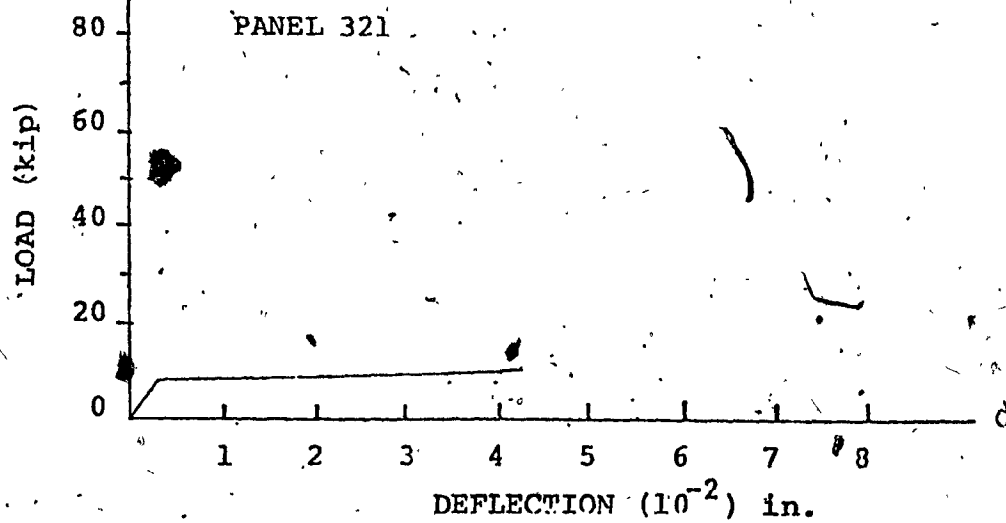1   2   3   4   5   6   7   8   δ

DEFLECTION (10^{-2}) in.
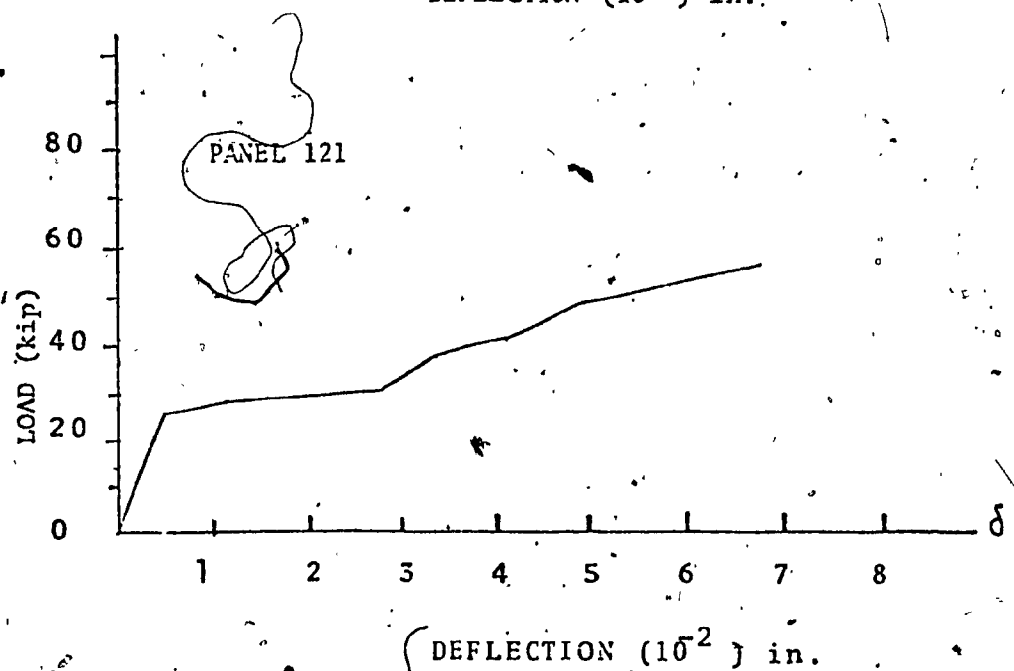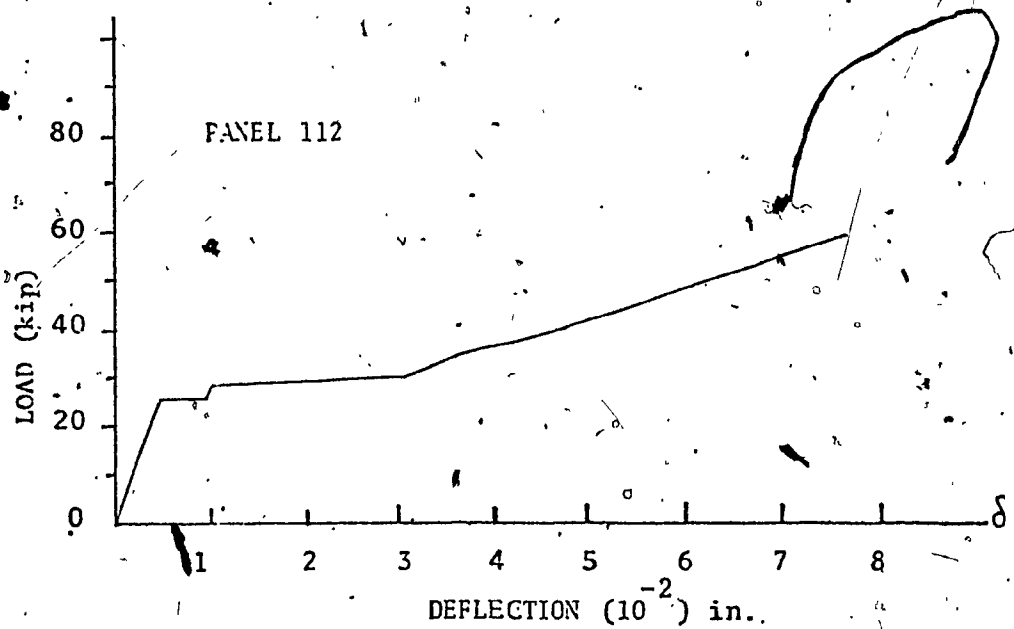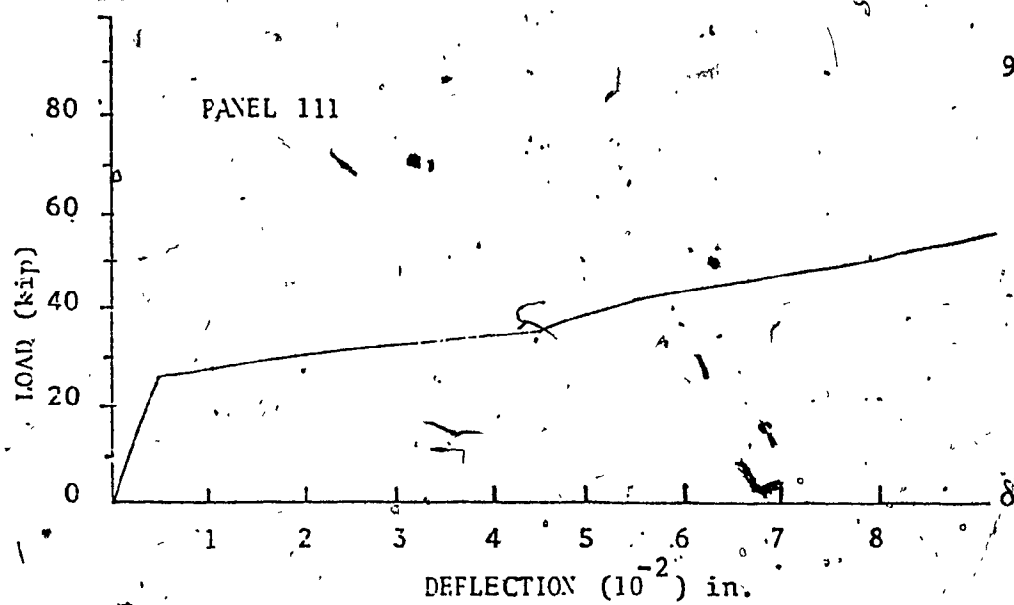
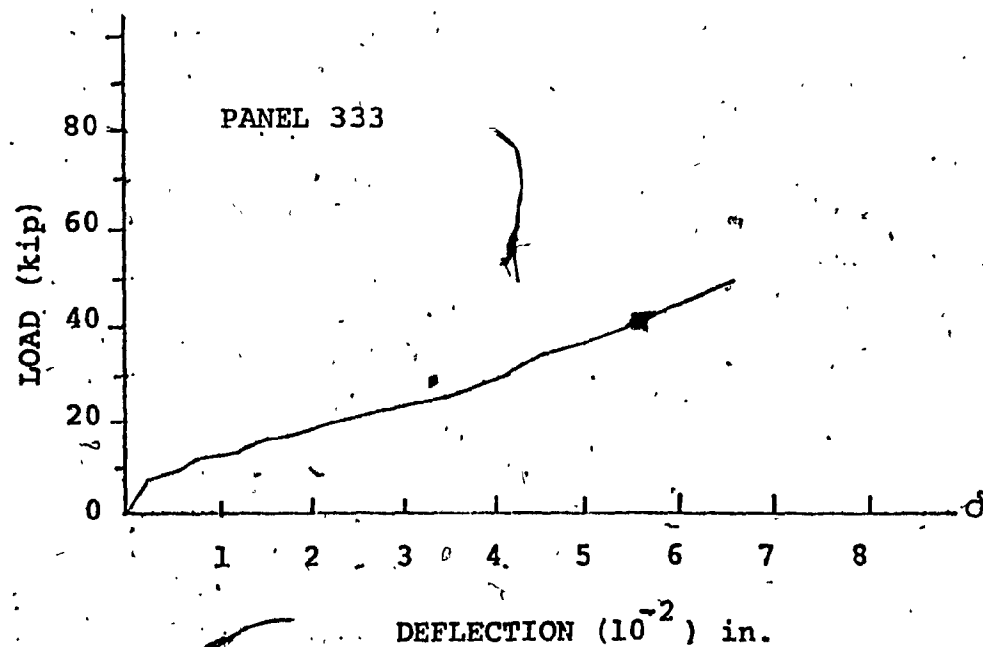FIG. A.1   LOAD DEFLECTION DIAGRAM

FIG. A.2 LOAD DEFLECTION DIAGRAM

PANEL 211

LOAD (kip)

DEFLECTION (10^{-2}) in.

PANEL 212

LOAD (kip)

DEFLECTION (10^{-2}) in.

PANEL 213

LOAD (kip)

DEFLECTION (10^{-2}) in.

FIG. A.3 LOAD DEFLECTION DIAGRAM

PANEL 221

PANEL 222

PANEL 223
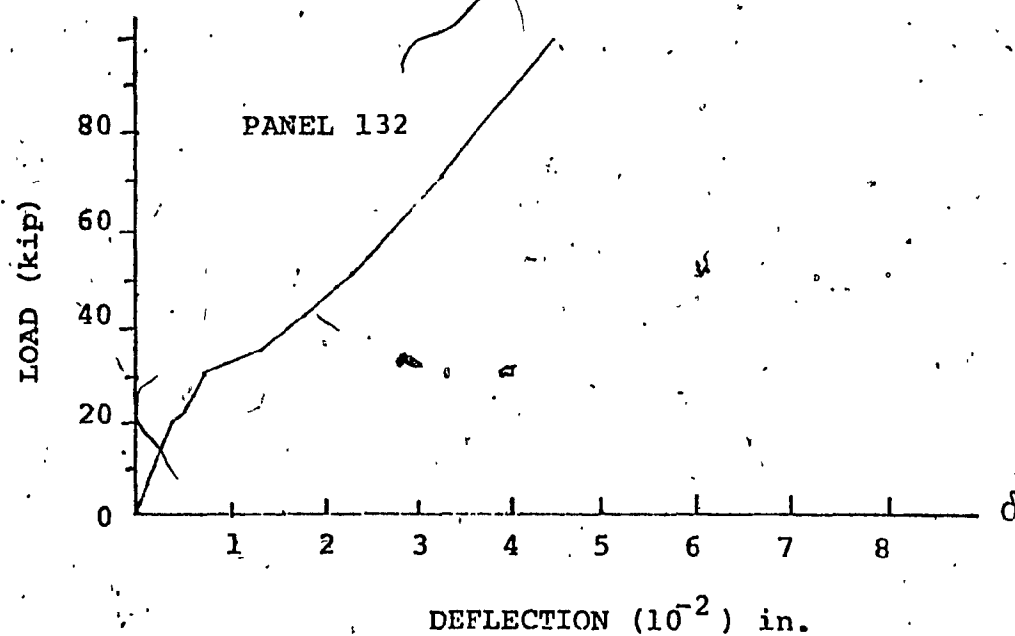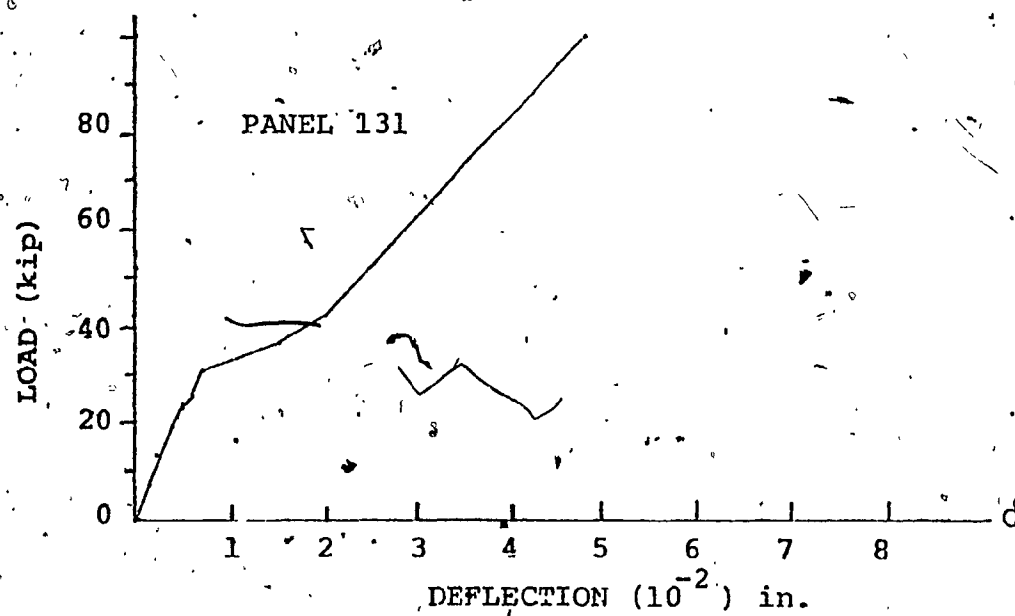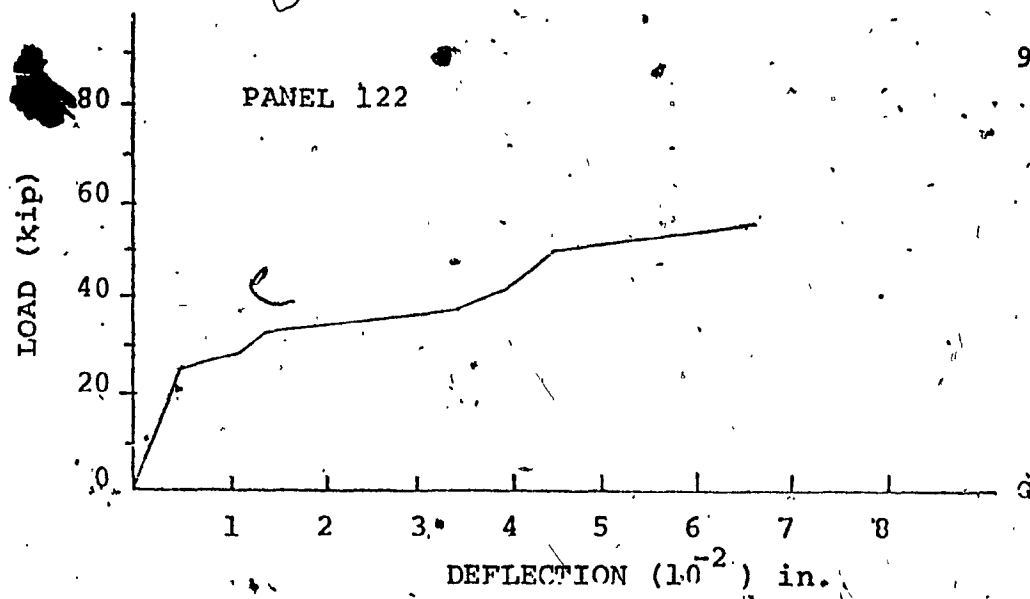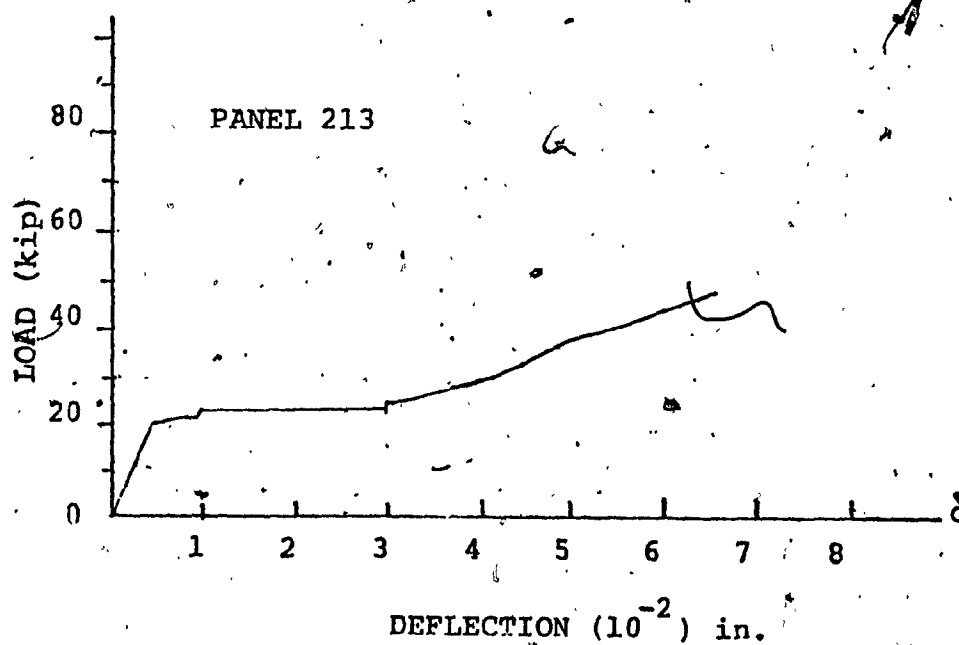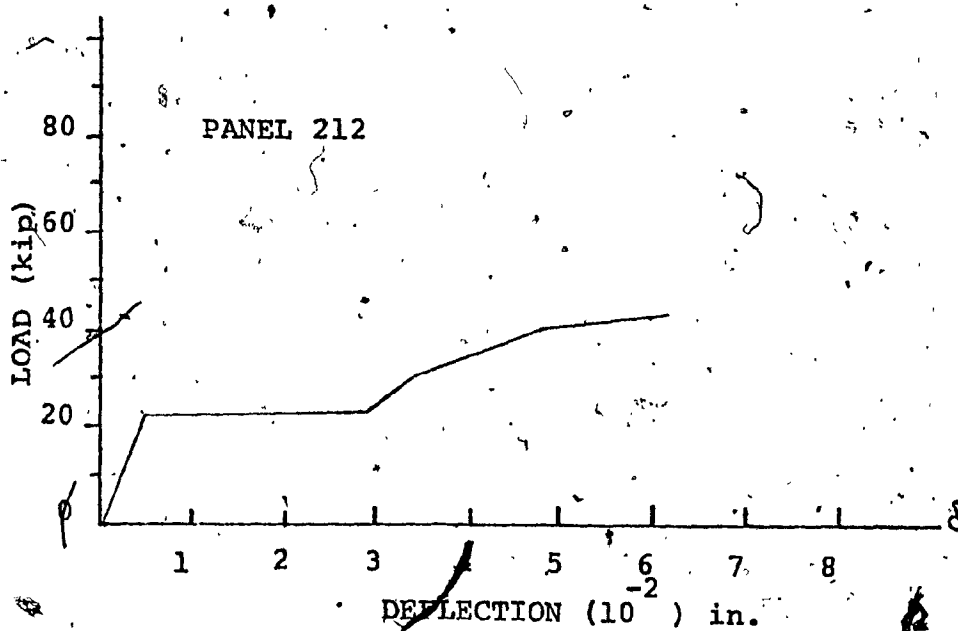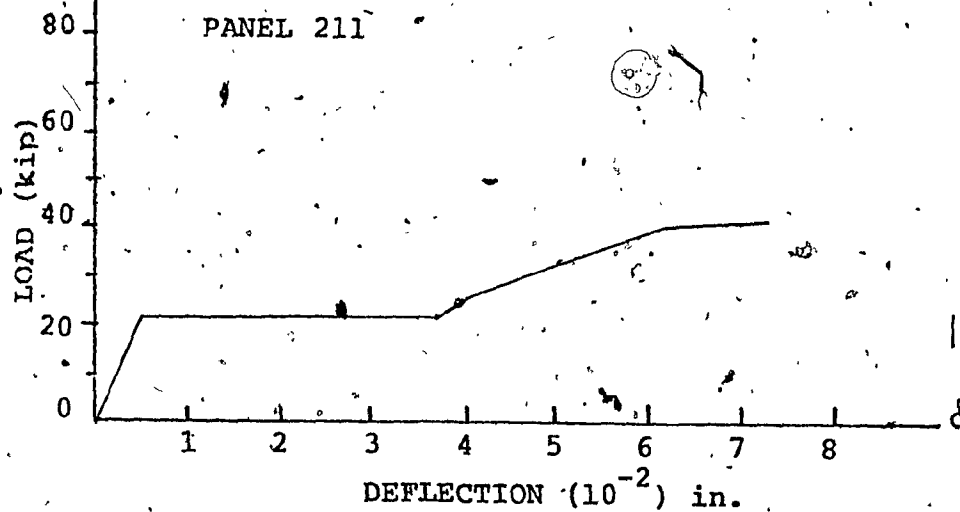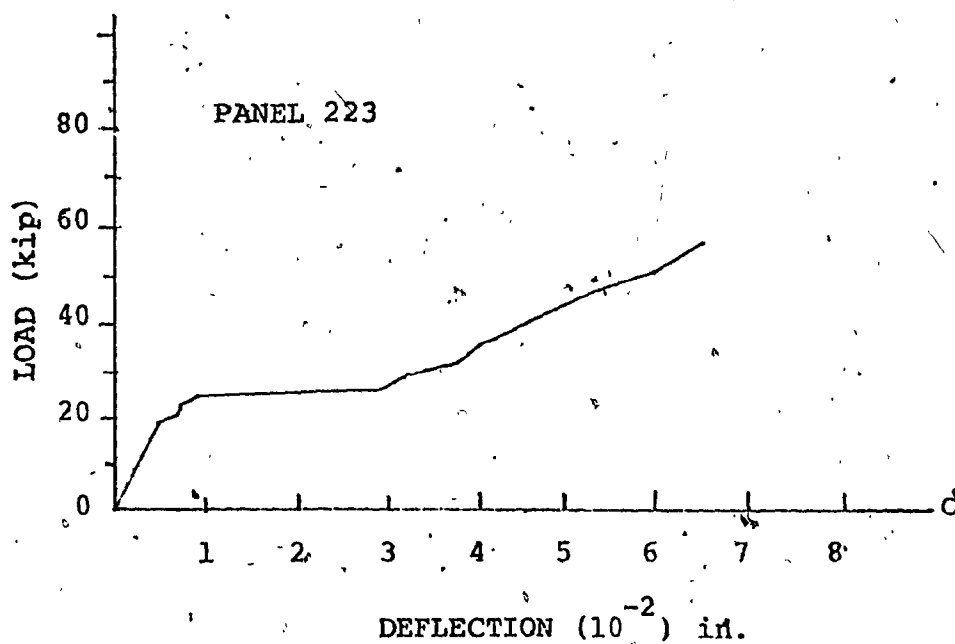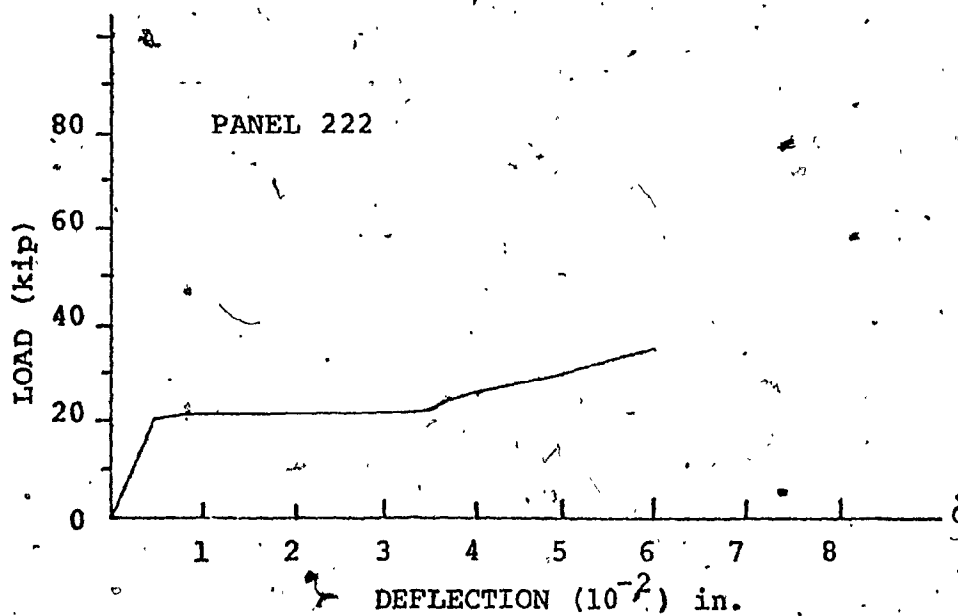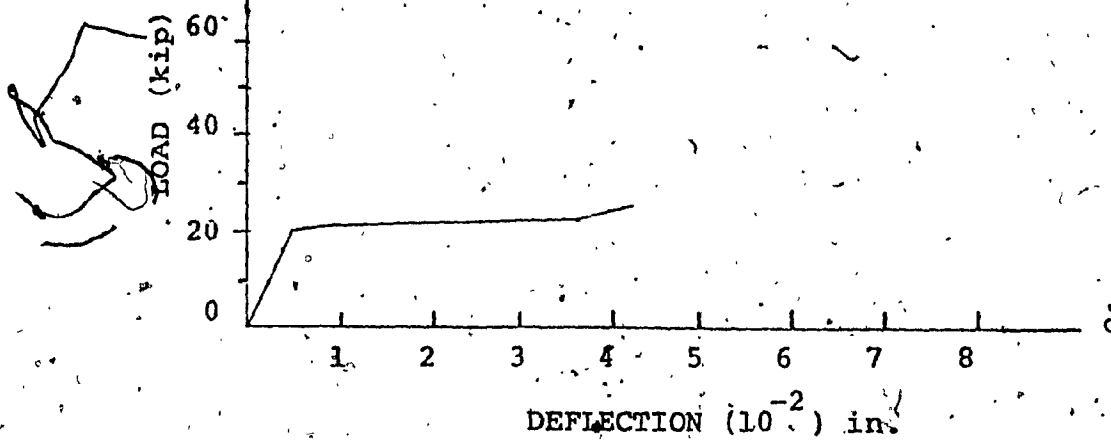
FIG. A.4   LOAD DEFLECTION DIAGRAM

FIG. A.5 LOAD DEFLECTION DIAGRAM

PANEL 311

LOAD (kip)

DEFLECTION (10^{-2}) in.

PANEL 312

LOAD (kip)

DEFLECTION (10^{-2}) in.

PANEL 313

LOAD (kip)

DEFLECTION (10^{-2}) in.
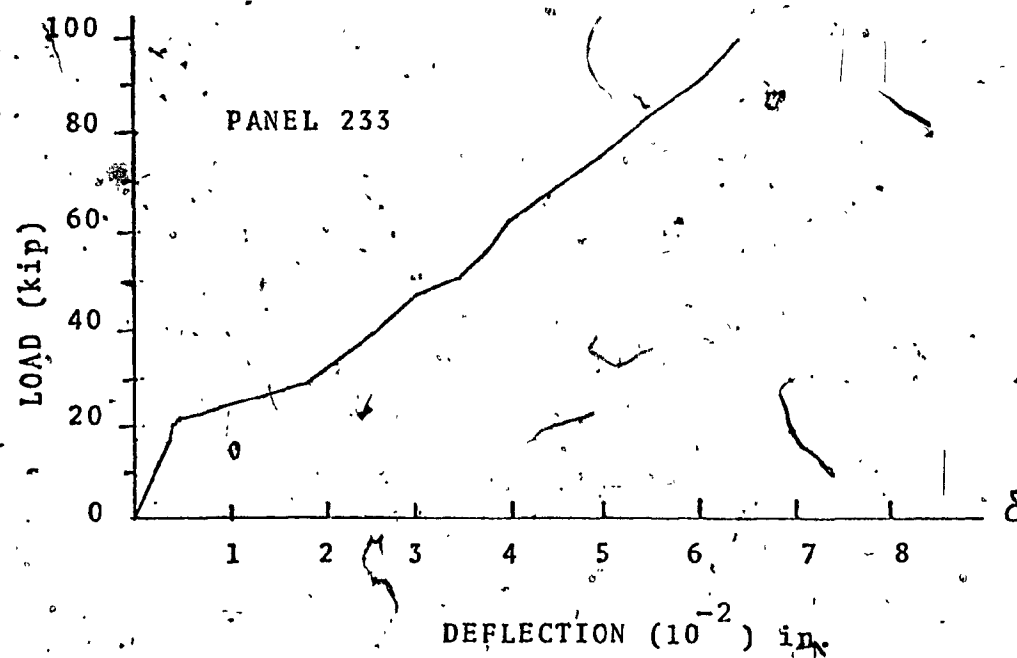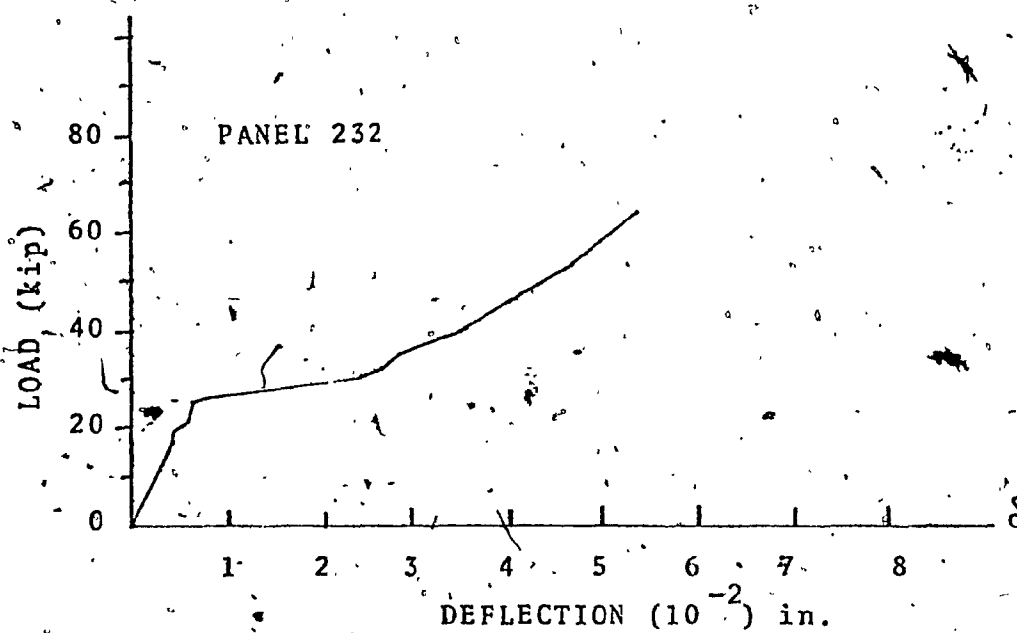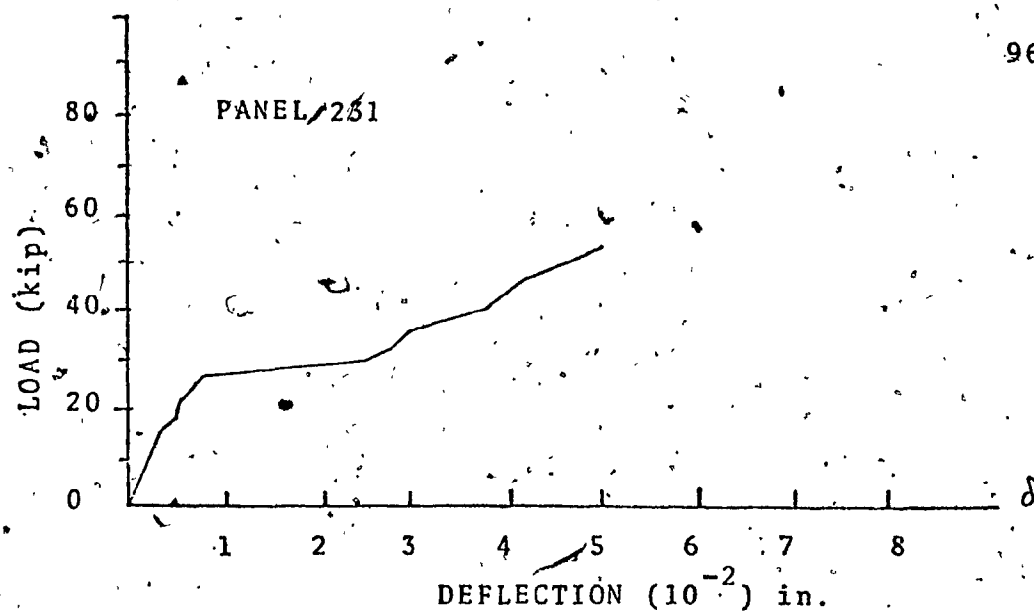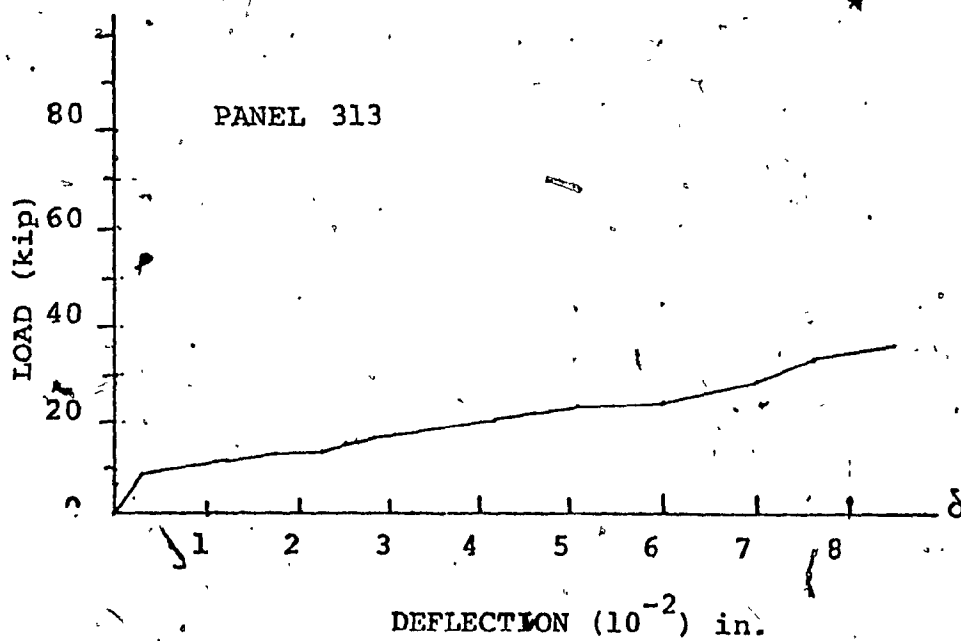
FIG. A.6 LOAD DEFLECTION DIAGRAM

FIG. A.7   LOAD DEFLECTION DIAGRAM

PANEL 331

PANEL 332

PANEL 333
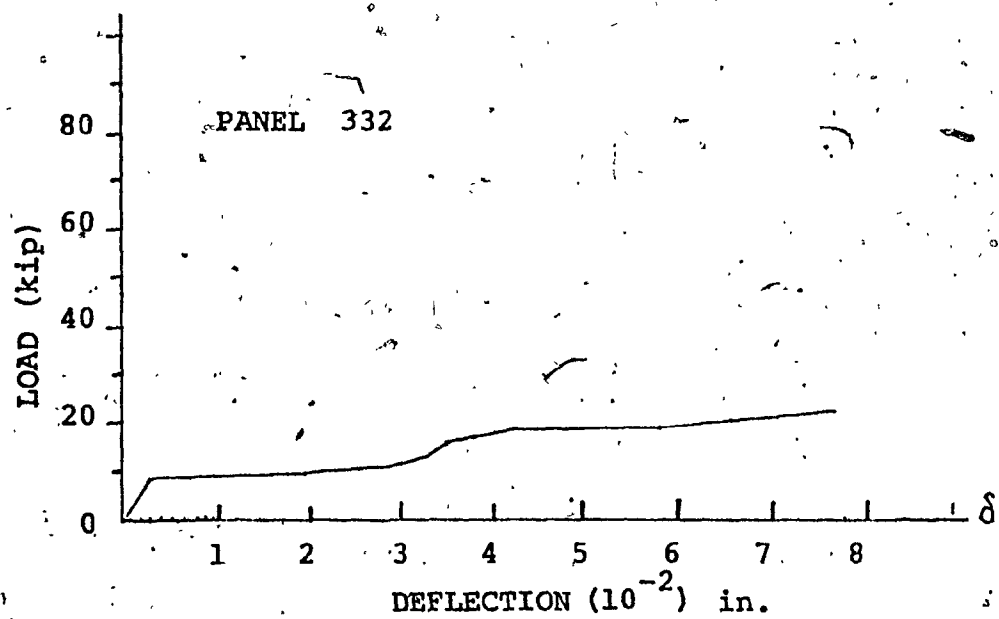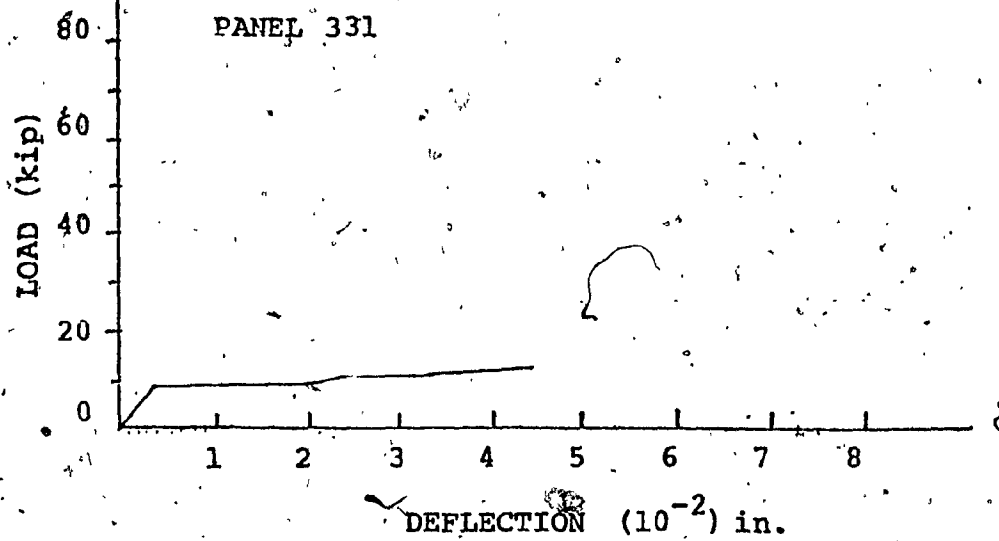
FIG. A.8   LOAD DEFLECTION DIAGRAM

APPENDIX B
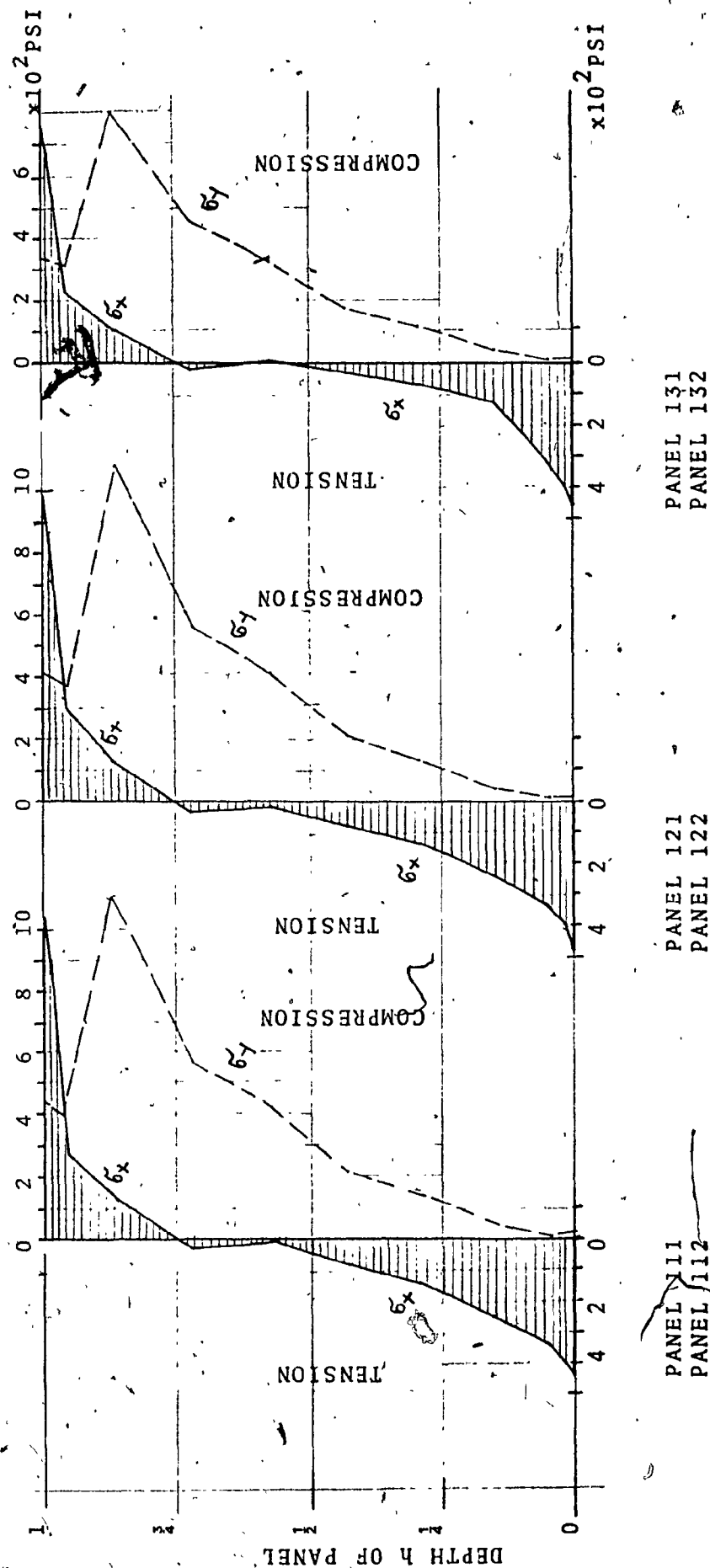
FIG. B-1 STRESSES σ_x AND σ_y AT MIDSPAN
UNCRACKED CONCRETE
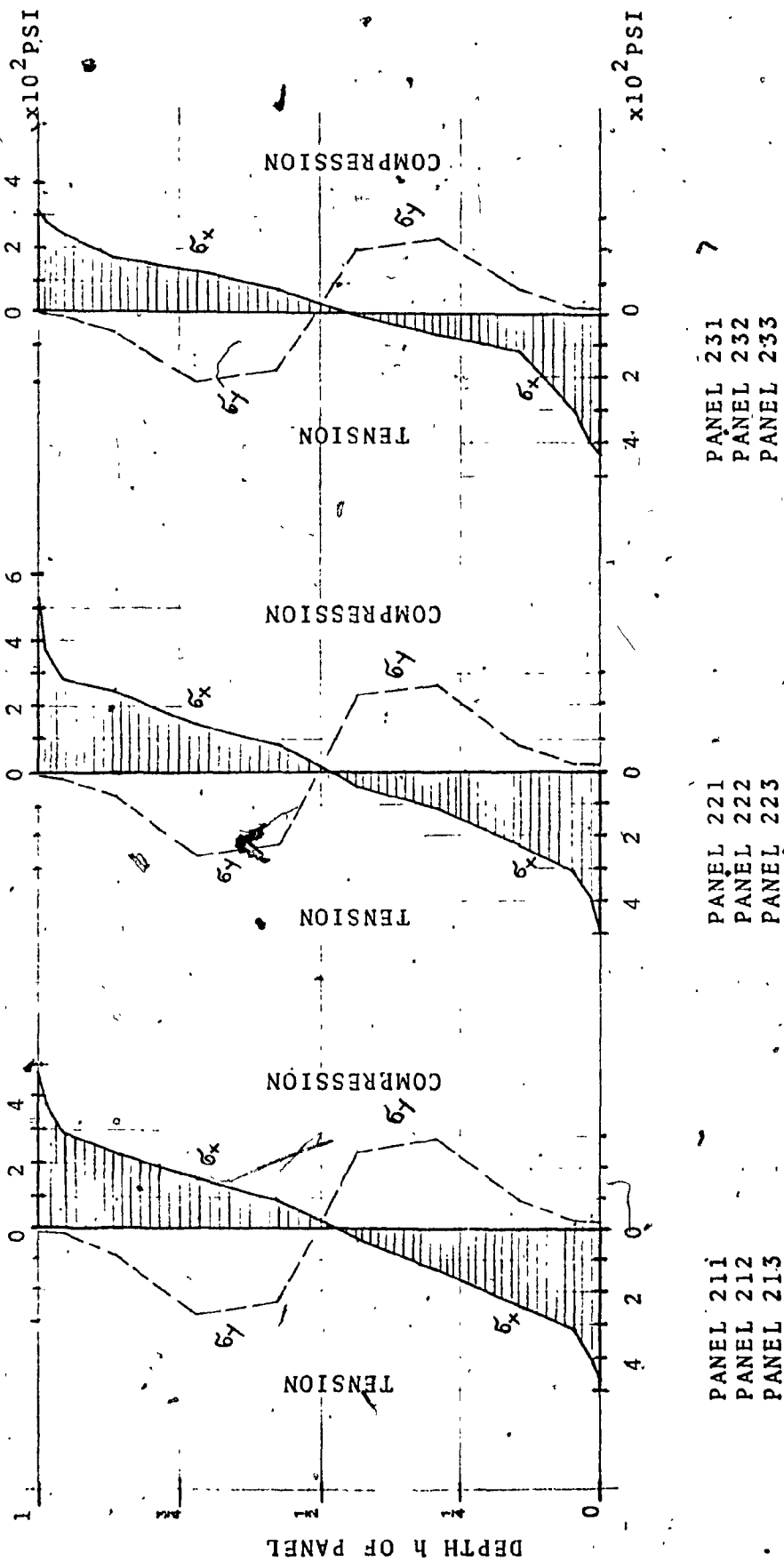
FIG. B-2 STRESSES σ_x AND σ_y AT MIDSPAN
UNCRACKED CONCRETE
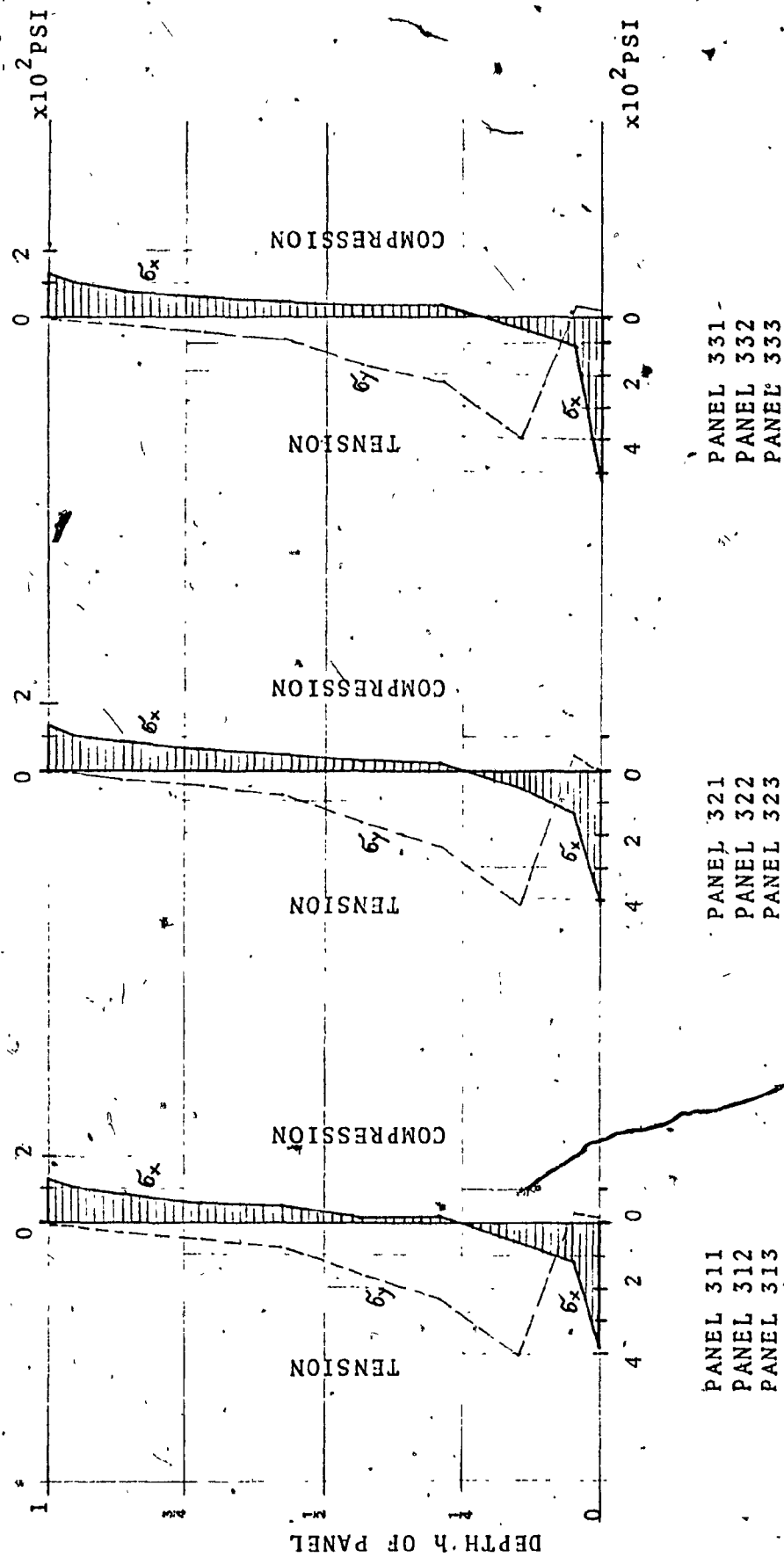
FIG. B-3 STRESSES σ_x AND σ_y AT MIDSPAN UNCRACKED CONCRETE
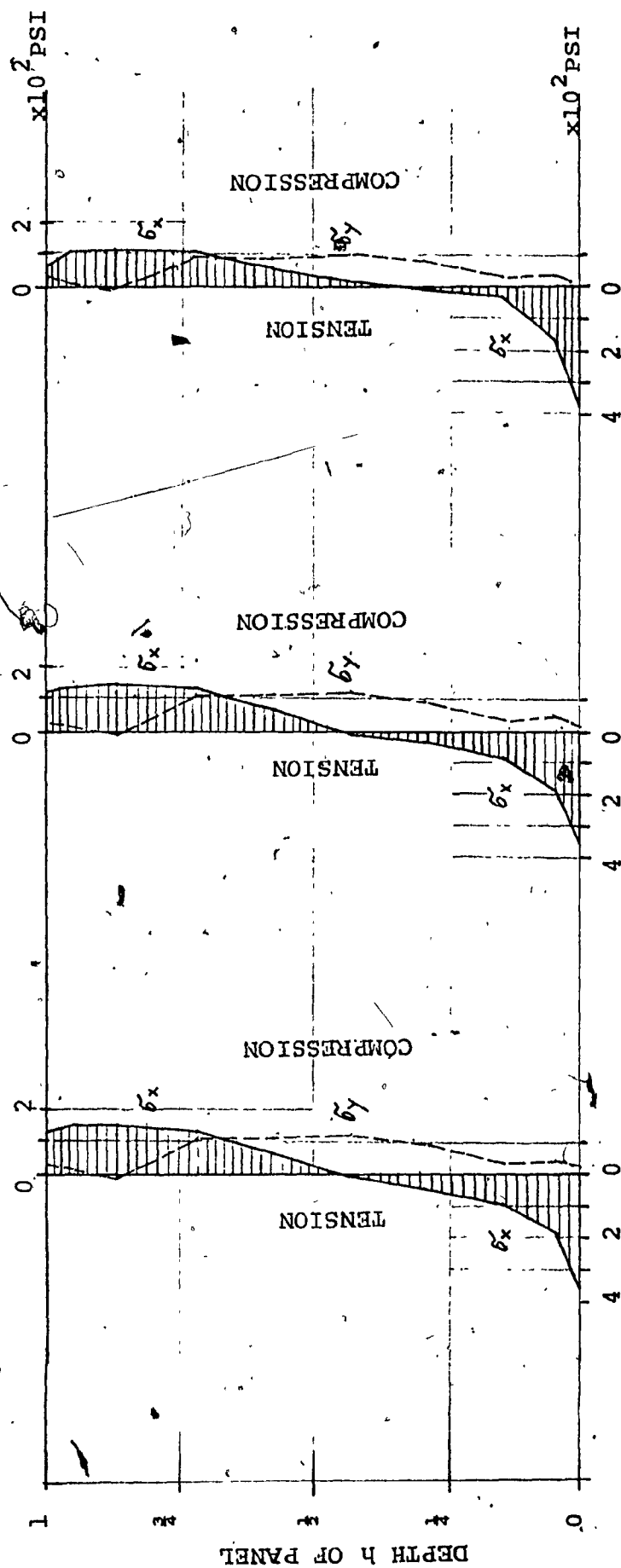
FIG. B-4 STRESSES σ_x AND σ_y AT MID SHEAR SPAN
UNCRACKED CONCRETE
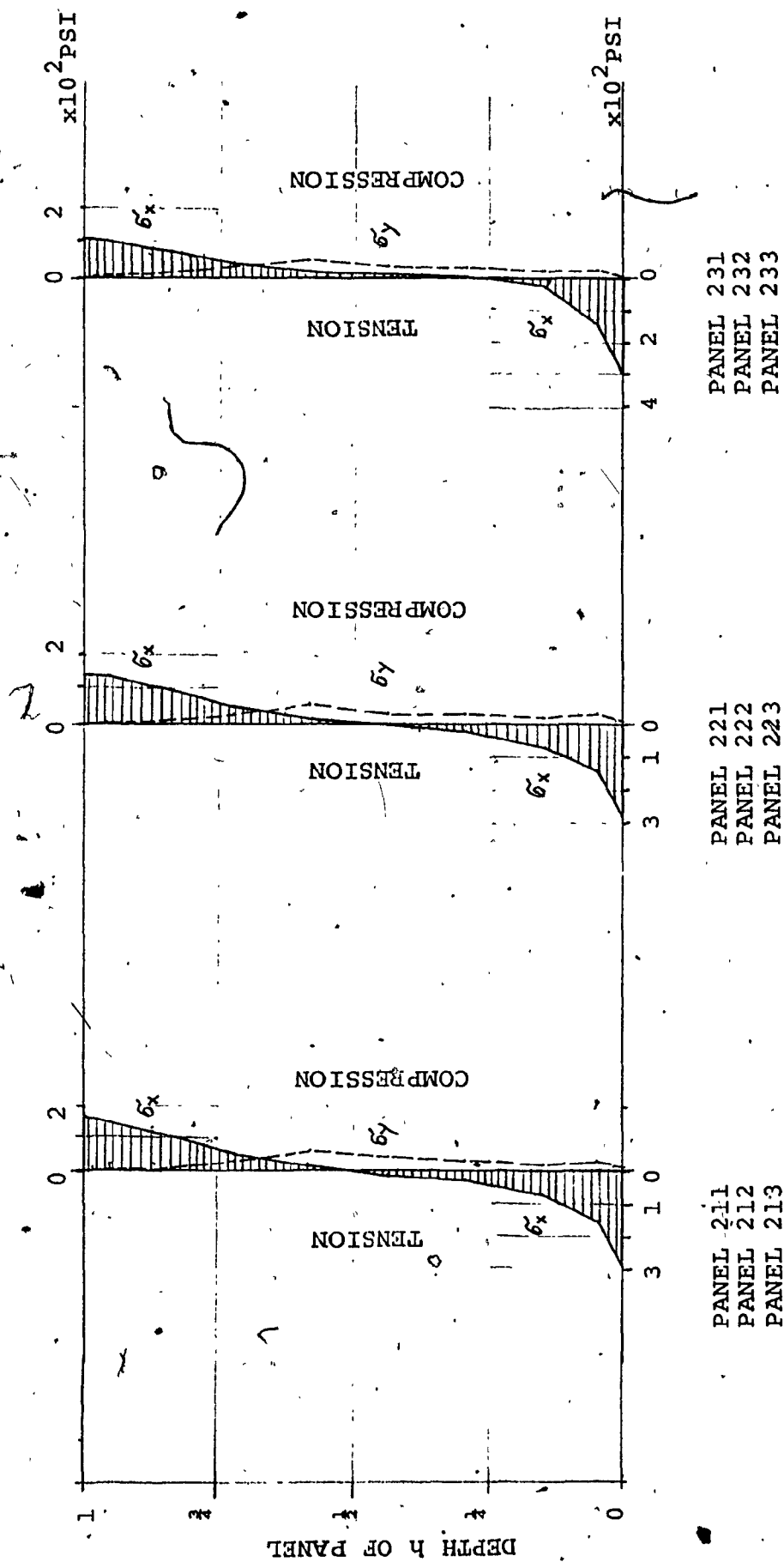
FIG. B-5 STRESSES σ_x AND σ_y AT MID SHEAR SPAN
UNCRACKED CONCRETE
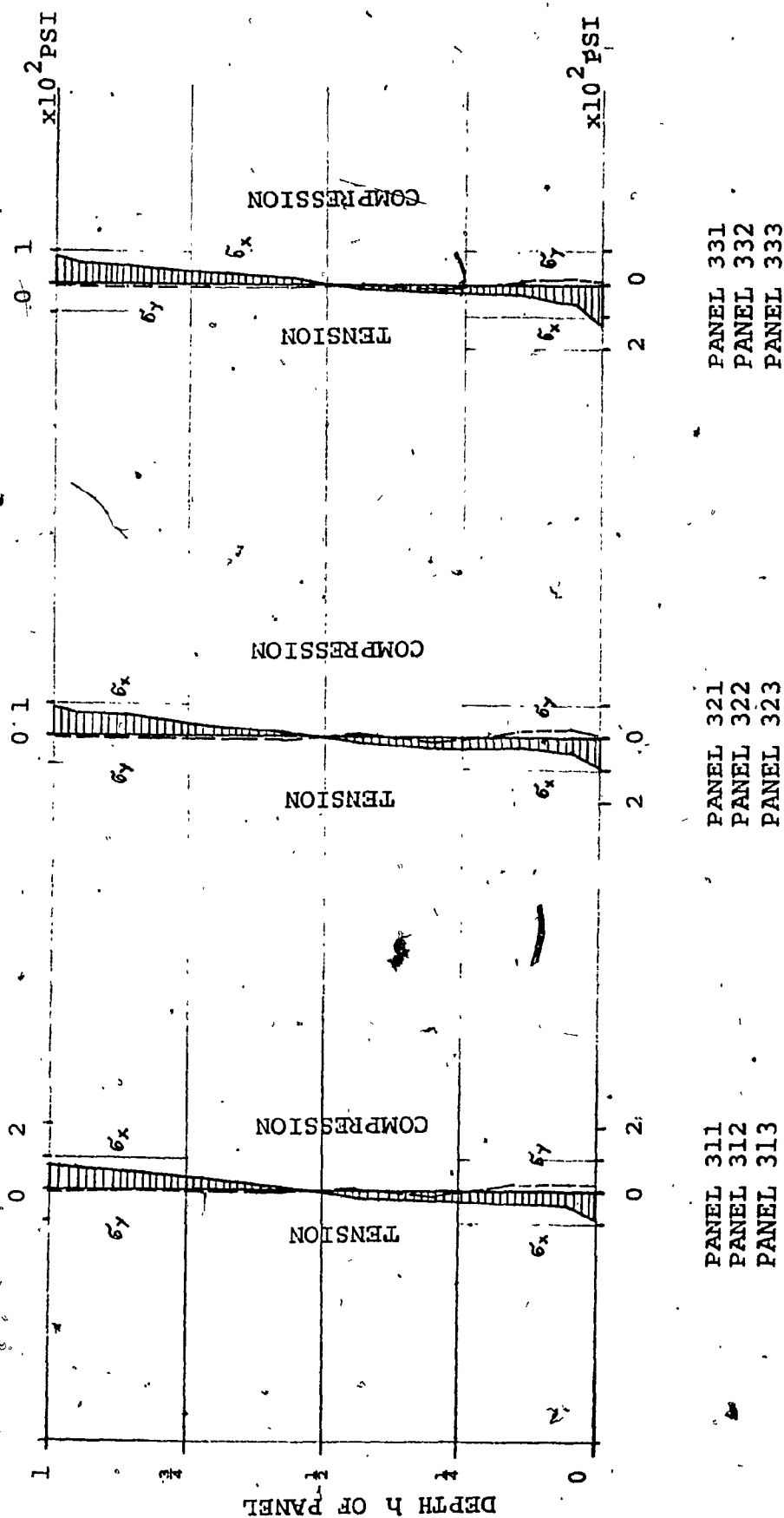
FIG. B-6 STRESSES σ_x AND σ_y AT MID SHEAR SPAN
UNCRACKED CONCRETE
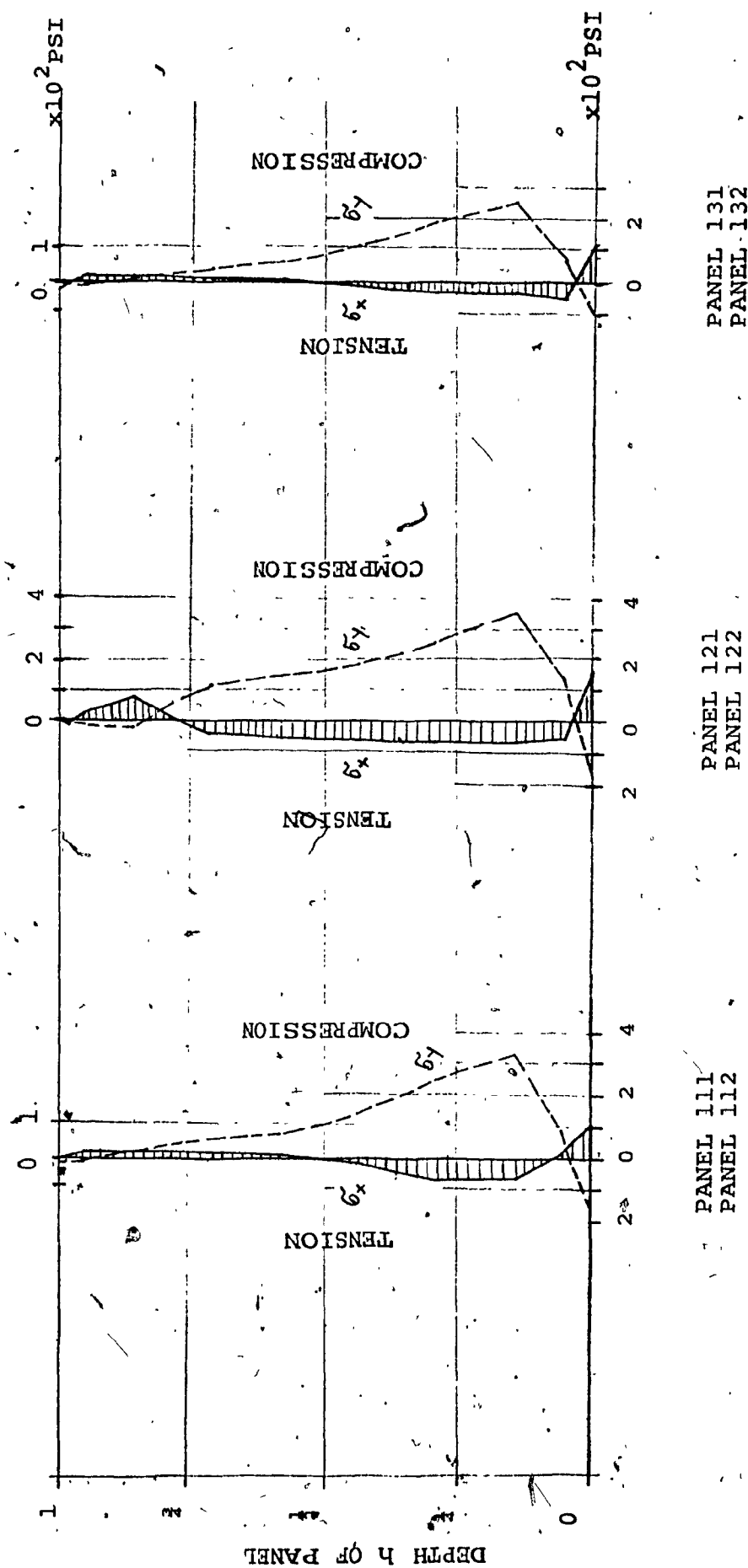
FIG. B-7 STRESSES σ_x AND σ_y AT SUPPORT
UNCRACKED CONCRETE

FIG. B-8 STRESSES σ_x AND σ_y AT SUPPORT
UNCRACKED CONCRETE